CWP-237
December 1996

The Influence of Near-surface Time Anomalies in the Imaging Process

Trino Salinas G.

— Master's Thesis —
Geophysics

Center for Wave Phenomena
Colorado School of Mines
Golden, Colorado 80401
303/273-3557

ABSTRACT

Land seismic data commonly suffer from time anomalies attributable to surface topography and laterally-changing near-surface conditions. Conventionally, these time distortions have been treated and modeled as simple time-invariant shifts under the assumptions that the anomalies are static and surface-consistent. In general, these assumptions are valid for areas with mild topography and slow near-surface velocity changes, allowing the static-correction to offer a satisfactory treatment to the near-surface-induced time distortions.

In rough terrain areas, however, where the near-surface characteristics include significant topographic changes and high-velocity rocks, the surface-consistent static approach has proven to be inaccurate, and more sophisticated methods have been required. Under those circumstances, wave-equation datuming and migration from the acquisition surface provide an accurate solution to this imaging problem. These solutions, nevertheless, work best when the near-surface velocity structure is well known. In practice, these techniques often fail to show satisfactory results due to difficulties in obtaining accurate estimates of the shallow velocity model.

Here, I analyze through demonstrations with synthetic examples how theoretic expectations about the quality of the near-surface treatment might change when the corrective algorithms work with imperfect shallow velocity estimates. In particular, when the near-surface velocity used in the datuming process is higher than the true velocity field, conventional static-datuming schemes may be more robust than the Kirchhoff datuming approach, offering better imaging quality after prestack depth migration.

Overthrust areas with significant surface topography along with complex subsurface velocity structure represent a great imaging challenge for seismic data processing. In an attempt to give some insight into this interesting and demanding imaging situation, I carry out a comparative analysis of imaging techniques on an overthrust model that takes into account rugged topography and a complex near- and subsurface velocity structure. The imaging approaches included in this study are prestack depth migration from topography, and a combination of prestack wave-equation datuming and prestack depth migration from a horizontal reference level. I also include solutions from methods such as tomo-statics and tomo-datuming based on a near-surface velocity structure derived from a tomographic inversion. In this comparative analysis, I find that although the velocity model obtained by turning-ray tomography reproduces, quite nicely, the main features of the true velocity field, it lacks the level of accuracy required to derive the benefit from the wave-equation datuming as compared to the conventional static-datuming approach; thus, the migrated sections obtained after the tomo-statics and tomo-datuming processes offer similar imaging quality.

Methods of residual-static corrections have long benefitted from the assumption

that the near-surface-induced distortions are static and surface consistent. However, in assessing the performance and robustness of algorithms designed to correct for time anomalies associated with the near-surface under the assumption of surface-consistency, one should be wary of using models that make the same assumption. More appropriately, the model data used in static-estimation algorithm testing should contain time distortions that are wave-theoretic. To generate those, I use a wave-equation-based methodology that combines wave-equation datuming and layer replacement. This near-surface modeling methodology is applied to the Marmousi data set to generate not just surface-consistent-static time shifts but more realistic time anomalies such as might be obtained after applying elevation-statics corrections. This methodology thus offers a means to contaminate data with time distortions consistent with the wave theory.

Following this modeling methodology, I use Kirchhoff datuming to superimpose a complex overthrust near-surface-induced time distortions atop a simple subsurface velocity model. The resulting synthetic data set is used to study the action of the datuming techniques on the stacking velocity analysis in a conventional (CMP) data processing sequence. To transfer the data from the topographic surface to the new datum level, I compare the wave-equation-based and simple static datuming approaches. When the datuming algorithms make use of an accurate near-surface velocity field, the data processed with Kirchhoff datuming yield stacking velocity functions virtually identical to those obtained from the data modeled at the new horizontal datum. The data processed with conventional statics, however, yield velocity functions that are too high or too low compared to the true ones. On the other hand, when a tomographic velocity model is used in the datuming process, the accuracy of the stacking velocities obtained from the data processed with the Kirchhoff approach depends upon the quality of the near-surface model derived from tomography. This indicates that when accurate near-surface velocities are available, Kirchhoff datuming is preferable for estimating reliable stacking velocity information; otherwise, conventional static-estimation schemes could be a satisfactory alternative approach.

TABLE OF CONTENTS

ACKNOWLEDGMENTS

I am thankful to my wife, Angela Maria, and my children, Maria Carolina and Mateo, for their patience and support during the whole time of my graduate studies.

I am grateful to the national oil company of Colombia Ecopetrol (Empresa Colombiana del Petroleos), and our research and development center ICP (Instituto Colombiano del Petroleo), for their financial support and confidence in my capacity to carry out this research.

I am greatly indebted to my advisor, Dr. Ken Larner, who always helped and encouraged me with his enthusiasm and enlightening suggestions that led me into this imaging research problem. Dr. Larner's accurate observations and practical ideas about the subject were the driving force to successfully accomplish the results offered in this dissertation.

I want to thank Drs. Norman Bleistein and John Scales for serving on my committee and for critiquing this dissertation, providing useful suggestions. I also would like to thank the faculty members of the Center for Wave Phenomena for allowing me to be part of such an outstanding research group. Furthermore, I thank Dr. Xianhuai Zhu of Union Pacific Resources Company for providing me all the information available for the synthetic overthrust model used in this work.

Special thanks are due to my friends: Gabriel Perez, Herman Jaramillo and Wences Gouveia for providing helful and interesting research discussions. And also thanks to Gabriel Alvarez who helped me understand the mysteries behind the SU programming in my early days at CSM.

Chapter 1

INTRODUCTION

The energy demand of the world is increasing every day, forcing the oil explorationist to look for hydrocarbon traps in locations where the problem complexity requires special imaging techniques. The easy targets have already been discovered, and the remaining ones might be in areas where the seismic method has had difficulties in the past. The rugged topography and complexity of their subsurface make foothills and overthrust areas attractive for new challenges. North and South America have interesting examples where giant fields have been discovered in such hostile environments for seismic activities. In mountainous thrust areas, the main issue is the distorting action of near-surface time anomalies on the seismic data due to a combination of rough topography and laterally changing near-surface conditions. Figure 1.1 shows a synthetic shot record that exemplifies near-surface-induced time distortions. The subsurface structure used in the modeling was based on characteristics frequently found in the Rocky Mountains area.

Accurate algorithms have been developed in the last few years to handle large dips. Those algorithms might be useless, however, if the topography and the near-surface complications are not properly taken into account during processing.

Land reflection data are often displayed and analyzed relative to different reference datums during the course of processing. Early in the processing sequence, the data reference level is changed from the recording surface to a floating datum that often follows a smooth version of the earth's surface. The floating datum is used in the common-midpoint (CMP) processing sequence through the stacking process, after which the data are moved to a final reference surface.

Although the data can be processed from a floating datum with special algorithms that can accommodate irregular and rugged geometry, traditionally seismic data are transferred to a flat, horizontal datum just before dip-moveout (DMO) and migration are performed. Most migration algorithms require input data from a flat surface for efficient performance and, more importantly, the data are interpreted from a flat, horizontal datum so as to tie with other data in a survey area. Historically, given difficulties in estimating accurate near-surface velocities required for deterministic wave-equation based solutions in the redatuming process (Berryhill, 1979), those time corrections have been treated as simple time shifts or elevation-static corrections. The assumptions behind the static corrections are that the near-surface time anomalies are attributable to variations in vertical raypaths (i.e., the surface-consistent statics assumption), and that no ray bending (via Snell's law) occurs at the base of the weathering layer (Wiggins et al., 1976). Underlying the surface-consistency assumption are three others: (1) the velocity of the weathering layer is much lower than that in the

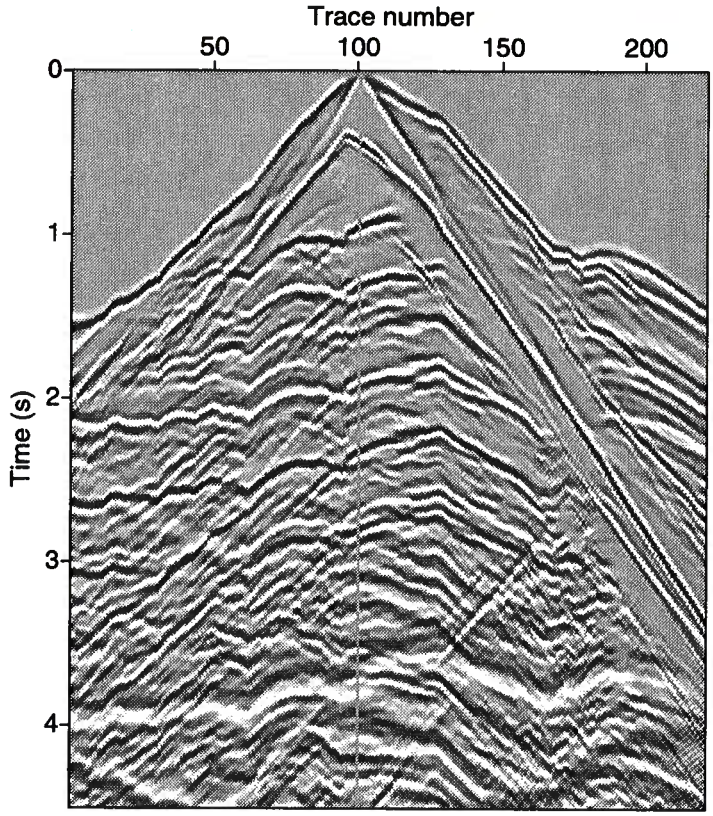

FIG. 1.1. Synthetic land shot gather showing near-surface-induced time distortions.

subweathering layer, (2) wave-theoretical influences on time anomalies can be ignored (Larner et al., 1996), and (3) source-receiver offset is small. In general, those assumptions are valid in regions of mild topography and slow near-surface velocity variations. However, in the presence of significant differences in elevation and more complicated velocity models, the surface-consistency and static assumptions become inaccurate, and more realistic methods might be required.

Unfortunately, a poorly appreciated aspect of data processing is the destructive action of using such vertical time shifts to perform datuming corrections (Berryhill, 1979, 1984; MacKay, 1994). Given the time-invariant nature of the static corrections, the moveout of the reflection and diffraction events can be seriously distorted. Those moveout distortions not only generate ambiguities in the velocity analysis process but also conspire against the success of other important wave-equation-based processing steps such as DMO and migration. To be able to represent the general behavior of the wavefield in the near-surface, a wave-equation-based method must be considered (see Figure 1.2).

Under these circumstances, there are two possible solutions to unraveling near-surface-induced distortions : (1) wave-equation-based redatuming as described by Berryhill (1979), and (2) migration algorithms that work directly from the irregular recording surface (Wiggins, 1984).

This study focuses on the applicability and limitations of both wave-equation-based and conventional static datuming techniques to deal with near-surface time anomalies under realistic conditions in which, near-surface velocities are poorly known. Furthermore, a simple wave-equation-based methodology for modeling near-surface time anomalies is tested on synthetic data. Moreover, nonconventional prestack imaging techniques are compared on an overthrust rugged terrain synthetic data from the Rocky Mountains area. Throughout this dissertation synthetic examples will be given that aim at drawing conclusions that are applicable to field data studies.

1.1 Previous work

A few techniques have been developed to process data from rugged terrain aiming to take proper account of the near-surface-induced time distortions. Assuming that the velocity of the near-surface can be estimated, one might compensate directly for the time distortions due to the weathering layers and the topography in the migration process or in a wave-equation datuming step (Berryhill, 1979, 1984; Yilmaz and Lucas, 1986). Wiggins (1984) proposed a Kirchhoff-type formulation to extrapolate and migrate data collected over an irregular surface. Reshef (1991) introduced an elegant finite-difference (FD) solution based on a simple phase-shift algorithm to deal with nonplanar reference data in the imaging process. Similarly, the "zero-velocity layer" migration technique (Beasley and Lynn, 1992) allows migration of data recorded on an irregular surface using conventional migration algorithms implemented to work from a horizontal reference surface. This migration approach was originally formulated to work with zero-offset data, but it can be extended to process prestack data.

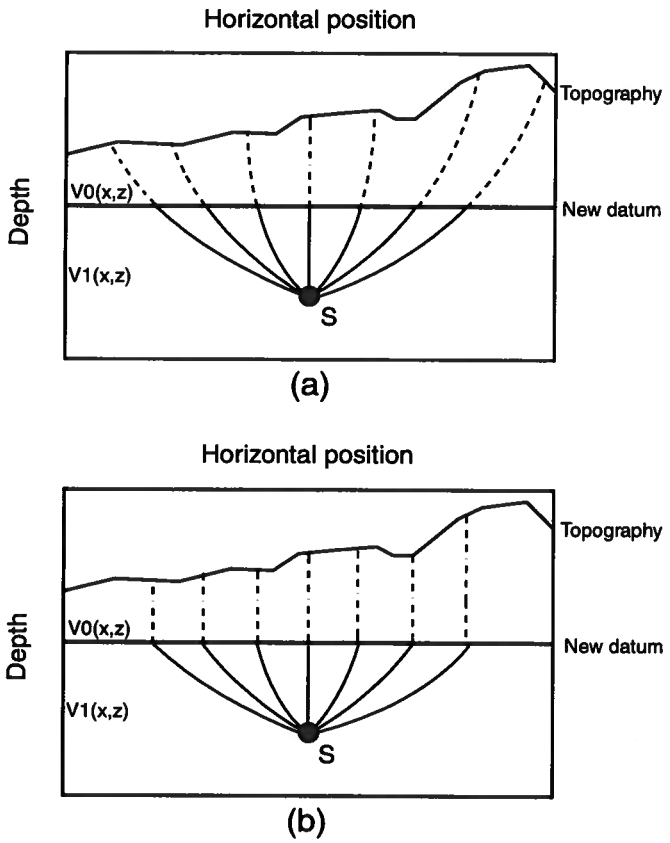

FIG. 1.2. (a) Ray-theoretical approach and (b) Elevation static correction method (after Zhu et al., 1995)

The "zero-velocity layer" scheme works on conventionally processed data that have static corrections applied and uses a particular modified version of the velocity model that includes a non-physical, zero-velocity layer between the irregular topographic surface and a datum level above that surface. Rajasekaran and McMechan (1995) offer a prestack, static-free processing approach to imaging of land data with complex topography.

In general, there are two possible approaches for including the near-surface information within the migration process: (1) with algorithms that incorporate the long-wavelength components of the near-surface time anomalies, performing migration from topography after stacking the data (Beasley and Lynn, 1992), and (2) with algorithms that work with prestack data including all the information (i.e., short- and long-wavelength components) of the near-surface structure in the migration-velocity field (Rajasekaran and McMechan, 1995).

Wave-equation-based datuming as described by Berryhill (1984) prepares data for a standard processing sequence, transferring the data recorded along an irregularly-sampled rugged surface to an ideal, regularly-sampled, horizontal datum. Berryhill (1979) analyzed the error in traveltime for dipping-reflector models using his wave-equation-based datuming technique and the simple static method. Shtivelman and Canning (1988) studied the limitations of the static datuming approach for zero-offset synthetic data and found analytic expressions for the error incurred as a result of that approximation. More recently, MacKay (1994) proposed an application of the zero-velocity layer concept to the datuming process: zero-velocity datuming.

Originally, wave-equation datuming, as part of a layer replacement scheme, was used in marine data to remove time distortions generated by the irregular water-bottom (Lynn et al., 1990; Yilmaz and Lucas, 1986). Layer replacement attempts to remove the nonhyperbolic near-surface time distortions by downward continuing data to a new reference level below the velocity anomalies, and then upward continuing to a horizontal surface using a homogenous replacement velocity. It works best where the near-surface velocity structure is well known, such as in marine data. Recent papers, however, have shown applications of this approach to land data as well, where information on the near-surface layer is generally more suspect (Bevc, 1993; Rajasekaran and McMechan, 1995; Schneider et al., 1995).

DMO is done routinely to eliminate the dip dependency of the stacking velocity in the presence of conflicting dips. Conventional DMO formulation assumes a horizontal recording surface for its derivation. In rugged terrain areas, however, this assumption is no longer valid, impairing DMO efficiency and benefits. Recently, Burke and Knapp (1994) pointed out that conventional DMO does not always improved data quality in areas with large topographic changes, as well as large lateral and vertical velocity gradients. To address this issue, Rodriguez et al. (1991) proposed an alternative DMO that handles near-surface time anomalies and rough topography.

As seen in this summary of the work done on imaging in areas of rugged terrain, some techniques in theory can accommodate, directly or indirectly, near-surface velocity structures within a seismic data processing sequence. In practice, however, those

techniques often fail to show satisfactory results due to difficulties in obtaining accurate estimates of the shallow-velocity model. Despite the importance of this subject, little work has been reported in the geophysical literature that systematically studies how errors in the near-surface velocity model compromise our ability to compensate for those associated time anomalies. This dissertation attempts to yield some insight about this issue by providing numerous synthetic examples that illustrate the problem.

1.2 Outline of the thesis

1.2.1 Wavefield-extrapolation operators for modeling and migration

In the next chapter, I review the derivation of wave-equation Kirchhoff datuming following the work done by Berryhill (1979), although some mathematical details are different. As a starting point, I consider the Kirchhoff approximation based on the Rayleigh II integral in three dimensions (Berkhout, 1985). Assuming 3-D propagation in a 2-D medium, I apply a stationary-phase analysis to find a wavefield-extrapolation operator that is independent of changes in the physical properties of the medium perpendicular to the seismic line direction (Bleistein, 1984).

Although in most of the synthetic examples included in this dissertation I use a nonrecursive Kirchhoff implementation of wave-equation datuming and migration, a short overview of recursive methods is provided (i.e., finite-difference wave-equation datuming). Furthermore, the benefits of a migration scheme that works directly from the recording surface are discussed. In Chapter 2, I also discussed general details of the computer implementation of the algorithms, including ray-tracing, operator aliasing control, and smoothing requirements for the velocity model.

1.2.2 Sensitivity of the datuming process to the near-surface velocity model

Kirchhoff datuming provides an accurate deterministic approach to unraveling near-surface-induced time distortions when the near-surface velocity model is known (Berryhill, 1979; Shtivelman and Canning, 1988). However, considering that even today our knowledge of the near-surface complexity is woefully lacking, it is pertinent to ask, what would happen to the datuming accuracy if the near-surface velocity model is poorly known. Also, which of the datuming algorithms would be less data distorting, in the presence of errors in the velocity field? Unfortunately, such errors are the case in practice; our estimates of the velocity field might be far from the true model (Bevc, 1994).

Chapter 3 addresses the above questions through demonstrations with synthetic data. In it, I undertake a sensitivity analysis of both a conventional static-estimation approach and Kirchhoff datuming to the near-surface velocity structure, on a model that exhibits rough topography and a simple subsurface structure. Improvement of the image of the subsurface is, of course, the driving force behind pre-processing steps that deal with the near-surface time anomalies. Therefore, I compare the robustness of

the two datuming approaches (i.e., Kirchhoff and static scheme) in terms of resulting imaging quality after prestack depth migration.

1.2.3 Modeling of near-surface time anomalies

Methods of residual-static corrections have long benefitted from the assumption that the near-surface-induced distortions are static and surface consistent. In spite of the success of these assumptions in the static-estimation process, those are just approximations to the true traveltime distortions (Larner et al., 1996). Therefore, to simulate more realistic near-surface time anomalies for testing of alternative residual static-estimation approaches, we need to go beyond the static and the surface-consistent assumptions.

Larner and Tjan (1995) proposed and tested with synthetic data an approach to estimating residual static corrections in structurally complex areas using prestack depth migration and multioffset modeling. For most of their tests, they considered the Marmousi data set (Versteeg and Grau, 1991) contaminated with randomly generated, surface-consistent static time shifts. Land data, however, typically suffer from time distortions that may be neither surface-consistent nor static, and will certainly contain variations along the surface with wavelengths longer than the cable length. In Chapter 4, I introduce a simple methodology for modeling time anomalies using a combination of wave-equation datuming and elevation static corrections. I also provide synthetic examples of the methodology using a simple model and the Marmousi data set.

1.2.4 Imaging in areas of rough terrain

Rugged terrain combined with a complex subsurface velocity model constitutes one of the most challenging imaging situations to seismic data processing. Conventional CMP processing has problems dealing with data acquired in areas with those characteristics. Most of the assumptions on which conventional processing is based are no longer valid under those circumstances. In Chapter 5, I compare different imaging techniques for a Rocky Mountain overthrust model. Those imaging approaches include prestack depth migration from topography, and a combination of prestack datuming (i.e., finite-difference and Kirchhoff approaches) and prestack depth migration from a flat surface. The modeled data set was provided by Dr. Xianhuai Zhu, of Union Pacific Resources Company. I also study the sensitivity of the datuming approaches to the velocity model following a methodology proposed by Versteeg (1993). Results of nontraditional approaches such as tomo-datuming and tomo-statics (Zhu et al., 1992, 1995) are also provided.

1.3 Contributions of this work

- I have analyzed the applicability and limitations of both wave-equation-based and conventional datuming techniques to deal with near-surface time anomalies, and the circumstances in which wave-equation-based methods would be

preferred over the traditional static approach. Several papers (Berryhill, 1979; Shtivelman and Canning, 1988; Bevc, 1993) have shown the benefits and the accuracy of the wave-equation datuming algorithms over the static approach for continuation of data through a near-surface velocity field. Little systematic analysis, however, has been done to estimate the error patterns that one should expect from the two approaches in the presence of inaccuracies in the near-surface velocity model.

- I have used a simple methodology to model realistic time anomalies using a combination of wave-equation datuming and elevation statics. In tests of algorithms designed to compensate for time distortions associated with the near-surface under the assumption of surface-consistency, the model data should contain time anomalies that are wave-theoretic as opposed to surface-consistent-static time shifts.

- I have compared the accuracy of different imaging techniques using an overthrust model based on the general characteristics of the structural geology and topography of the Rocky Mountains area. The results of this comparative analysis are aimed at learning which imaging approach is best suited to dealing with such an overthrust complexity in the presence of rough terrain.

I have concluded from these studies that although wave-theoretic downward continuation to a chosen datum is preferable to simplistic vertical-path static correction of the near-surface-induced time distortions, this holds only when the near-surface velocity model is known accurately. Where the near-surface is not so well known, conventional statics correction may actually be preferable. Wave-equation datuming (upward or downward) and thus layer replacement to or from an irregular topographic surface allow us to enhance efficiency in the study of the influence of the near-surface irregularities on imaging of subsurface structure in otherwise costly model data sets.

Chapter 2

WAVEFIELD-EXTRAPOLATION OPERATOR FOR MODELING AND MIGRATION

Modeling and migration are two closely related techniques. Modeling involves forward extrapolation that simulates the wave propagation process. Migration, however, not only involves backward extrapolation to unraveling the wavefield propagation but also an imaging step. Removing the imaging step from the migration process results in the useful wave-equation datuming process. Seismic datuming is the wavefield extrapolation process that transforms seismic measurements from the actual data acquisition surface (old datum) to a simulated recording surface (new datum) down in the subsurface. In practice, the conventional datuming procedure for nonzero-offset data can be summarized in three main phases: (1) downward extrapolation of the receivers to the new datum, (2) reordering of the data from common-shot gathers to common-receiver gathers, and (3) downward extrapolation of the sources to the new datum, using reciprocity (see Figure 2.1).

Wave-equation datuming could be formulated as a boundary value problem following a Kirchhoff integral scheme (i.e., summation approach) or directly by considering a finite-difference (FD) representation of a simplified version of the wave-equation (MacKay, 1994). Berryhill (1979) considered a poststack wave-equation datuming approach using a Kirchhoff integral formulation and later generalized the method to the prestack case (Berryhill, 1984). Considering that the goal is to extrapolate the seismic data from one datum to another without computing the wavefield at intermediate steps, the most efficient choice seems to be a nonrecursive Kirchhoff extrapolation method. Also, the irregular geometries that must be used in rugged terrain areas make the Kirchhoff formulation a convenient way to extrapolate data.

To remove the distorting action of the overburden by extrapolating the recorded seismic wavefield from one datum to another, one needs to know the velocity field between the two reference surfaces. In the marine case, where the near-surface time anomalies are associated with the water-bottom topography, the overburden model can be estimated simply by using $f - k$ zero-offset migration. The migrated section with water-velocity delineates the water-bottom shape (Berryhill, 1986). For land data, however, the estimation of the near-surface velocity model is far more complicated than that for its marine analog. Traditionally, first-arrival refraction analysis has provided an approximate and fast option for estimating the low-velocity layer model. Schneider et al. (1995) presented one of the few published applications of wave-equation datuming in land data. They derived the near-surface velocity model using a standard first-arrival refraction-analysis method. A better velocity model estimation method, however, is turning-ray tomography. Stefani (1995) provides interesting

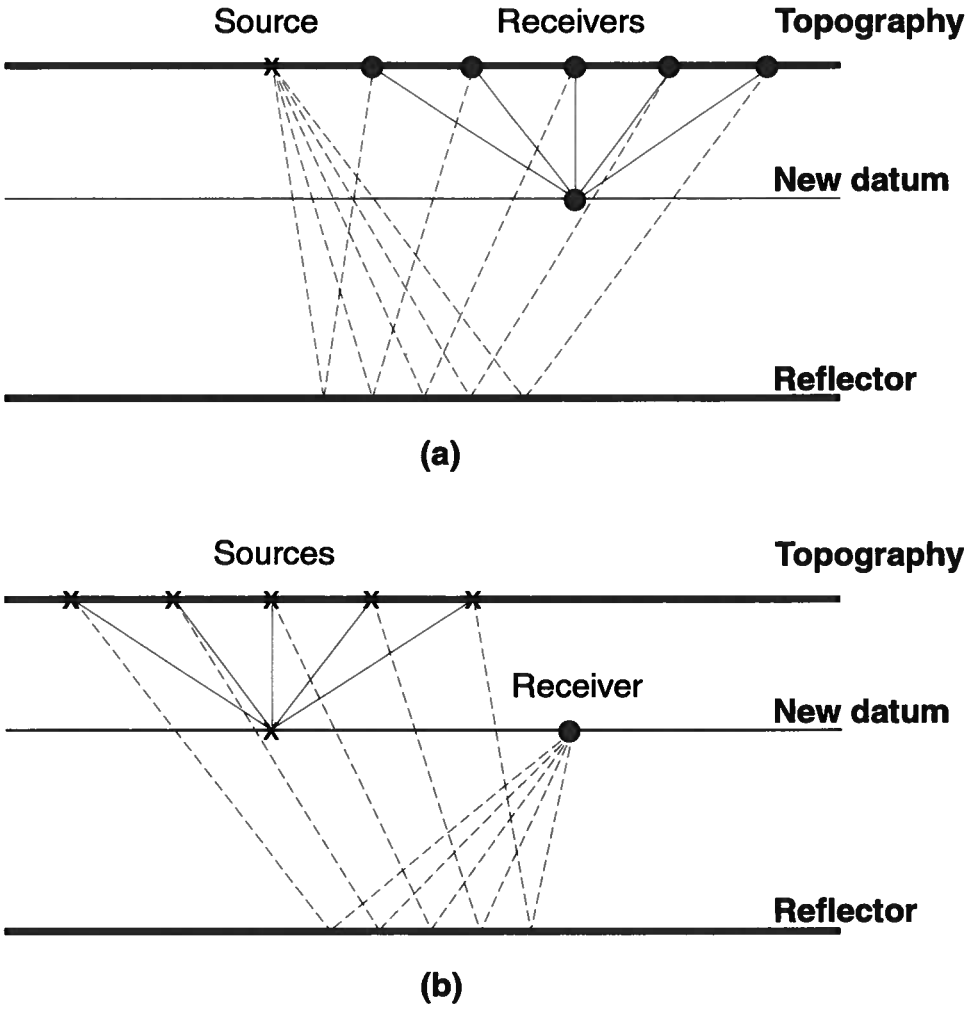

FIG. 2.1. Wave-equation datuming for nonzero-offset data : (a) downward continuation of receivers and (b) downward continuation of shots.

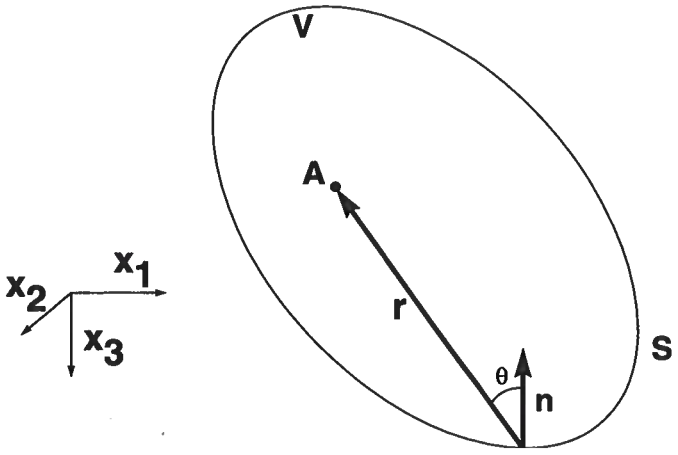

FIG. 2.2. Pressure field inside a volume V, bounded by a surface S, in the derivation of the Kirchhoff integral.

synthetic data examples of the application of turning-ray tomography to estimation of near-surface velocity models. Despite these advances, wave-equation datuming has primarily been used on marine data, largely because the estimation of low-velocity layer model remains considerably more difficult for land data.

2.1 Kirchhoff-datuming formulation: Theoretical overview.

The Kirchhoff integral formulation is derived from Green's theorem by relating a pressure-field P at an interior point A of a closed surface S (see Figure 2.2) to observations of the wavefield on the surface S, as follows

$$P(r_A,\omega) = \zeta(r_A) \oint_S [P\nabla G - G\nabla P]\cdot \mathbf{n}\, dS\ , \tag{2.1}$$

$$\zeta(r_A) = \begin{cases} -\frac{1}{4\pi} & r_A \ \epsilon \text{ interior} \\ -\frac{1}{2\pi} & r_A \ \epsilon \ S \\ 0 & \text{otherwise} \end{cases}$$

where G is a Green's function that satisfies the acoustic wave-equation, and $\mathbf{n}$ is the unit vector normal to S. Both scalar fields, P and G, are functions of spatial coordinates $r' = (x_1, x_2, x_3)$ and temporal frequency ω.

Figure 2.3 illustrates the geometry applicable to the characteristics of the seismic experiment in the analysis of equation (2.1). The closed surface S consists of surfaces S_0 and S_1. Docherty (1991a) proved that the contribution of surface S_1 to any interior point on S is zero by using a stationary argument. In general, we will need to know only one wavefield, $P(r',\omega)$ or its derivative in the direction normal to the surface S_0 (Cauchy conditions), in order to evaluate the integral of equation (2.1). Once the boundary condition is established, equation (2.1) is solved by taking its limit as the

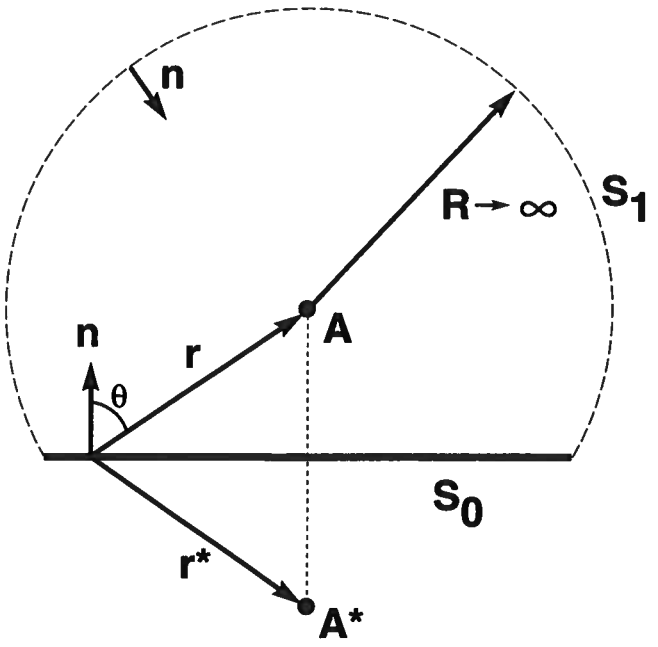

FIG. 2.3. Closed surface S for the derivation of the Rayleigh II integral (after Berkhout, 1985).

observation point r_A approaches the surface S. If a Green's function is found that is zero everywhere on the integration surface, the normal derivative of $P(r',\omega)$ will not be needed. When the undulations of the recording surface are small over a wavelength, such a Green's function (Wiggins, 1984) can be approximated by

$$G = \frac{e^{-ikr}}{r} - \frac{e^{-ikr^*}}{r^*} , \tag{2.2}$$

$$\frac{\partial G}{\partial \eta} = 2\frac{\partial}{\partial \eta} G_{fs} , \tag{2.3}$$

$$G_{fs} = \frac{e^{-ikr}}{r} \tag{2.4}$$

where G_{fs}, is the free-space Green's function (Scales, 1994), $r = \mid r' - r_A \mid$, is the distance between location $(x_1, x_2, x_3)_A$ and a point on the surface S with coordinate r', $r^* = \mid r' - r_{A^*} \mid$, is the distance between location $(x_1, x_2, x_3)_{A^*}$ and a point on the surface S with coordinate r', $k = \omega/c$ and c is the velocity of the homogeneous medium. This choice of Green's function, which vanishes on surface S_0, eliminates the normal derivative of $P(r',\omega)$, providing the Rayleigh II integral (Scales, 1994),

$$P(r_A,\omega) = \frac{1}{2\pi}\int_{\xi_1} P(r',\omega) \int_{\xi_2} \frac{\partial r}{\partial \eta}\frac{(1+ikr)}{r^2} e^{-ikr} d\xi_2 \, d\xi_1 , \tag{2.5}$$

$$r = \sqrt{(x_1 - \xi_1)^2 + (x_2 - \xi_2)^2 + {x_3}^2} \,,$$

where ξ_1 and ξ_2 are the integration variables in the x_1- and x_2- directions, respectively (see Figure 2.2). A rigorous discussion on the derivation of equation (2.5) can be found on Berkhout (1985).

In the derivation of his approach to wave-equation datuming, Berryhill (1979) started with the time-domain representation of the Rayleigh II integral, then assumed that there was no change in the physical properties of the medium in the ξ_2- direction. To incorporate the wavefield contribution of that ξ_2- direction in the calculation, he convolved the data with a time-domain shaping operator based on general geometric characteristics of the wavefield. In this work, I specialize the 3-D extrapolation equation (2.5) to the two-and-one half (2.5-D) dimensional geometry by performing a stationary-phase calculation on ξ_2 under the assumption that the data $P(r', \omega)$ are independent of ξ_2 (Bleistein, 1987). This assumption is justified by considering that the phase function associated with the data $P(r', \omega)$ exhibits slower variations compared to that of the phase of the Green's function (see Figure 2.1a).

Integrals of the form

$$I(\lambda) = \int f(\eta) e^{i\lambda\Phi(\eta)} d\eta \,, \tag{2.6}$$

are approximated asymptotically (Bleistein, 1984), when the parameter $\lambda \to \infty$, by

$$I(\lambda) \sim \left[\frac{2\pi}{|\lambda||\Phi''(\eta_0)|}\right]^{1/2} f(\eta_0) e^{i\lambda\Phi(\eta_0) + i\pi/4 \mathrm{sgn}\lambda \mathrm{sgn}\Phi''(\eta_0)} \,, \tag{2.7}$$

where η_0 is the stationary point, the point where the derivative of the phase Φ is zero.

Here, the goal is to obtain an analogous asymptotic expansion for the two-and-one-half-dimensional extrapolation formula. For the integral in equation (2.5), the phase function to be considered is

$$\begin{aligned} \Phi &= r \,, \\ r &= \sqrt{(x_1 - \xi_1)^2 + (x_2 - \xi_2)^2 + {x_3}^2} \,, \end{aligned} \tag{2.8}$$

with formal large parameter $\lambda = -\omega/c$. The first derivative of the phase function Φ with respect to ξ_2 is given by

$$\frac{\partial\Phi}{\partial\xi_2} = \frac{\xi_2 - x_2}{r} \,, \tag{2.9}$$

which is zero when $\xi_2 = x_2$. The phase is stationary when the its first derivative is zero. That is, in the two-and-one-half-dimensional survey, the dominant contribution occurs directly below the observation point. Also required in the stationary-phase

calculation is the second derivative of the phase Φ with respect to ξ_2 evaluated at the stationary point,

$$\Phi'' = \frac{\partial^2 \Phi}{\partial \xi_2^2} = \frac{1}{r} \ , \quad \xi_2 = x_2. \tag{2.10}$$

There is only one stationary point. To complete the stationary-phase calculation, I must know the sign of the second derivative, Φ'', at $\xi_2 = x_2$. From equation (2.10),

$$\text{sgn}\left[\frac{\partial^2 \Phi}{\partial \xi_2^2}\right] = 1. \tag{2.11}$$

These results allow us to state the stationary-phase approximation of equation (2.5) as,

$$\begin{aligned} P(r_A, \omega) &= \sqrt{\frac{c}{2\pi}} \int_{\xi_1} P(r', \omega) \frac{\partial r}{\partial \eta} \frac{(1 + i\omega r/c)}{\sqrt{|\omega|} r^{3/2}} e^{-i\omega r/c - i\pi/4 \text{sgn}\omega} d\xi_1 \ , \\ r &= \sqrt{(x_1 - \xi_1)^2 + {x_3}^2} \ . \end{aligned} \tag{2.12}$$

Using the shorthand on the previous equation,

$$i\text{sgn}\omega e^{-i\pi/4\text{sgn}\omega} = e^{i\pi/4\text{sgn}\omega} = \sqrt{\frac{i\omega}{|\omega|}} \ . \tag{2.13}$$

I end up with the following 2.5-D wavefield extrapolation formula, which permits downward continuation of upgoing waves and upward continuation of downgoing waves,

$$P(r_A, \omega) = \frac{1}{\sqrt{2\pi c}} \int_{\xi_1} \frac{P(r', \omega)}{\sqrt{r}} \frac{\partial r}{\partial \eta} \sqrt{i\omega} \left[1 + \frac{c}{i\omega r}\right] e^{-i\omega r/c} d\xi_1 \ . \tag{2.14}$$

For upward continuation of upgoing waves and downward continuation of downgoing waves, I use the conjugate transpose of the equation (2.14); that is,

$$P(r_A, \omega) = \frac{1}{\sqrt{2\pi c}} \int_{\xi_1} \frac{P(r', \omega)}{\sqrt{r}} \frac{\partial r}{\partial \eta} \sqrt{-i\omega} \left[1 - \frac{c}{i\omega r}\right] e^{i\omega r/c} d\xi_1 \ . \tag{2.15}$$

Equation (2.15) clearly shows how one would treat integration over a nonplanar acquisition surface. The surface geometry influences three features in the previous equation. The delayed-time, r/c, depends on the surface geometry through r; $1/\sqrt{r}$ and the obliquity factor $\partial r/\partial \eta$ also depend on the surface geometry and are weighting factors in the integration process. The third component is the surface element, $d\xi_1$, which also contributes to the amplitude calculations.

In equation (2.15), the first term within brackets is associated with the far-field solution and the second term is related to the near-field solution. In practice, the second term is neglected (i.e., "far-field approximation") to gain computational efficiency. This equation could be compared to equation (A-1) in Berryhill (1979).

My implementation of Kirchhoff datuming is based on the far-field approximation of equation (2.15), that means that I consider only the far-field solution in the wavefield extrapolation process.

2.2 Recursive versus nonrecursive extrapolation

Basically, there are two general approaches to wavefield extrapolation: (1) recursive and (2) nonrecursive (see Figure 2.4). In a nonrecursive extrapolation scheme, the wavefield is propagated from the surface to the target points in one step. This extrapolation operator must contain the complete propagation action of the overburden structure that needs to be taken into account. Usually, some form of ray-tracing modeling is used to get the extrapolation operator. Examples of this extrapolation procedure can be found in Bleistein et al. (1987), and Berryhill (1979). My implementation of Kirchhoff extrapolation operators follows a nonrecursive approach combined with a paraxial ray-tracing algorithm. This approach is efficient and accurate for the purpose of this study.

In recursive extrapolation approaches, the wavefield can be propagated either from interface to interface or, in general, from one extrapolated output level to the next. This approach uses local velocities so lateral velocity variations can be handled properly. FD and phase-shift forms of extrapolation operator are examples of a recursive approach while Kirchhoff-type operators can be formulated as either recursive or nonrecursive extrapolation operators (Bleistein et al., 1987; Berkhout, 1985).

Recently, Bevc (1995) proposed a pseudo-recursive Kirchhoff migration scheme to increase imaging quality for the Marmousi data set. He obtained better images with his pseudo-recursive migration than those generated with conventional Kirchhoff migration using traveltimes calculated with a FD eikonal solver. This layer-stripping kind of migration combines Kirchhoff wave-equation datuming and Kirchhoff migration. The simplest nonrecursive Kirchhoff migration works with only one propagation path from the surface to the image point, therefore multiple arrivals cannot be accommodated. By contrast, the pseudo-recursive migration approach considers many propagation paths, thus increasing the control over multiple arrivals as in other recursive approaches. The layer-stripping migration could treat topographic variations and near-surface time anomalies implicitly in the first datuming step.

2.3 Zero-velocity layer datuming: Finite-difference approach

The "zero-velocity layer" concept was introduced by Beasley and Lynn (1992). Initially this concept was proposed as a mathematical trick for doing migration from irregular surfaces using conventional migration algorithms that work from a horizontal datum level. Subsequently, MacKay (1994) applied the zero-velocity concept to the datuming process. The idea behind this approach is to take advantage of the action of each of the terms involved in the FD formulation for depth extrapolation proposed by Claerbout (1985). This formulation considers two elements: (1) the diffraction term,

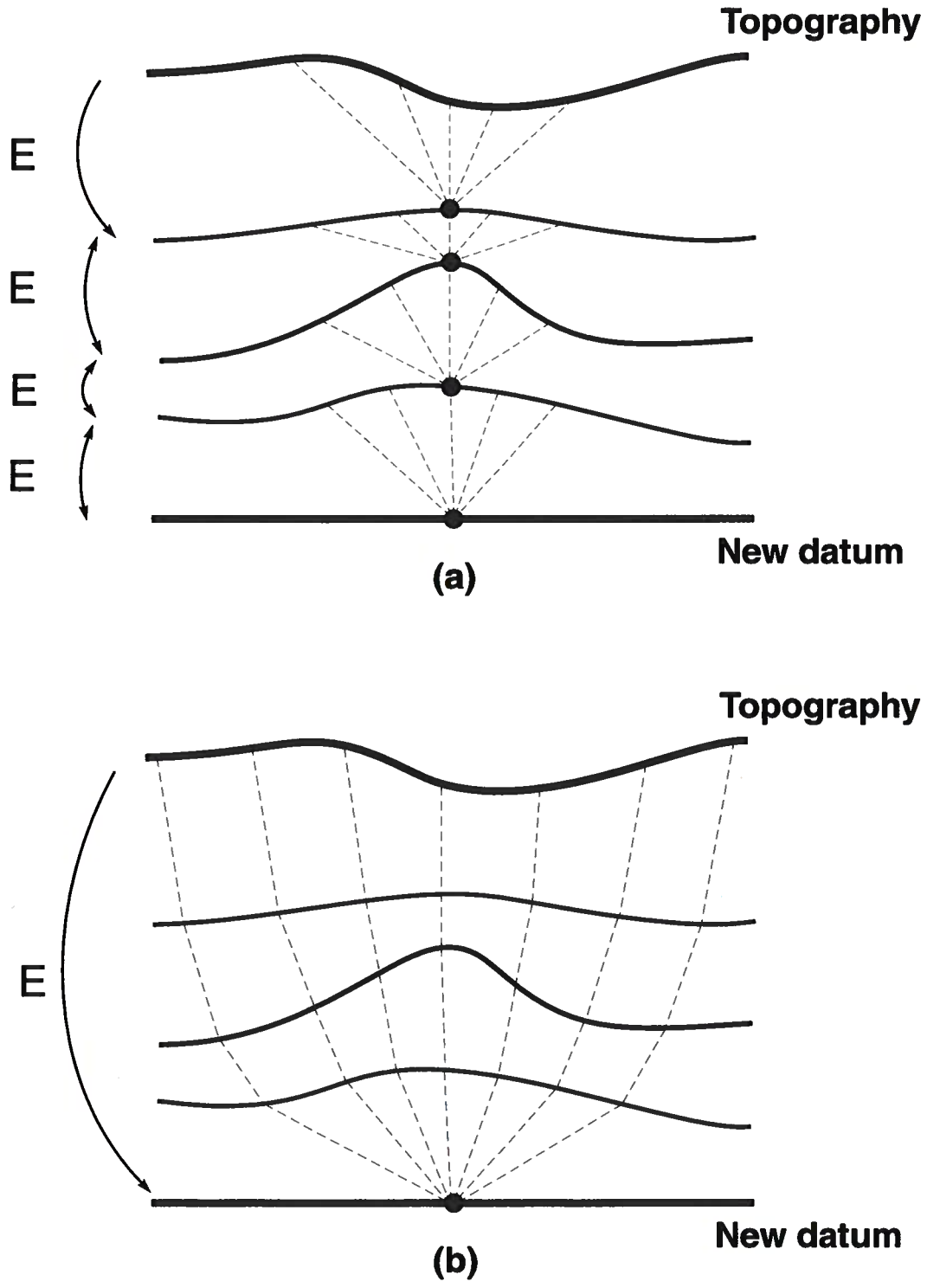

FIG. 2.4. Wavefield extrapolation : (a) recursive and (b) nonrecursive approach

its action being to collapse diffractions, and (2) the thin-lens term, which takes into account lateral velocity variations by differentially time-shifting data traces.

The "zero-velocity layer" scheme works on conventionally processed data that have had static corrections applied to transfer data to a flat datum at or above the highest elevation along the recording surface. Unlike conventional algorithms (i.e., migration or datuming), the velocity field between the flat datum and the acquisition surface is set to zero for the diffraction term. The thin-lens or time-shifting term, however, considers the same replacement-velocity field used in the elevation-static calculations. Therefore, while working in the zero-velocity layer, the extrapolation operator reverses the static corrections applied but does not collapse diffractions or propagate waves laterally. Once the process encounters the nonzero-velocities below the recording surface, the diffraction term turns on and the full migration or datuming action begins. The velocity field beneath the true acquisition surface must represent the best knowledge of the subsurface geology.

This approach gives an elegant and simple way to correct wavefield distortions that arise in traditional static datuming techniques. This scheme, however, not only requires the application of static corrections before migration or datuming, but also includes a non-physical, zero-velocity layer that impairs the use of the computationally attractive phase-shift algorithms (Reshef, 1991).

In this study, I use a FD datuming as a benchmark to assess the quality of my Kirchhoff datuming implementation. The FD datuming was performed using the ProMAX software of Landmark Advance Geophysical Division. Its implementation is based on that of the zero-velocity datuming of MacKay (1994). In all the applications, I used a one-way 70 degree explicit FD wave-propagation algorithm even though normal practice suggests that a one-way 30 degree operator would be sufficient. This suggestion is based on the belief that near-surface velocity tends to be slow and thus most of the energy travels vertically. Normally, this consideration is true; however, in overthrust areas this presumption might no longer be valid.

2.4 Kirchhoff prestack depth migration from topography

The Kirchhoff migration approach is attractive as a seismic exploration imaging tool because of its potential for flexibility in handling input data and for computational efficiency. In contrast to full-waveform, finite-difference extrapolation techniques, which are constrained to geometries of individual physically- realizable experiments (i.e, common-shot gathers), Kirchhoff methods can process selected input data from any arbitrary gather domain (i.e., common-offset gathers) according to a particular processing goal. One major advantage of Kirchhoff migration is the ability to image subsurface points independently of one another (i.e., target-oriented migration). Another important attribute of the Kirchhoff migration is its ability to accommodate irregular grid spacing or rough topography. Kirchhoff migration involves an integration (in practice, a discrete summation) of a wavefield over the acquisition surface. Irregular sampling of the wavefield over the recording surface is readily handled by

the discrete sum.

The migration from the acquisition surface incorporates the topographic and near-surface velocity information directly into a fully prestack approach. Thus, the time corrections associated with near-surface are applied implicitly during migration rather than as an explicit, separate step (McMechan and Chen, 1990). Furthermore, this approach accounts for both normal- and dip-moveout as migration is performed. Moreover, the same velocity field is required for statics, moveout corrections, and migration. This particular characteristic adds a complete internal consistency to the process. That same consistency, however, is the primary drawback of the approach in practice. All near-surface anomalies (topographic and velocity variations) must be included in the velocity distribution used in the migration process. Of interest is the degree of precision required in the velocity field to obtained a solution that is competitive in quality with that obtained from conventional approaches.

Migration from the acquisition surface could be implemented using a 2D FD scheme (McMechan and Chen, 1990; Reshef, 1991) or a Kirchhoff-integral formulation (Wiggins, 1984; Ellis and Kitchenside, 1989). Considering the robustness of the integral formulation in handling land data, which typically involve nonuniform acquisition geometries, I follow a Kirchhoff approach.

The Kirchhoff migration can be represented by

$$U(x,z) = \int_{\xi} d\xi \; W(x,z;\xi) \; D(\xi, t_s + t_r) \quad , \tag{2.16}$$

where,

$U(x,z)$	output seismic section at grid point (x,z),
ξ	surface position parameter,
$W(x,z)$	amplitude weighting factor,
$D(\xi, t_s + t_r)$	filtered version of the input data,
t_s	traveltime from shot x_s to the point (x,z),
t_r	traveltime from receiver x_r to the point (x,z).

The weighting factor $W(x,z)$ includes spherical-spreading corrections as well as the obliquity factor, a function of the incident angle at each source and receiver (see Figure 2.5).

My migration code is an extension of **sukdmig2d.c** developed by Dr. Zhenyue Liu. This code is part of the Seismix Unix system (SU) (Cohen and Stockwell Jr., 1996). The new version of **sukdmig2d.c** allows migration of data directly from a surface having variable topography. This implementation should be considered a kinematic prestack depth migration rather than a true-amplitude one. The obliquity factor and spherical spreading parameters used within the integration process as weights are estimated based on a reference $v(z)$ velocity model. The essential steps in the prestack depth migration algorithm are shown in Figure 2.6.

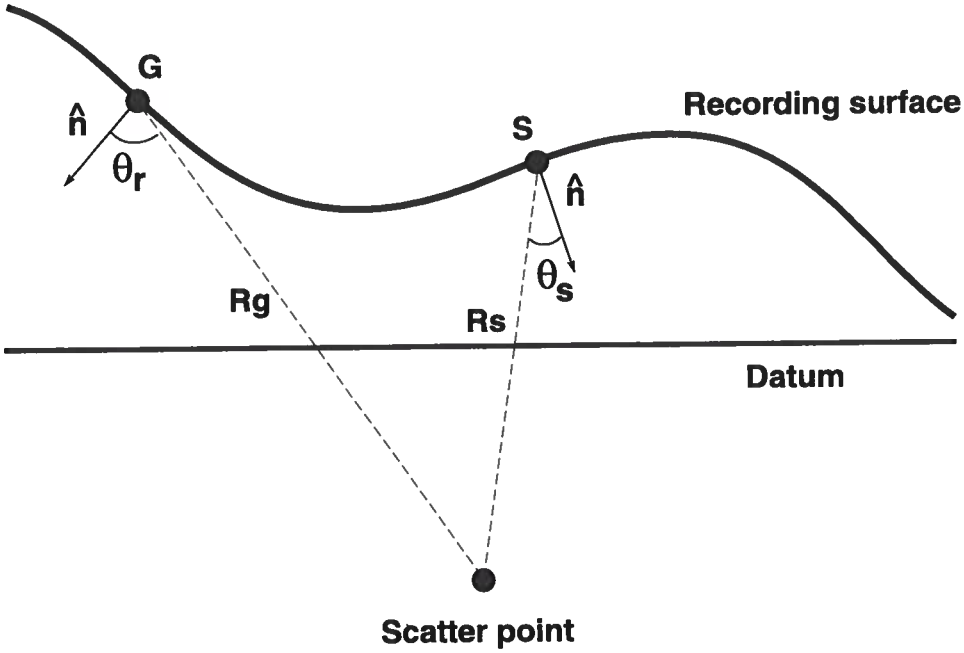

FIG. 2.5. Migration from recording surface.

2.5 Computer implementation of the Kirchhoff approach

2.5.1 Ray-tracing

Traveltime computation is the core of every Kirchhoff-type implementation. The various approaches to address traveltime estimation in $v(x, z)$ media (Beydoun and Keho, 1987; Nichols, 1994) fall into two commonly used methods: ray-tracing and FD eikonal solvers. The ray-tracing algorithm calculates traveltimes, amplitudes and phase on each ray. Since the rays usually do not pass through output grid points, a step of interpolation or extrapolation is required to obtain traveltime estimations at grid locations. Unlike ray-tracing algorithms, the FD eikonal solvers calculate traveltimes and amplitudes at output grid locations. In the presence of multiple-arrivals (i.e, caustics), most FD eikonal solvers calculate only first-arrival traveltime, which often may not be the time of the most energetic arrival. Under these circumstances, as pointed out by Geoltrain and Brac (1993), the first-arrival traveltimes do not yield satisfactory results in the migration process. The first-arrivals in such cases do not characterize the timing of significant reflection energy in places below complex velocity overburden.

The computational cost of traveltime calculation dominates Kirchhoff implementations. Therefore it is essential to fine tune the ray-tracing step to achieve a good balance between speed and accuracy. To increase efficiency in this process, it is wise to generate traveltime tables at specific source locations on the surface of the area of interest. Later, if required, values in those tables could be interpolated on the

Pseudo-code for Kirchhoff prestack depth migration

```
Initialization:
Read input traces and parameters
Compute reference traveltimes, angles, and anti-aliased filter parameters
For each seismic trace {
        Interpolate traveltimes to source/receiver positions
        Filter the trace (for integration and half-differentiation)
        Compute amplitude weighting factor and anti-aliasing filter
        Interpolate traveltimes and amplitudes along x axes
        For each lateral position {
                Interpolate traveltimes and amplitudes along z axes
                Sum amplitudes at each depth sample
        }
}
Scale and output migrated section
```

FIG. 2.6. Prestack depth migration algorithm

fly to estimate traveltimes in shot/receiver positions within the migration process. Furthermore, to avoid the calculation of traveltimes and amplitudes on the entire model, the interpolation process could be done in two stages. First, one could interpolate between the source or receiver positions. Assume that the traveltime tables $\tau(x, z; x_{s1})$ and $\tau(x, z; x_{s2})$ from sources x_{s1} and x_{s2} to subsurface positions (x, z) are available. To estimate traveltime tables from sources located at intermediate position between x_{s1} and x_{s2}, one could use the following linear relation,

$$\tau(x, z; x_s) = \alpha\, \tau(x, z; x_{s2}) + (1 - \alpha)\, \tau(x, z; x_{s1}) \ , \tag{2.17}$$

where x_s is the new source position $(x_{s1} < x_s < x_{s2})$, and $\alpha = (x_s - x_{s1})/(x_{s2} - x_{s1})$. In a $v(x, z)$ medium, the interpolation error is a function of $\partial v/\partial x$, and higher derivatives. Since errors in the interpolation procedure augment with increasing magnitudes of these derivatives, interpolation might be risky in the presence of strong lateral velocity variations (Liu, 1993). To overcome this problem, one could interpolate a traveltime perturbation rather than the true one. The traveltime perturbation tables are estimated based on a reference velocity model, $v(z)$ and the true velocity model, $v(x, z)$. The reference velocity model represents a laterally smoothed version of the true velocity model. Therefore, the traveltime perturbation tables are calculated by

subtracting the reference traveltime table from the total traveltimes tables. The reference velocity model is also used in the calculation of the weighting parameters for the integration process and the slowness vector used in the design of the anti-alias filter. In a $v(z)$ medium, the interpolation scheme used is exact, considering that the traveltimes are invariant for lateral reference shift; that is for any horizontal displacement h,

$$t(x+h, z; x_s+h) = t(x, z; x_s) \tag{2.18}$$

The second interpolation stage is done between grid points within the traveltime functions. Usually, the traveltime tables are built using a coarse grid, and, later in the process, those tables are interpolated into a finer grid to preserve resolution in the wavefield extrapolation.

In my Kirchhoff implementations, I use paraxial ray-tracing to generate traveltime functions. This technique uses local approximation of the wavefront given by the dynamic ray-tracing equations to extrapolate traveltimes and amplitudes at receiver locations in the vicinity of the central rays. The traveltime extrapolation in the vicinity of a central ray, however, is sensitive to instabilities in the dynamic parameters. Therefore, to get stable and accurate results with this algorithm, smooth velocity models are usually required. In the next section, I provide some details of the smoothing technique used in this development. As with all ray-based methods, there are shadow-zones where no geometric ray can be found. To circumvent that problem, the ray-tracing code uses a FD eikonal solver to fill up the shadow-zones in the traveltime tables. Since reasonable accuracy is obtained with relatively few rays, the paraxial ray-tracing approach is computationally efficient. The paraxial ray-tracing algorithm, implemented as shown in Figure 2.7, was developed by Dr. Zhenyue Liu, and I have extended it to handle variable topography.

2.5.2 Smoothing of the velocity field

In general, ray-tracing algorithms are sensitive to abrupt changes in the velocity model. Paraxial ray-tracing method is no exception, requiring a smoothed velocity model to give accurate amplitudes and traveltimes. The Paraxial ray-tracing, which offers an efficient means for extrapolating amplitudes and traveltimes to receiver points in the vicinity of a central-ray, is based on local approximations of the wavefront curvature. These approximations, however, depend upon the size of the curvature of the raypath; the smaller the curvature, the better the quality of the raypath. Some smoothing algorithms are based on windowed-averaging operators. Other smoothing approaches consider circular bell-shaped operators such as that used by Versteeg (1993) in his migration sensitivity analysis. In this work, I use a velocity-smoothing technique based on damped least-squares developed by Liu (1993). This approach is based on the observation that the curvature of the raypath determines the stability of the traveltime calculation. Liu (1993) showed that the curvature of the raypath could be given as a function of the first derivatives of the velocity field with respect to both spatial variables. Then, he proposed a scheme that minimizes

Pseudo-code for paraxial ray-tracing

```
Initialization:
Read velocity model and parameters
For each specified shot position {
        Restrict the velocity model
        For each shooting angle {
                Trace the central ray
                Estimate traveltimes in the vicinity of the central ray
        }
        output traveltime for this source position
}
```

FIG. 2.7. Paraxial ray-tracing algorithm

in the least-square sense, a weighted sum of the deviations between the true velocity model and the smoothed one, attenuating the first spatial derivatives of the velocity structure. Furthermore, to minimally distort traveltimes, the smoothing operation is performed on the slowness model. Therefore, conversion of velocity to slowness is done as the first step, then the smoothing procedure is applied, followed by a conversion of slowness back to velocity.

2.5.3 Control of operator aliasing

The Kirchhoff method implies an amplitude summation along a traveltime curve that is the trajectory of the migration operator. For a constant background, this curve is defined by the double-square-root (DSR) diffraction traveltime equation. The DSR equation describes downward continuation of both shots and receivers into the earth (Claerbout, 1985). When the summation curve is too steep for the spacing interval and frequency content of a given seismic trace, a distortion called operator aliasing arises. This phenomenon has the same characteristics as that observed in data acquisition when the group interval is too large for the frequency content and dips present in the seismic survey. Operator aliasing, however, is different from and independent of that data aliasing.

To avoid ambiguities in the summation process, one needs to augment the number of time samples in the estimation of a trace contribution as the slope of the operator increases. Berryhill (1979) used a running-average operator of length proportional to the difference in traveltime of adjacent points in the integration process. The average operator generates a constant sample interval along the summation surface by

filtering out the high-frequency component of the trace contributions associated with the steepest parts of the operator.

In my implementation of wavefield extrapolators, I use an algorithm proposed by Lumley et al. (1994). They use an N-point triangle filter to anti-alias the migration operator. In principle, this approach locally low-pass filters the seismic data to fulfill the following sampling criterion,

$$f_{max} \leq \frac{1}{2\Delta T} = \frac{1}{2(\partial t/\partial x)\Delta x} \ , \tag{2.19}$$

where ΔT is the traveltime difference along the migration operator between adjacent traces, $\partial t/\partial x$ is the local slope of the operator at the point where the trace intercepts the operator, Δx is the trace spacing and f_{max} is the maximum unaliased frequency. The z-transform representation of this N- point triangle filter is

$$g(z) = \frac{-z^{-k-1} + 2 - z^{k+1}}{(k+1)^2(1-z)(1-z^{-1})} \ , \tag{2.20}$$

where the length of the triangle filter is $N = 2k + 1$. In the frequency domain, the amplitude spectrum of the filter has notches at the frequencies,

$$f_n = \frac{\omega_n}{2\pi} = \frac{n}{(k+1)\Delta t} \ , \quad n = 1, 2, 3, ... \tag{2.21}$$

To design the length of the filter, Lumley et al. (1994) equate the desired maximum unaliased frequency, f_{max}, expressed by equation (2.19), to the first notch given by equation (2.21). Therefore, the optimum filter length has to satisfy the following inequality:

$$N \geq max \left[4(\frac{\partial t}{\partial x})\frac{\Delta x}{\Delta t} - 1, 1 \right] \tag{2.22}$$

Originally, this anti-alias filter was used for 3-D seismic migration; however, it is applicable to other Kirchhoff space-time operators such as wave-equation datuming, DMO, and NMO corrections.

Chapter 3

SENSITIVITY OF THE DATUMING PROCESS TO THE NEAR-SURFACE VELOCITY MODEL

3.1 Static-shift versus wave-equation datuming

Wave-equation datuming has proven to be an accurate deterministic solution to unraveling near-surface-induced distortion when the near-surface velocity field is perfectly known. Several papers have shown the accuracy and benefits of using a wave-equation-based datuming technique as opposed to the traditional simple static datuming approach.

Unlike datuming with time-invariant shifts, wave-equation datuming corrects the time distortions caused by topography and laterally changing near-surface conditions in a way that is consistent with wavefield propagation. By honoring the wave-equation, this process ensures that subsequent processing steps that assume simple hyperbolic moveout of reflections in CMP gathers, or complicated moveout consistent with wave propagation beneath the near-surface layers, can be accurately applied. After wave-equation datuming, migrated sections show increased reflector continuity and better representation of true subsurface structure than do those generated after static corrections have been applied. In practice, however, the application of wave-equation datuming has not been straightforward. For land data, the major difficulty is found in the estimation of the near-surface velocity model. Another complication to this process is due to the nonuniform acquisition geometries frequently found in land seismic data (e.g. missed shots, crooked line geometry, irregular shooting combined with low signal-to-noise ratio). Traditionally, first-arrival refraction analysis gives an efficient means of building models of low-velocity layers. Recently, turning-ray tomography (Stefani, 1995) has proven to be a robust and accurate technique for estimating near-surface velocity models where conventional refraction analysis fails. These methods, however, give just approximations to the true near-surface velocity model. Therefore, it is relevant and pertinent to ask,

- What happens to the accuracy of the datuming effort if the near-surface velocity model is poorly known?
- Which datuming approaches are more tolerant of errors in the presence of inaccuracy in the near-surface velocity model?

This chapter is devoted to a sensitivity analysis of datuming processes to errors in the near-surface velocity model. I address the above questions through demonstrations with simple synthetic examples, aiming to give some insight into the errors one can expect from each approach when working with imperfect velocity models.

3.1.1 Accurate near-surface velocity model

The initial step in any sensitivity analysis is the generation of an ideal reference result. To get such a reference, I assume that my knowledge about the velocity model is perfect. Later in this chapter, I relax this assumption introducing some perturbation to the true velocity model. The synthetic data used in this analysis were generated using a simple ray-tracing modeling code (Docherty, 1991b). It consists of 161 shots, each of them with 161 traces, and the shot and group interval are both 25 m. The data have a Ricker wavelet with a dominant frequency of 25 Hz. Figure 3.1 shows the structural velocity model. The model includes simple sinusoidal topographic relief and a three-reflector subsurface geometry above a homogeneous half-space. The two labeled dots A and B in Figure 3.1 indicate the surface locations of the shots selected for comparison of the corrective action of the different approaches.

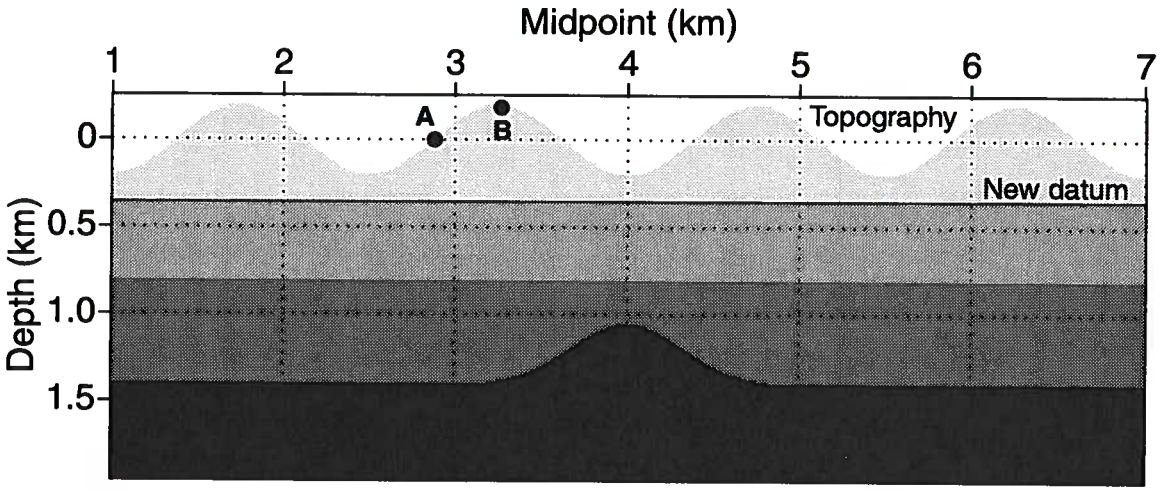

FIG. 3.1. Structural velocity model. The model includes a sinusoidal topographic relief and a simple subsurface structure. The labeled dots A and B indicate the surface locations of the shots selected for comparison of the action of the different approaches. The shading denotes velocity; the darker the shading, the higher the layer velocity.

The wavelength of the sinusoidal topographic surface is 1500 m, and the height of the anomaly is 200 m, so this model does not include the shorter wavelengths generally addressed with conventional static-estimation methods. The velocity ranges from 2000 m/s at the near-surface to 4000 m/s in the deepest formation. Two shot records showing the reflections from the two deepest interfaces as they would appear for sources and receivers on the topographic surface are shown in Figure 3.2. The main characteristic on the shot gathers is the nonhyperbolic moveout observed on the reflection events. These prominent features in the data portray the distorting action of the sinusoidal topographic anomalies.

There are basically two different approaches for treating near-surface time anomalies in a deterministic fashion. The first approach consists of redatuming the data to a new level of reference below the near-surface velocity anomalies to prepare the data for conventional processing. This approach could be performed using invariant-time shifts or a wave-equation-based datuming scheme.

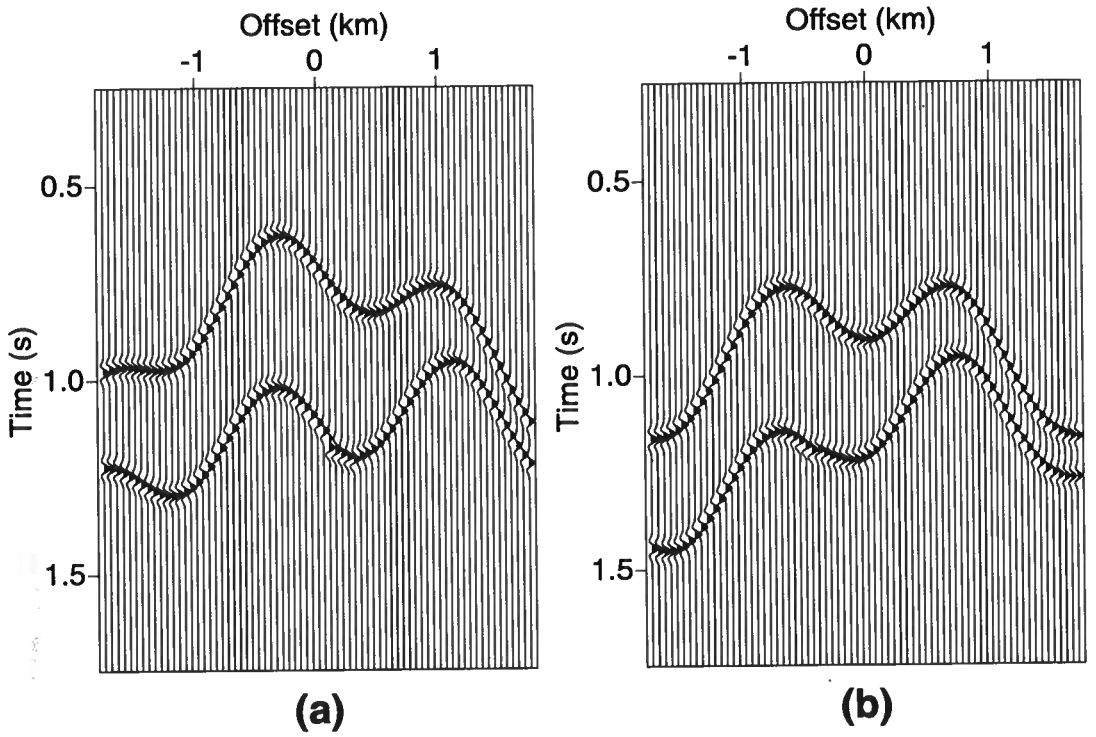

FIG. 3.2. Synthetic split-spread shot gathers from topography: (a) shot A, and (b) shot B.

The second approach is to migrate the data directly from the acquisition surface, incorporating the near-surface model as part of the migration-velocity field. All these methods should work best with a reliable estimate of the near-surface velocity structure as input. Figure 3.3a shows the same shot gathers as in Figure 3.2 after the sources and receivers have been transferred from topography to a flat datum at 350 m. Here, I use the conventional redatuming approach based on simple static time shifts. The static corrections consider the near-surface time distortions to be those of vertical paths above the datum level, ignoring the slant paths that more properly are associated with reflection events (see Figure 1.2). Although, the nonhyperbolic moveout present on the input data is greatly reduced, the remaining moveout distortions will cause problems for wave-equation-based processes such as velocity analysis, DMO, stack

and migration.

In areas of rough topography the static approach usually breaks down, and more sophisticated datuming techniques such as wave-equation-based algorithms are required. Figure 3.3b shows the shot gathers after Kirchhoff datuming was performed to move the data from surface to a flat reference datum. Since, I have used the correct velocity model to perform the wavefield extrapolation, the shallower reflection event, quite nicely, recovers the familiar hyperbolic moveout. The moveout of the deeper reflection, on the other hand, remains nonhyperbolic, as it should, considering the lateral velocity variation associated with the anticlinal overburden observed in the subsurface velocity model. Due to limitations of aperture, small artifacts could be observed at the edges of the shot gathers. Here, it is important to remember that the extrapolation processes are done in the shot and receiver domain. These artifacts, due to lack of data at the edges, are common in all migration-type processes, especially those applied in a shot or receiver domain. These new shot gathers simulate the seismic data that would have been recorded if the acquisition surface were located at the level 350 m. Unlike the static scheme, Kirchhoff datuming removes the distortions caused by the sinusoidal topography in a manner consistent with the wave-equation.

Let us examine how these differences look after prestack depth migration. Figure 3.4a offers the migrated stack section after static-corrections. This image shows the wavefield distortions imposed by the simple static-datuming solution. The time shifts applied to the original seismic data have distorted the reflections from their desired hyperbolic shape leading, after migration, to an erroneous image that shows an imperfect diffraction focusing response. The additional event observed on top of the shallower reflector at a depth of about 700 m (Figure 3.4a) is the result of migrating data that were kinematicly over-corrected by the conventional static-datuming approach; thus, after migration, it also looks over-migrated. In fact, that extra event is associated with the middle- to far-offset traces of the former shallower reflector. Nonzero-offset data are more influenced by the moveout distortions than are zero-offset data. The imaging inaccuracy, however, is not in the migration process itself, but in the distorted input data. As can be seen in Figures 3.3, and 3.2, the static time corrections are larger than those generated by the Kirchhoff datuming approach. This observation is most evident at far-offsets. After static-datuming corrections, the data for shot A show the shallower reflection at a time of 0.72 s for an offset of -1.75 km, while the Kirchhoff solution locates the same reflection at a time of 0.78 s (prior to the correction, that reflection appeared at a time of about 0.96 s).

Figure 3.4b displays the stack migrated section after Kirchhoff datuming. As expected, this section displays a proper solution to this imaging problem of migration performed after the data are re-datumed using wave-theory. This good image also shows accuracy of the modeling code (Docherty, 1991b) used for this example since the algorithm for the modeling program CSHOT differs from that for datuming.

This example gives an idea of the deterioration in imaging quality one can expect in the surface-consistency approach to static corrections even when the information on near-surface velocity is perfect. The amount of smearing in the results increases with

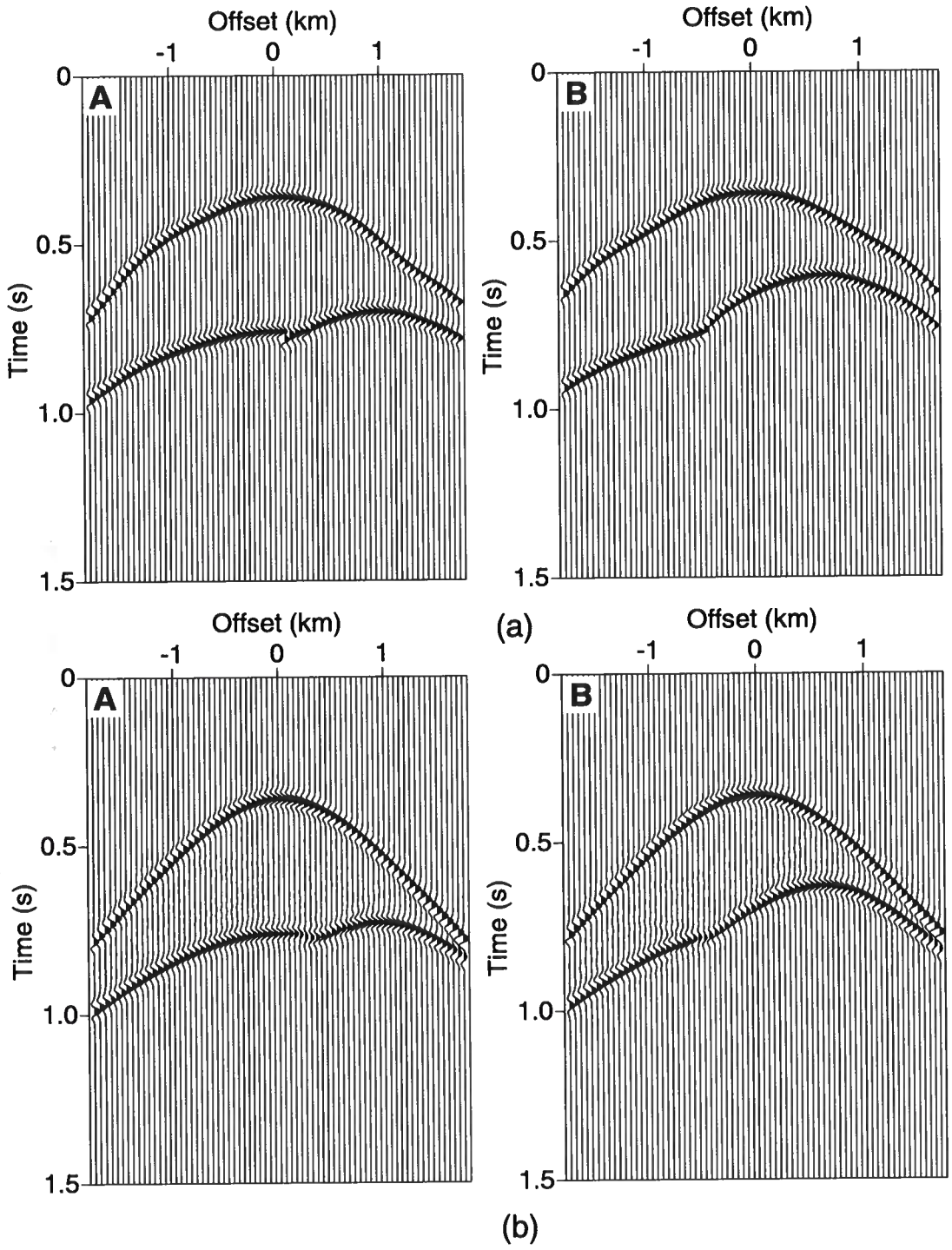

FIG. 3.3. Shot gathers A and B after datuming corrections to transfer the data to a flat surface at 350 m (a) with static time shifts, and (b) with the Kirchhoff approach.

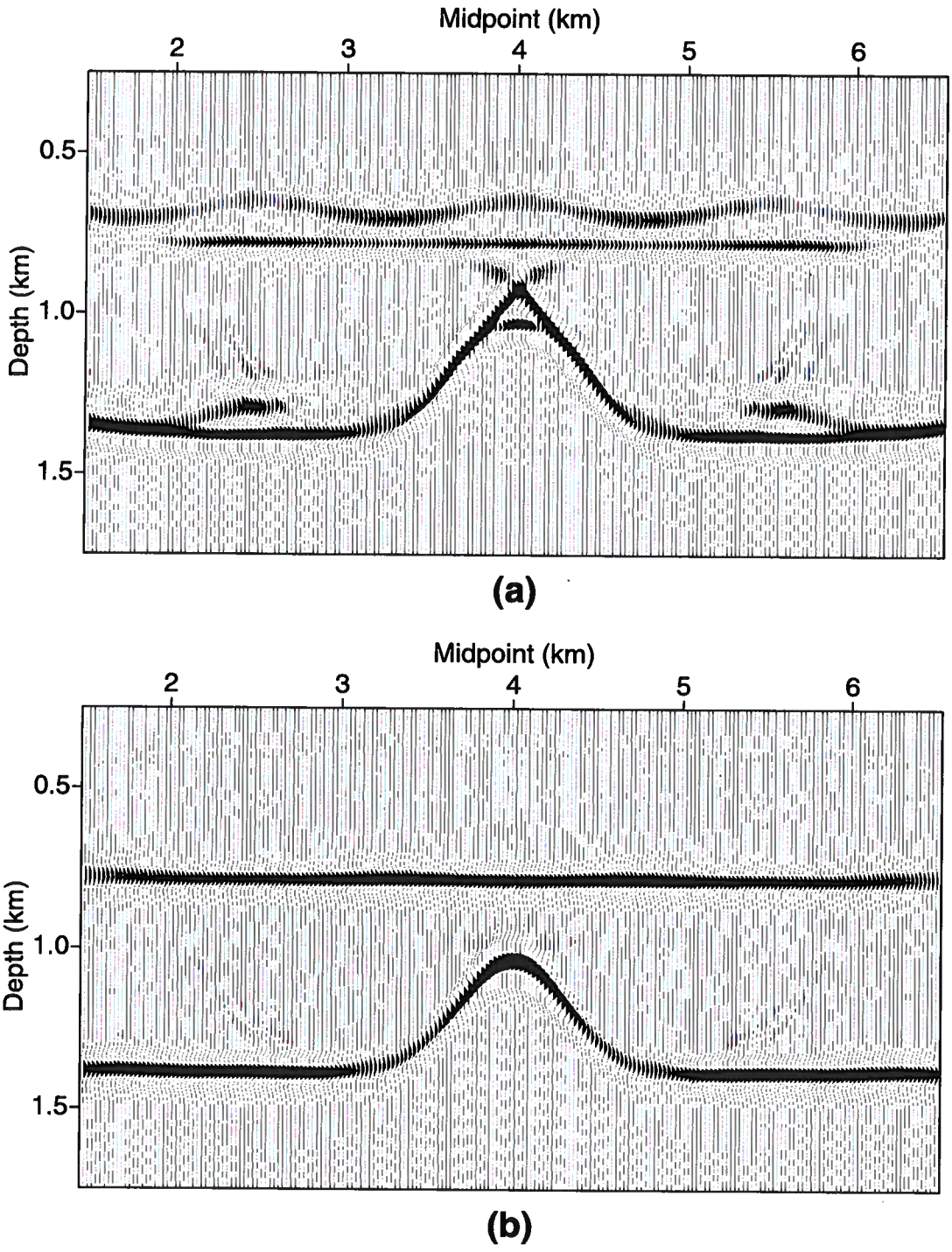

FIG. 3.4. Prestack depth migration (a) after static-datuming corrections, and (b) after the Kirchhoff datuming.

the vertical distance to the datum level, that is, the difference between the old and new levels of reference. Therefore, the accuracy of the conventional static solutions is best for cases of small datuming distance. The over-migration of the data seen in Figure 3.4a is a phenomenon that might resemble situations frequently encountered in seismic data processing. Seismic data, however, could be under- or over-migrated due to multiple reasons, such as inaccuracy in the migration velocity field, anisotropy, ignoring of three-dimensionality in 2-D data, wrong migration technique or improper procedure to account for near-surface time anomalies (Beasley and Lynn, 1992).

In practice, the data-smearing problem illustrated in Figure 3.4a is treated by changing the migration velocity field, under the assumption that remaining diffraction tails in the seismic sections are attributable to inaccuracy in the velocity model. This approach is valid when the velocity field is indeed wrong, but it is poor if the problem, as seen here, is caused by improper treatment of induced near-surface time anomalies. No modification in the migration velocity field would compensate for all the wavefield distortions generated by the conventional static-corrections approach. Such a solution tries to correct for a wavefield distortion imposing a velocity change that has no physical justification. Additionally, where a fine tuning of the migration velocity is attempted to account for the improper treatment of near-surface time anomalies, the seismic image would have lateral and vertical mis-positioning problems that could conspire against an accurate interpretation of any oil prospect.

Figure 3.5 shows the result of the second approach for dealing with near-surface time anomalies. The migration algorithm used to obtain this migrated stack section works directly from the acquisition surface. Here, I processed the original data without including any datuming step. Figure 3.5 should be compared with Figure 3.4. The migrated stack sections that were generated honoring the wave theory (Figures 3.4b and 3.5) are almost identical; both are much superior in imaging quality to that obtained after applying static datuming corrections. For this model, we conclude that migration from the original topographic surface and wave-equation datuming followed by prestack migration from the new datum level are comparably accurate.

3.1.2 Perturbed near-surface velocity model

Now, let us repeat the above tests, but now with an erroneous near-surface velocity model. From the first example is clear that wave-equation based (i.e., datuming and migration) methods are superior to the conventional static approach when the near-surface velocity is well known. We will see that this relative quality of solutions is not always true when the datuming processes are performed using a poorly known velocity model.

Again, the essential issue is the sensitivity of datuming quality to inaccuracies in the near-surface velocity. To perturb the velocity model, we include errors in percentage from the true velocity model in Figure 3.1. We will consider the results of the two datuming techniques when the velocity of the near-surface layer is 5, 10, and 15% too high and also when the velocity is 15% too low (correct velocity for the

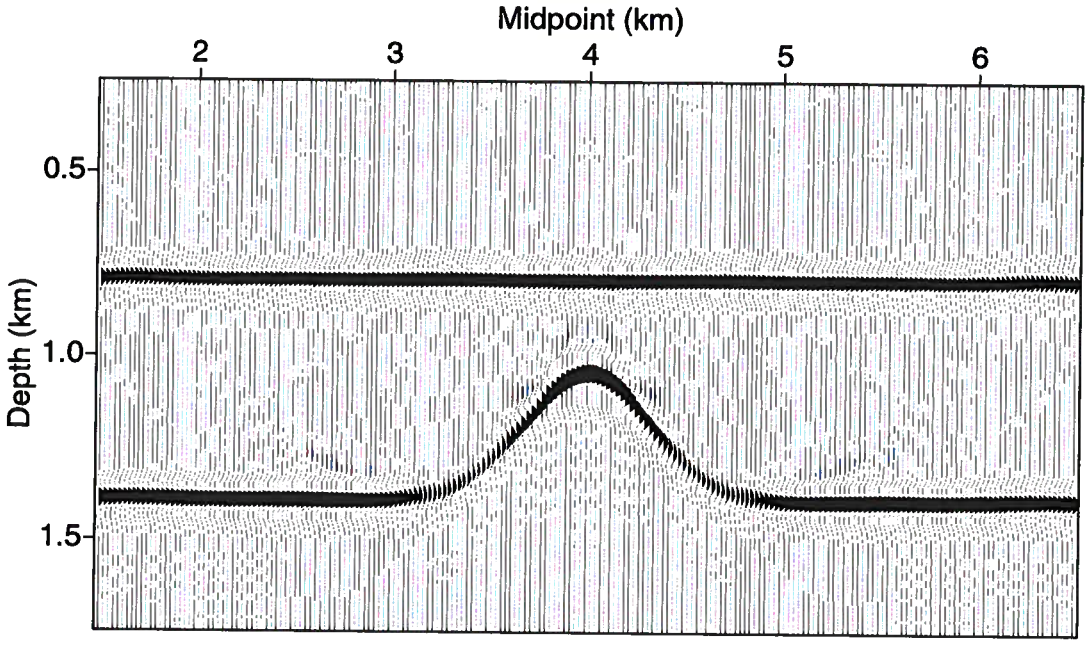

FIG. 3.5. Prestack depth migration from the sinusoidal acquisition surface.

first-layer = 2000 m/s). Migrated sections for all the velocity errors studied are shown in Figures 3.8 through 3.11. Shot gather displays, however, will include only velocity errors of 15% too high and 15% too low (Figures 3.6, and 3.7).

This sensitivity analysis will allow us to draw some qualitative conclusions in terms of robustness of each datuming scheme when working with imperfect velocity models. Figure 3.6a shows the shots gathers from Figure 3.2 after static-corrections to go from surface to a flat datum at 350 m. Here, the near-surface velocity used is 15% too high. The remaining moveout distortions in the reflection events are evident, as seen in Figure 3.6a. Figure 3.6b shows the shots gathers from Figure 3.2 after Kirchhoff datuming using a first-layer velocity 15% too high. As with datuming using static-corrections, Kirchhoff datuming leaves highly distorted moveout in the reflection events. The moveout distortions for the conventional static approach, however, are less severe than those exhibited by the Kirchhoff datuming solution, especially for the deeper reflector. Since the first-layer velocity is too high, the static correction are smaller than those obtained by using the true velocity, giving a moveout closer to the true one shown by Figure 3.3b. Therefore, the velocity error compensates to a certain degree, the moveout distortions generated by the conventional static datuming procedure. Furthermore, the resulting reflectors are all slightly deeper in time than they should be. These timing errors are simply the familiar distortions in converting from depth to time with a wrong velocity.

Results of the 15% decrease in the near-surface velocity (Figure 3.7) shows similar

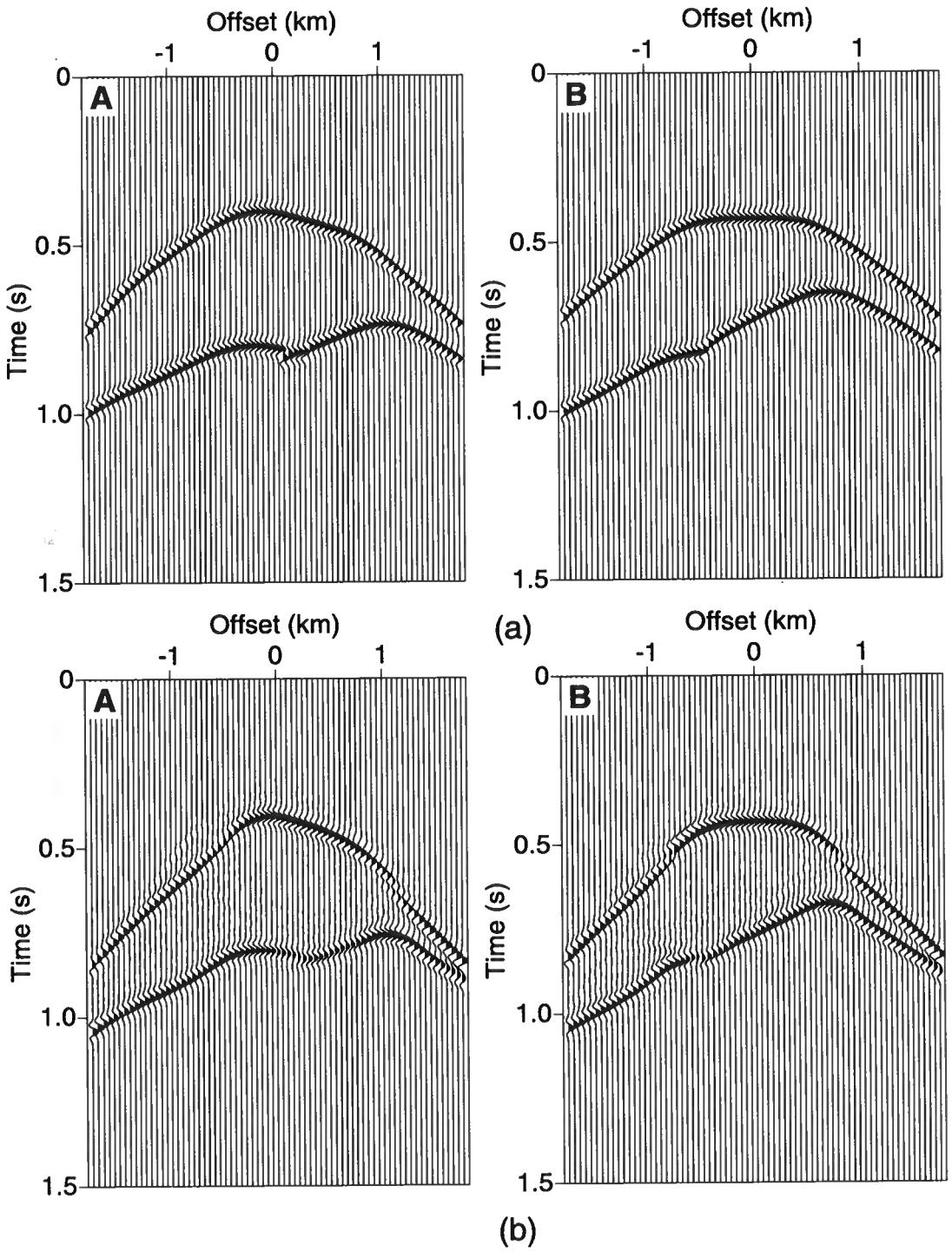

FIG. 3.6. Shot gathers A and B after datuming corrections to transfer the data to a flat surface at 350 m using a near-surface velocity that is 15% too high (a) with static-time shifts, and (b) with the Kirchhoff approach.

moveout distortions, but the timing errors are naturally in the opposite direction. Here, since the first-layer velocity is too low, the static corrections are larger than those calculated with the true velocity. Therefore, the moveout distortions due to the static approach are not compensated for by the error in the near-surface velocity. It is easy to imagine the potential problems for wave-equation-based processes such as velocity analysis, DMO, and migration due to the moveout distortions seen in Figures 3.6 and 3.7.

To establish the robustness of the two datuming approaches in terms of imaging quality, I applied prestack depth migration to the data after applying static-corrections and Kirchhoff datuming for each error-level. For the migration process, I consider a perfect knowledge of the subsurface velocity structure. Figure 3.8a shows the migrated section processed with static-corrections using a velocity 5% too high, and Figure 3.8b shows the migrated section after Kirchhoff datuming using a velocity 5% too high. Similarly, migrated sections after each datuming procedure using velocities 10 and 15% too high and 15% too low are shown in Figures 3.9, 3.10, and 3.11. It is interesting to observe the general behavior of the two datuming algorithms when the near-surface velocity information is incorrect. The conventional static approach seems to be less sensitive to errors in velocity than is Kirchhoff datuming (Figures 3.9, and 3.10). Surprisingly, the images of the anticline structure and the horizontal deeper reflector in the geologic model are better resolved and have better continuity across the section when the data have been processed with static-correction as opposed to Kirchhoff datuming. Particularly, static-corrections worked better than did Kirchhoff datuming when the velocity used for the datuming process was higher than the true value. Nevertheless, although the data processed with static corrections show a general improvement in imaging quality over that of data treated with the Kirchhoff datuming approach in the deeper reflection, for the shallow reflection the images are comparably distorted by the two datuming algorithms. This observation indicates that imaging of reflections from shallow interfaces is more sensitive to moveout distortions than are those from deeper features. Deeper in the velocity model, the surface-consistent static assumption becomes more appropriated; slanting of the raypaths in the weathering layer is more significant for shallow reflectors than for deeper ones, reducing the accuracy of the static solution for earlier seismic events. On the other hand, when the velocity used in the datuming process is lower that the true one (Figure 3.11), both images are extremely distorted. As mentioned earlier, under these circumstances the errors in the near-surface velocity do not compensate for the moveout distortions incurred by the erroneous static-datuming approach.

Schneider et al. (1995) offer an interesting field application of layer replacement on land data from a Western U.S. overthrust belt. They use standard refraction analysis procedures to derive the velocity structure of the near-surface, followed by wave-equation velocity replacement based on a Kirchhoff datuming scheme. They compare stack sections processed with a static solution and Kirchhoff datuming using the estimated near-surface velocity model. Their stack sections show a general improvement in the shallow reflectors when Kirchhoff datuming, as opposed to the

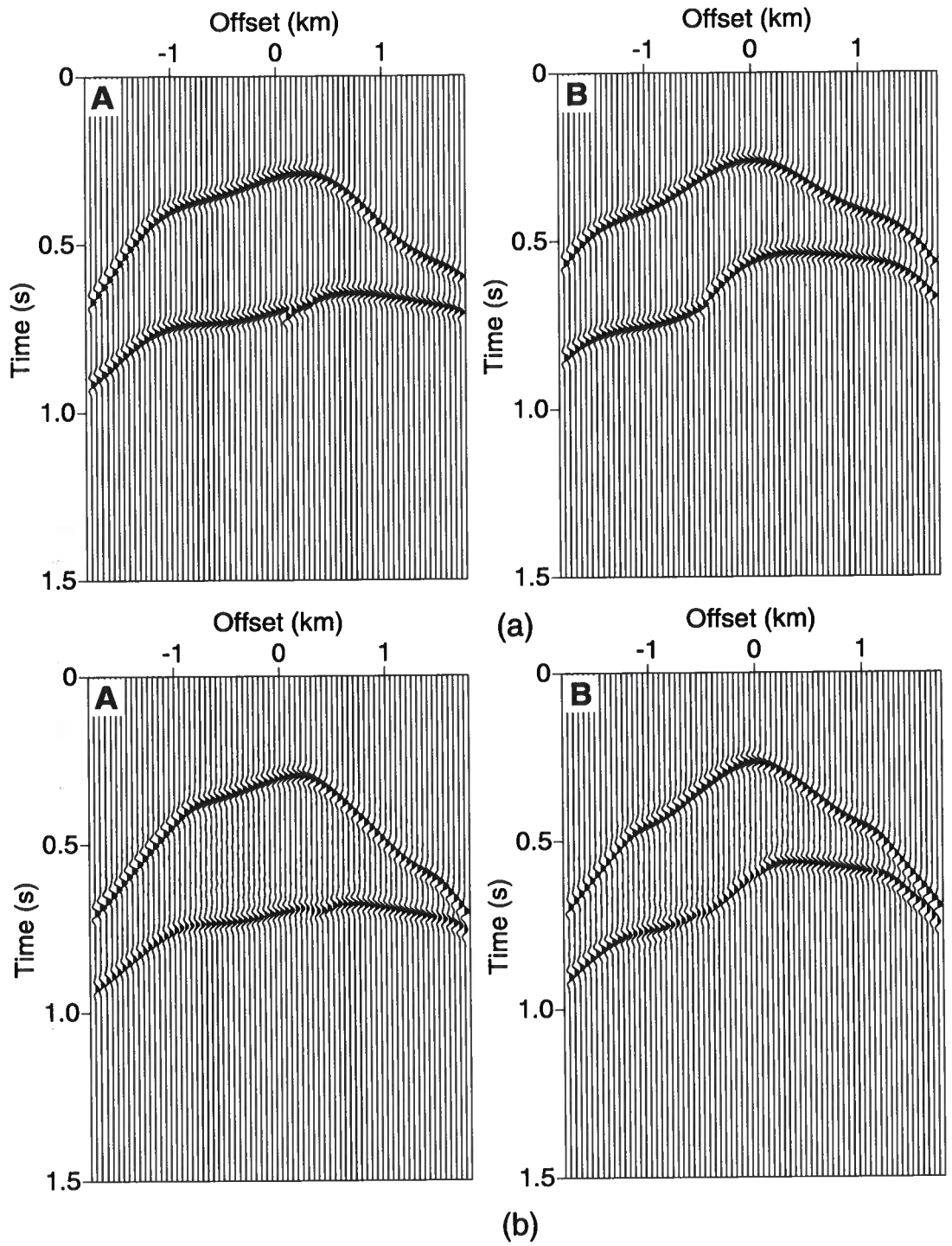

FIG. 3.7. Shot gathers A an B after datuming corrections to transfer the data to a flat surface at 350 m using a near-surface velocity that is 15% too slow (a) with static-time shifts, and (b) with the Kirchhoff approach.

conventional static-corrections, is used. In some parts of the line 2, however, the stack obtained with a static solution exhibits better reflection continuity than does that with Kirchhoff datuming. This may indicate that their low-velocity layer model is not accurate enough to see the benefits of the Kirchhoff datuming approach, as shown in the previous synthetic examples. In the central part of the near-surface velocity structure used in this field application, there is a sudden increase in velocity. This particular characteristic of the low-velocity-layer model may be the reason that a static approach often yields better results than does the more sophisticated Kirchhoff datuming.

3.2 Comparison of imaging results

3.2.1 Discussion

From the previous section, static-corrections seem to be more robust than the Kirchhoff datuming in the presence of imperfect near-surface velocity models. Kirchhoff datuming exaggerated the energy focussing process in all the tests I performed with erroneous velocities. To explain this behavior, let us examine how the two datuming schemes work. As explained in Chapter 2, Kirchhoff datuming extrapolates a wavefield considering an area of influence defined by the aperture of the summation operator. The shape of the extrapolation operator is governed by the velocity structure observed between the old and the new reference surfaces, and the distance between them. I use ray-tracing to estimate the amplitudes and shapes of these operators. When the proper velocity field is used, the Kirchhoff extrapolation procedure can go forward or backward in time correctly following the wave theory. Therefore, no distortion is observed in the extrapolation process (see Figures 3.3 and 3.4). Unlike Kirchhoff datuming, the conventional static datuming approach assumes only the vertical-path propagation, neglecting completely the slant paths arising from Snell's law. Also, as mentioned earlier, the conventional static datuming is based on the surface-consistent assumption.

When the near-surface velocity is wrong, the Kirchhoff datuming operator is not accurate either. Therefore, the summation step implied by the Kirchhoff datuming process will add together contributions from traces at incorrect traveltimes, causing a focusing and defocusing action that destroys event coherency. For the static-datuming approach, however, the errors in velocity change only the vertical time shifts applied to each trace because there is no repositioning in this scheme. Therefore, at least in this sense, the conventional static approach may be less sensitive to velocity errors than is Kirchhoff datuming.

Let us analyze how the Kirchhoff datuming operators change when one uses erroneous velocities. As the velocity increases, the Kirchhoff datuming operator broadens (see Figure 3.12). The traveltimes from one reference surface to the other are smaller than those estimated with the correct velocity, giving a less-curved looking operator. Furthermore, the minimum time of the operator is also reduced, as illustrated by Figure 3.12. These characteristics of the operator indicate that the horizontal component

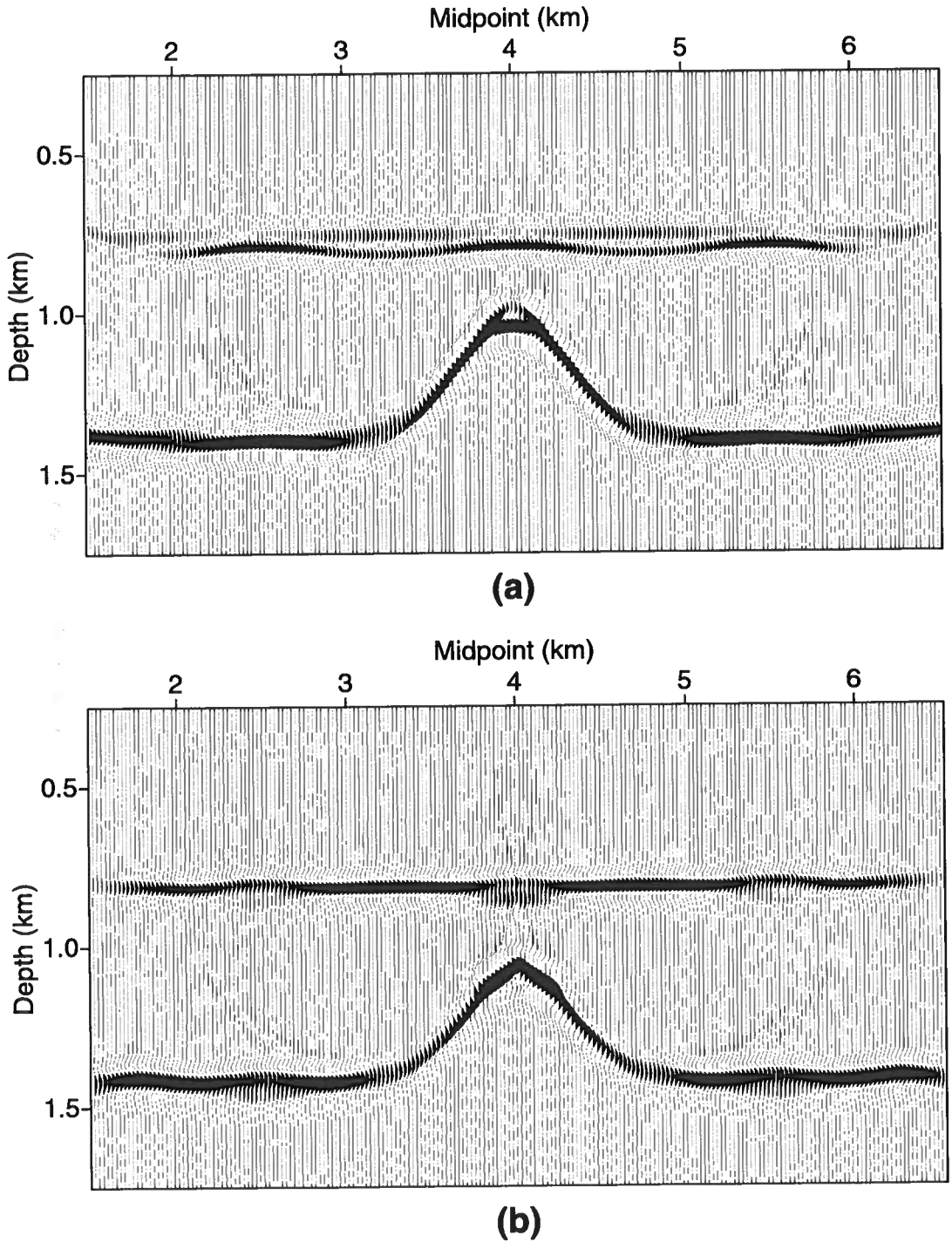

FIG. 3.8. Prestack depth migration after datuming-corrections using a near-surface velocity 5% too high (a) with static time shifts, and (b) with the Kirchhoff approach.

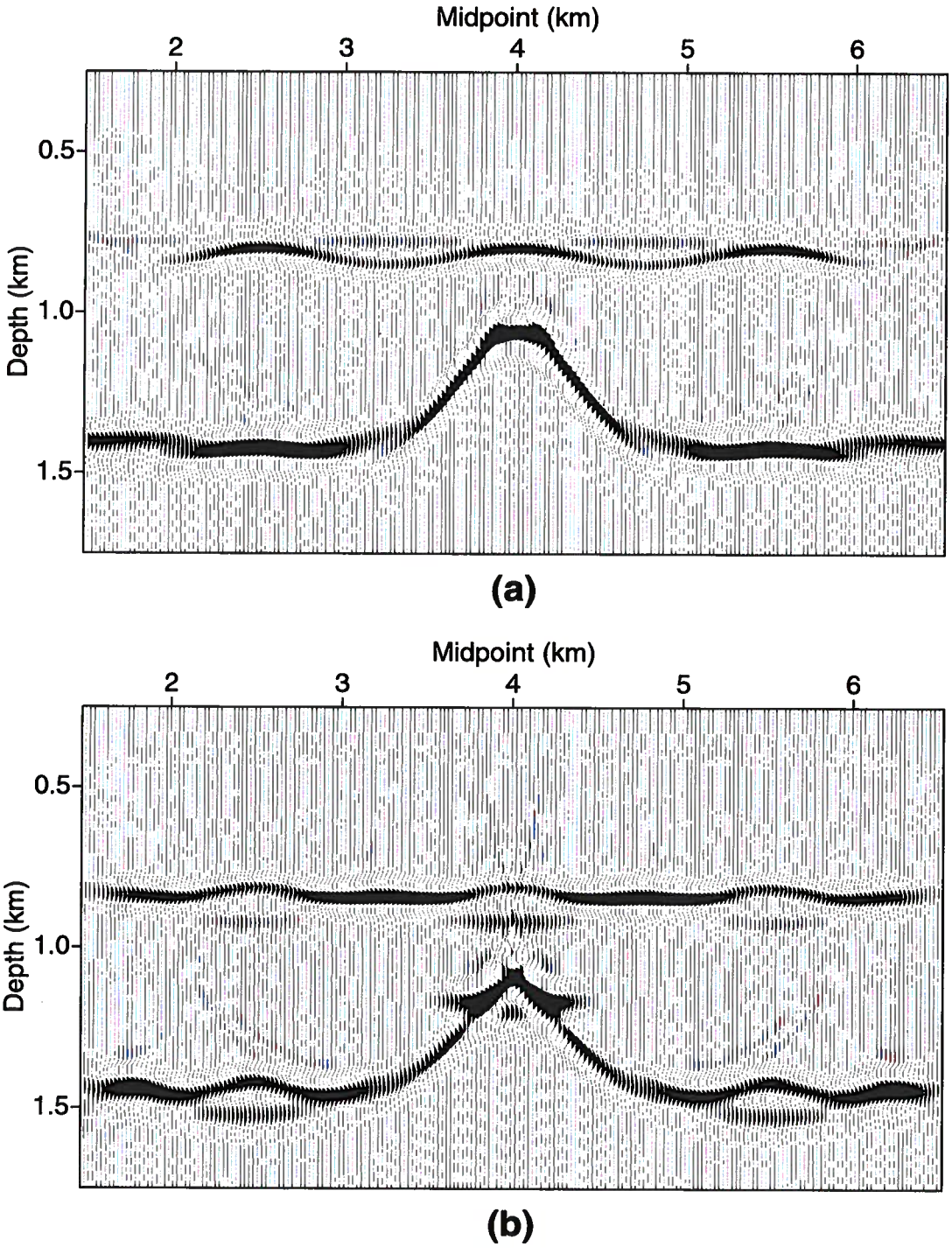

FIG. 3.9. Prestack depth migration after datuming-corrections using a near-surface velocity 10% too high (a) with static time shifts, and (b) with the Kirchhoff approach.

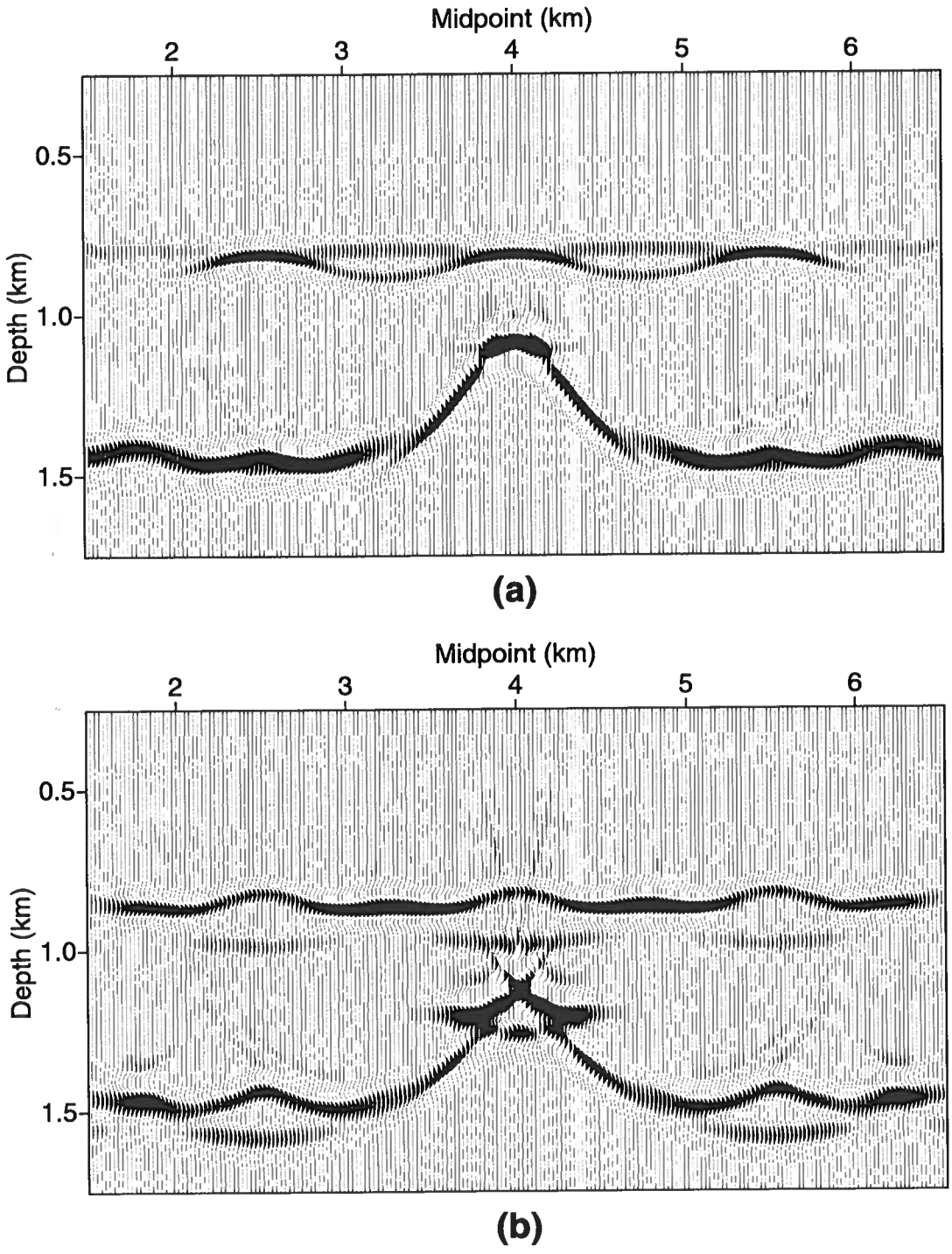

FIG. 3.10. Prestack depth migration after datuming-corrections using a near-surface velocity 15% too high (a) with static time shifts, and (b) with the Kirchhoff approach.

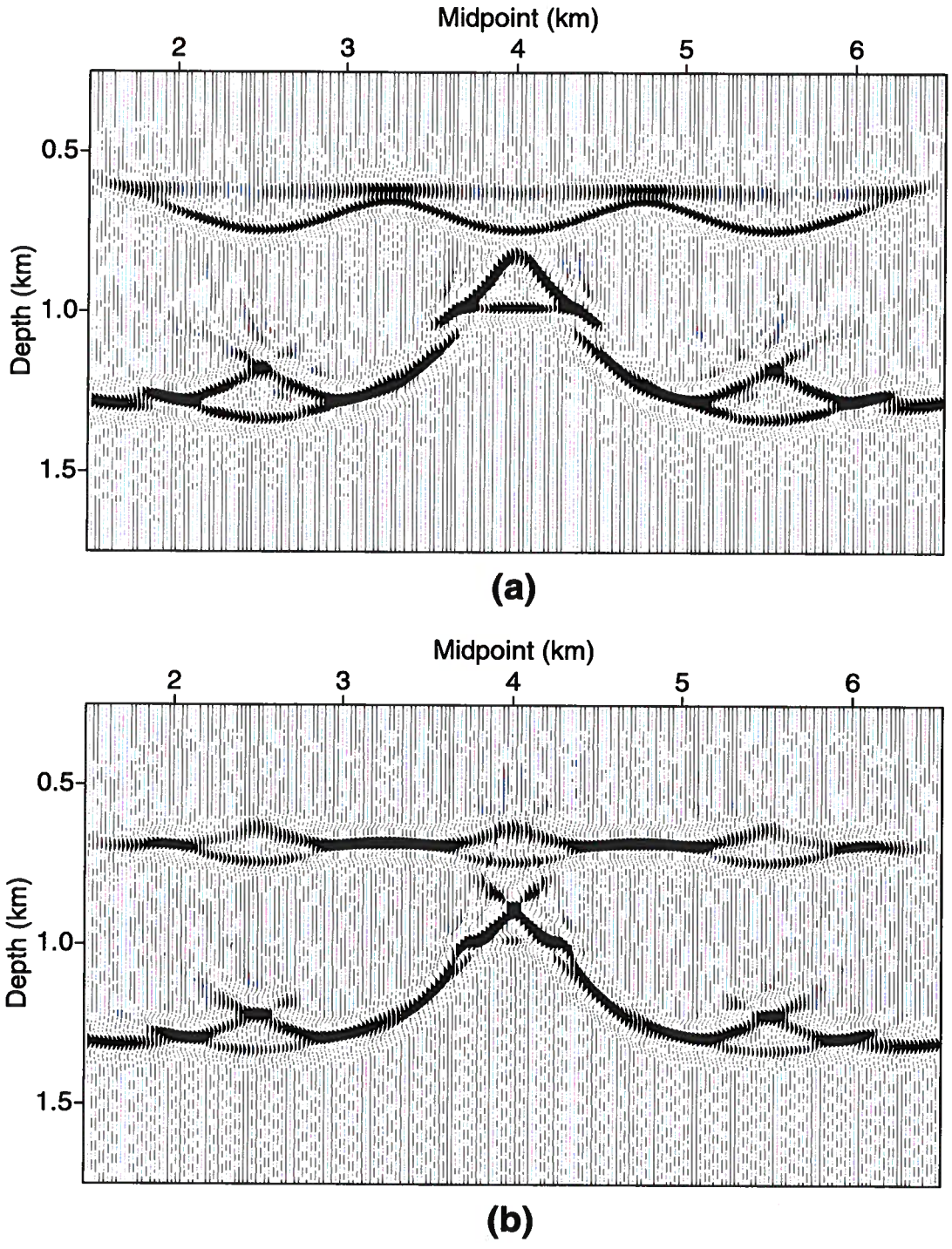

FIG. 3.11. Prestack depth migration after datuming-corrections using a near-surface velocity 15% too low (a) with static time shifts, and (b) with the Kirchhoff approach.

of the extrapolator gets stronger as the velocity increases; thus the focusing action of the process is exaggerated. The operator associated with a too-high velocity focuses the data more than it should, producing moveout distortions in the reflection events. Later in the processing sequence, the prestack migration thus will process a data set that exhibits a severe focusing problem due to errors in the Kirchhoff datuming operator. Therefore, the migration results appear overmigrated, as seen in Figures 3.9 and 3.10. For the static-datuming approach, however, the focusing problem is not an issue; thus, this approach does not distort the data as much as does the Kirchhoff datuming scheme when the near-surface velocity model is too high. Under this condition, the moveout distortions inherited by the static-datuming approach are partially compensated for by the errors in the near-surface velocity, giving moveout closer to the true ones than those obtained with the Kirchhoff datuming scheme. On the other hand, when the velocity of the near-surface is too low, the moveout distortions for data processed with the conventional static approach, instead of being attenuated, are enhance by the errors in the near-surface velocity. This analysis gives some explanation for the better images that may be obtained with the conventional static corrections than those with the wave-equation datuming when the near-surface velocity is too high. It also explains why the situation changes when the shallow velocity is too low.

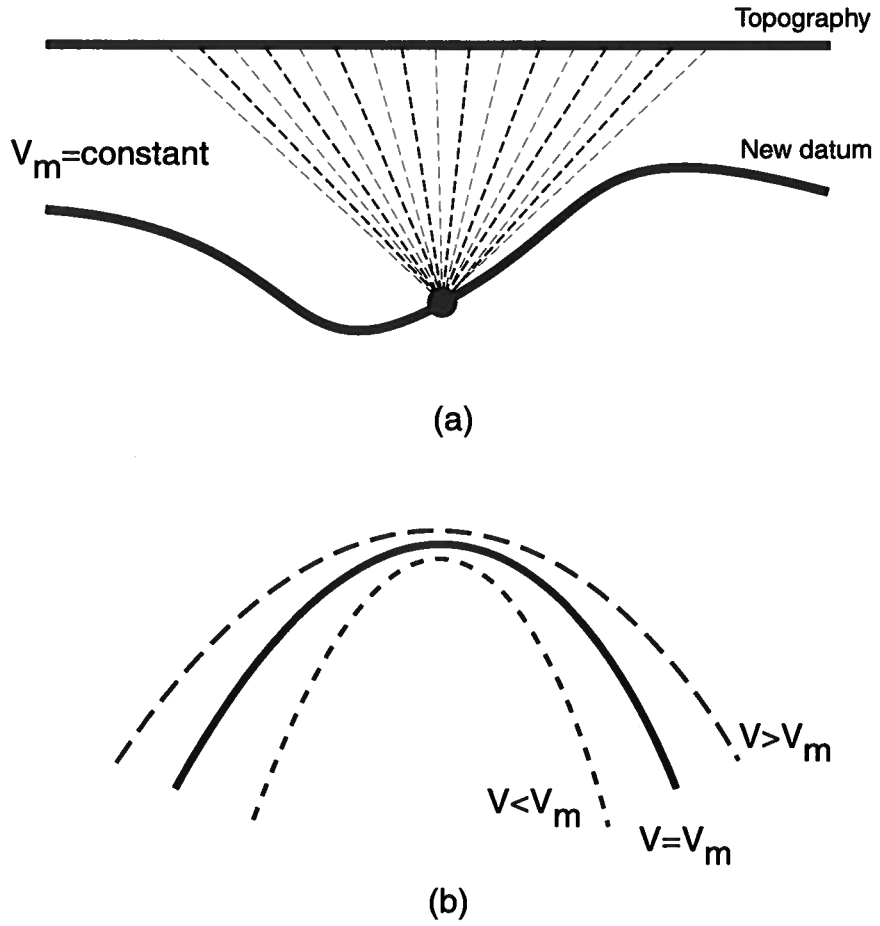

FIG. 3.12. Sensitivity of the Kirchhoff datuming operator to erroneous velocities: (a) downward continuation process, and (b) extrapolation operators. Three operators are shown; two of them use velocities higher and lower than the velocity V_m of the medium.

Chapter 4

MODELING OF NEAR-SURFACE-INDUCED TIME DISTORTIONS

4.1 Introduction

Traditionally, near-surface-induced time distortions have been treated and modeled as static and surface-consistent time shifts, which are based on the assumptions that most of the wavefield energy follows a nearly vertical raypath in the near-surface and that no ray-bending occurs at the base of the weathering layers (Wiggins et al., 1976). Although these assumptions have been widely accepted, it is known that the true traveltime distortions obey a more complicate pattern (Larner et al., 1996). The multi-directional raypaths of the wavefield propagation depend directly upon the complexity of the near-surface velocity structure. Despite the complex nature of the propagation process in the near-surface, historically, simulated residual time anomalies have been simply generated as surface-consistent, static time shifts in an attempt to assess the quality and robustness of new static-estimation procedures. More appropriately, the model data used in static-estimation algorithm testing should contain time distortions that are wave-theoretic.

In this chapter, I discuss a different way to modeling near-surface time distortions. Here, I use an alternative wave-equation-based methodology to generate not surface-consistent, static time shifts but more realistic time anomalies. By honoring the wave-equation, this scheme ensures that these time anomalies may be good examples of the type of near-surface-induced time distortions frequently found in field data.

4.2 Traditional approach: Surface-consistent assumption

Over the years, static-estimation techniques have taken advantage of the static and surface-consistent assumptions. Several methods have been developed under these assumptions to estimate time corrections that account for time distortions related to laterally changing near-surface conditions. Conventionally, new static-estimation techniques have been tested using synthetic data that suffer from precisely surface-consistent, static time shifts. Usually, the ideal time perturbations included on the synthetic data tests are randomly generated numbers with zero mean. Obviously, these time anomalies do not have any near-surface velocity model associated with them. These tests, therefore, could be considered biased because they just include in the contaminated synthetic data, just the kind of time anomalies for which those algorithms were formulated. The success of any approach under these circumstances always leaves a doubt as to whether or not the technique is good enough to be applicable to field data.

Land data normally suffer from time anomalies that are neither surface-consistent nor static and that certainly include laterally changing conditions along the near-surface, with wavelength longer than the cable length. As demonstrated by Wiggins et al. (1976), those long-wavelength time anomalies are not well resolved by reflection static-estimation methods based on the surface-consistent assumption.

4.3 Wave-equation-based approach

Here, I use a simple methodology for generating realistic near-surface-induced time distortions that honors the wave-equation and takes into account a near-surface velocity structure in the modeling process. These time anomalies will allow us to assess the accuracy and robustness of alternative residual-static estimation schemes under conditions similar to those found in conventional processing of field data. This approach to modeling time anomalies combines wave-equation datuming and elevation-static corrections (see Figure 4.1). This tool is useful for study of models with complex near-surface, but with subsurface velocity structure of any complexity. In this way, instead of doing a costly FD modeling for the complete velocity structure, one could use a two-step modeling procedure.

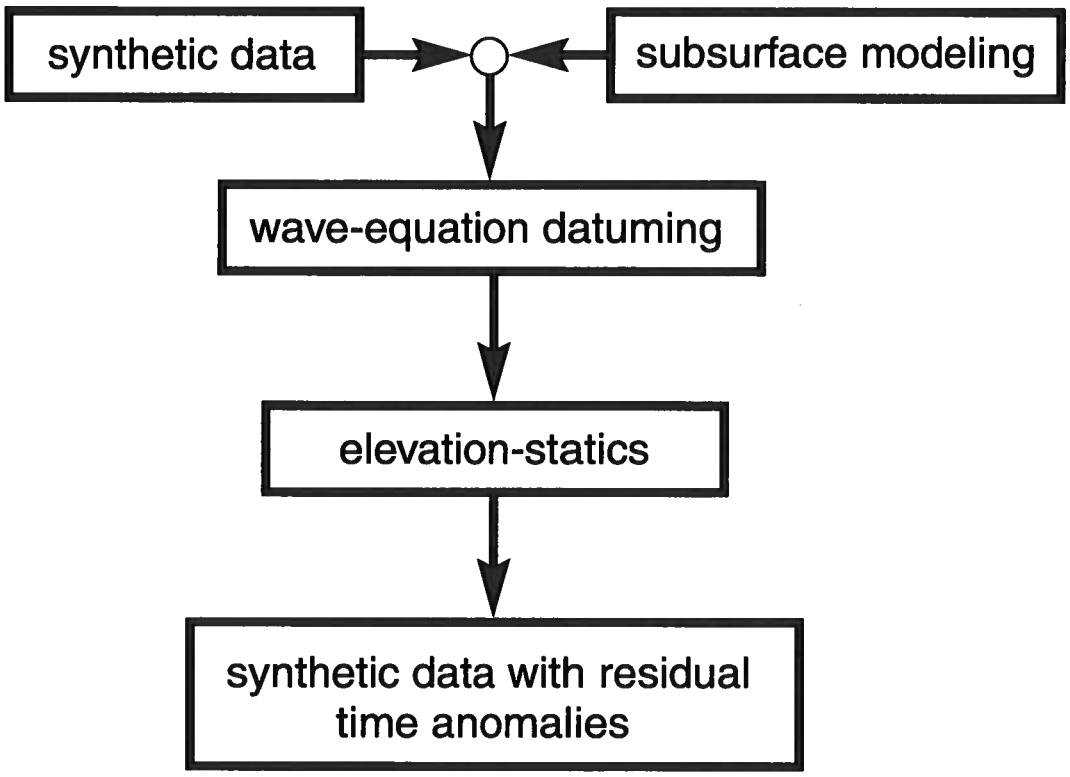

FIG. 4.1. Modeling of near-surface-residual time anomalies

The first step would be to model relative simple subsurface velocity structure

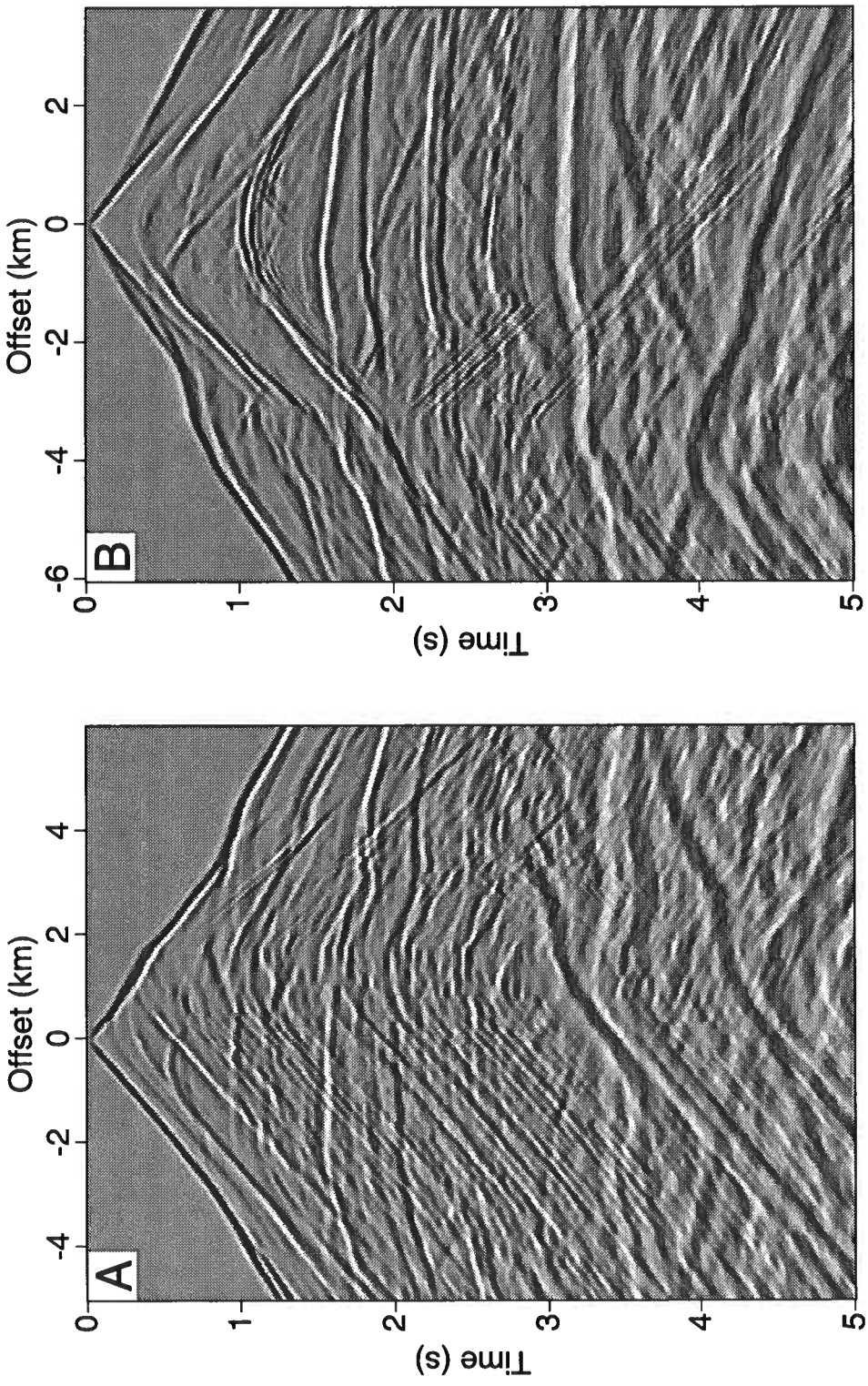

FIG. 5.3. Synthetic shot gathers modeled at a datum level of -1.22 km.

The negative offset-traces of shot gather A in Figure 5.2 exhibit short- to medium-wavelength time anomalies associated with rapid changes in the topographic relief. Furthermore, since this shot record was modeled on top of a high-velocity outcrop, a large break in the first-arrivals associated with a lateral reduction in the near-surface velocity is observed at offsets of about 1.2 km, as is a strong discontinuity in the reflection events at an offset of -0.25 km. The sharp edges of the near-surface velocity anomalies generate diffraction patterns in deeper reflections, as well, such as those observed at an offset of -0.25 km. Since shot gather B was modeled at a location where elevation changes are small and near-surface structure is modest, the major time distortions show only relatively long-wavelength components (see Figure 5.2). In this shot record, the high-velocity anomaly in the near-surface does manifest itself at an offset of -5.5 km and time of 2.3 s, where a large break is observed on the reflection events. Time anomalies associated with the near-surface are relatively easy to identify because they generally distort the traces following a vertical pattern (i.e., roughly in agreement with the surface-consistent and static assumptions).

To evaluate the accuracy of the datuming procedures another data set, to be used as a reference, was generated using the overthrust model; this time, however, the shots and receivers were located at the datum depth level of -1.22 km shown in Figure 5.3. The new reference surface is located below the largest of the near-surface velocity anomalies, and thus, the near-surface-induced time distortions present in these data are less severe (Figure 5.3). For consistency with the former data set, this modeling task was also performed with a finite-difference code.

The data exhibit many of the problems frequently found in land reflection seismic data from overthrust environments, which nowadays are one of the most attractive, and challenging areas for oil exploration.

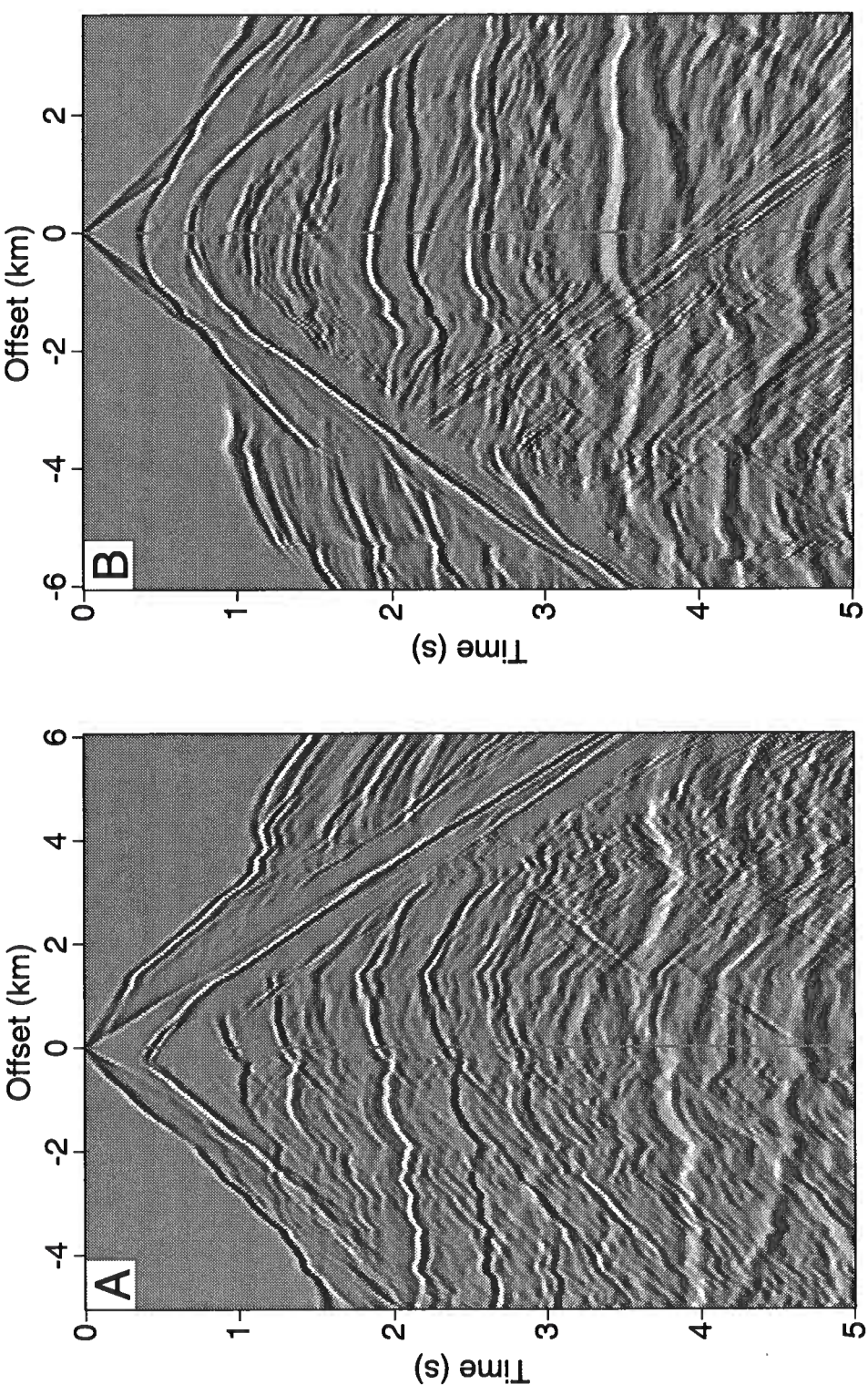

FIG. 5.2. Synthetic shot gathers of the overthrust Rocky Mountains model. Shot records A and B are located at lateral positions 5 km and 10 km, respectively.

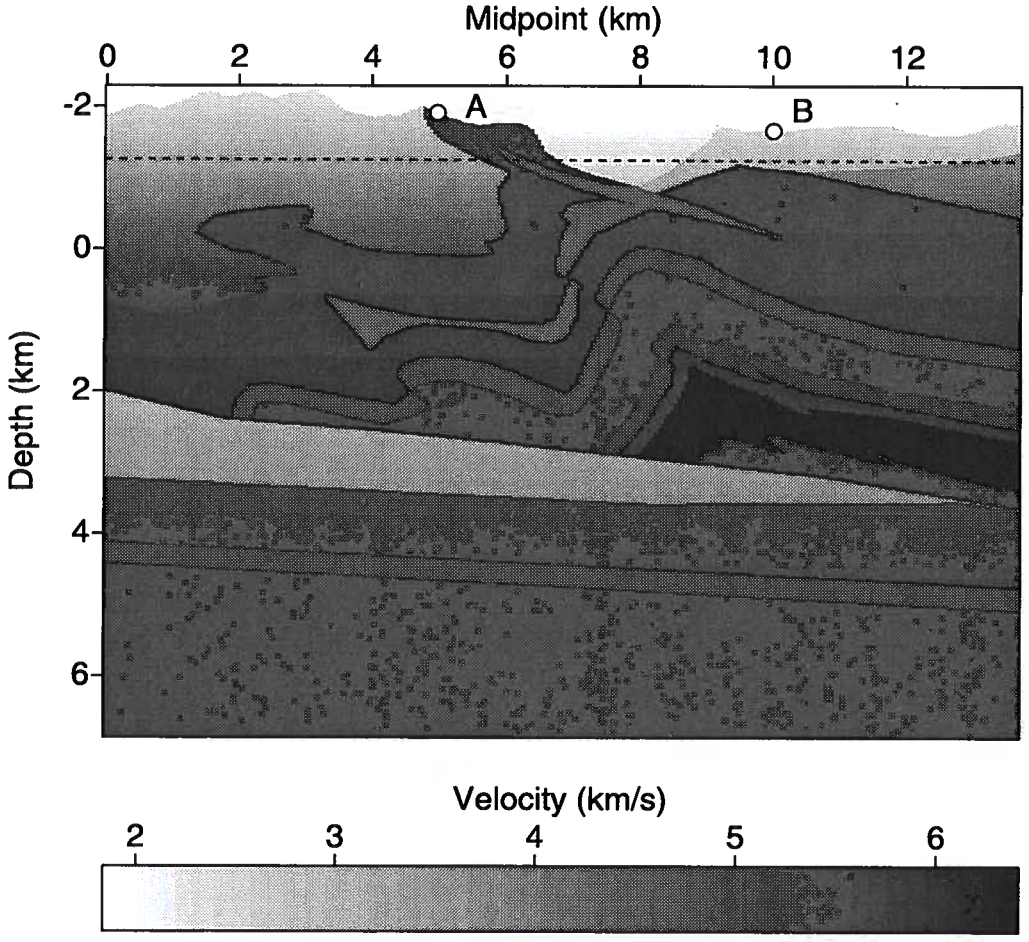

FIG. 5.1. Rocky Mountains overthrust velocity structure. Velocities along the near-surface range from 2040 m/s to 5425 m/s (6700 ft/s to 17800 ft/s). Dots A and B represent the locations of two shot records used in the comparative study. The dashed line indicates the surface level to which the datuming process is performed.

5.2 General description of the synthetic data set

The complex-structure model used in this analysis was kindly provided by Dr. Xianhuai Zhu, of Union Pacific Resources Company. The structural model was built following the general characteristics of structural geology and topography frequently encountered at the Rocky Mountains of the U.S.. In particular, the topographic profile was taken from a seismic line shot recently in an area of interest (Zhu et al., 1995). The structural features in this model (Figure 5.1) indicate that the area corresponds to a compressional tectonic style characterized by intense overthrust faulting and folding. Fault planes break up roughly at 45 degrees in the central part of the model where the subsurface is most complex; however, because of folding, the reflectors exhibit dip as large as 90 degrees.

The near-surface of the model is highly complex, with elevation differences up to 600 m and strong, abrupt lateral velocity contrast as large as 240%. In the central part of the near-surface model (close to location A in Figure 5.1) the presence of an outcropping high-velocity rock mass results in a lateral velocity change from 2135 m/s to 5120 m/s (7000 ft/s to 16800 ft/s). This feature poses the major difficulty in getting a satisfactory solution to this imaging problem. Since the velocity of this geologic anomaly in the near-surface is so high, wave propagation paths in the shallow section depart significantly from the vertical paths that are assumed for conventional statics processing. Proper treatment of this problem requires special imaging techniques such as wave-equation datuming and prestack depth migration.

To represent accurately the complexity of the model in the synthetic data, a commercial full waveform finite-difference code (ProMAX from Landmark) was used in the modeling process. The generated data set consists of 274 shot records with sources and receivers in a split-spread geometry along a topographic surface. Each shot has 240 channels, recorded with 4-ms sample interval. Both, the shotpoint interval and the receiver group spacing are 50 m (165 ft), yielding a maximum CMP multiplicity of 120, with offset ranging from 50 m to 6040 m (165 ft to 19800 ft). The source wavelet is a zero-phase Ricker type with a dominant frequency of 12 Hz, and in order to image the deepest features, the record length is 6 s.

Figure 5.2 shows two representative shot records, A and B, located at surface positions 5 and 10 km from the left edge of the structural model, respectively (see Figure 5.1). The strong distorting action of the near-surface features is seen in the long- and short-wavelength components of time anomalies on refraction and reflection seismic events.

Chapter 5

IMAGING IN AREAS OF RUGGED TERRAIN: ROCKY MOUNTAIN OVERTHRUST SYNTHETIC DATA SET

5.1 Introduction

Overthrust areas with significant surface topography along with complex subsurface velocity structure pose one of the greatest imaging challenges for seismic data processing. Part of the problems faced by the conventional common-midpoint (CMP) processing sequence and traditional imaging methods in such environments results from recording data along an inconvenient, rugged acquisition surface. Traditionally, time anomalies associated with topography and laterally-changing near-surface conditions have been treated as time-invariant shifts, and for a long time, the processing of land data has benefitted from static corrections when the underlying assumptions are approximately fulfilled. On the other hand, when the near-surface includes high-velocity rocks and rough topography, the surface-consistent and static assumptions may be largely in error. Under such circumstances the conventional static datuming approach to account for near-surface-induced time distortions is inaccurate for the wavefield components that do not propagate vertically. As mentioned in previous chapters, this simple datuming technique leaves moveout distortions on reflection data whose occurrence not only impairs the interpretation of the correct stacking velocities but also compromises the performance of subsequent wave-equation-based processes such as dip moveout (DMO) and migration.

To illustrate the aforementioned problems, I compare different imaging techniques on synthetic data from a complex overthrust model that includes rough terrain. Among the imaging algorithms used in this comparative analysis, I include prestack depth migration from the acquisition surface, and a combination of prestack datuming and prestack depth migration from a horizontal reference level beneath the more complex portions of the near-surface velocity structure. I also compare prestack datuming results using finite-differences and Kirchhoff approaches. Moreover, I perform a sensitivity analysis of datuming procedures to inaccuracy in the shallow velocity structure following a methodology offered by Versteeg (1993). Finally, I compare the two datuming schemes in terms of (1) the ambiguities in velocity analysis that arise from moveout-induced distortions and (2) the influence of errors in the near-surface velocity model on the stacking velocity functions. For this purpose, I use a complex near-surface velocity structure but a simple subsurface model.

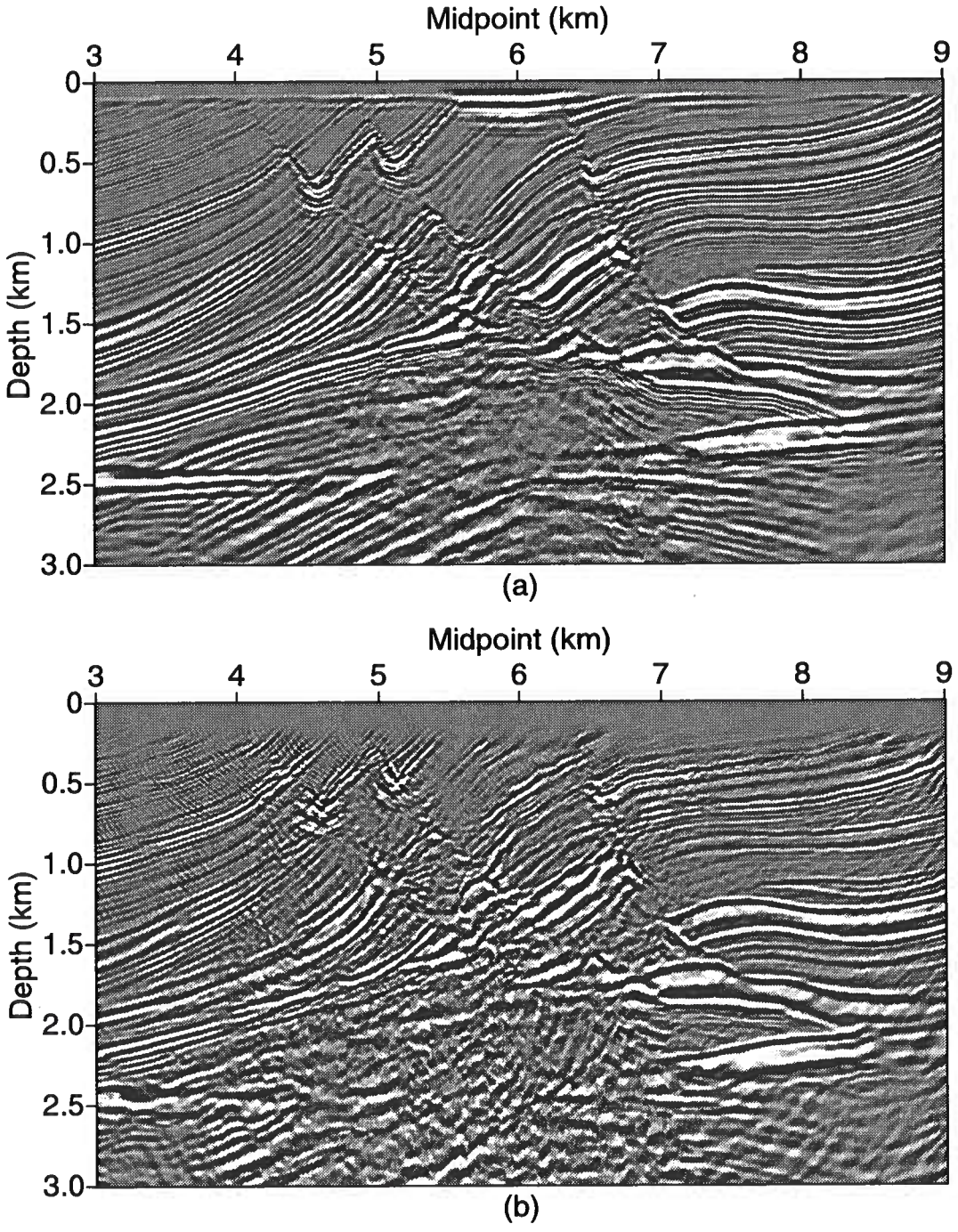

FIG. 4.15. Prestack depth migration of the Marmousi (a) original data, and (b) data contaminated with residual time anomalies.

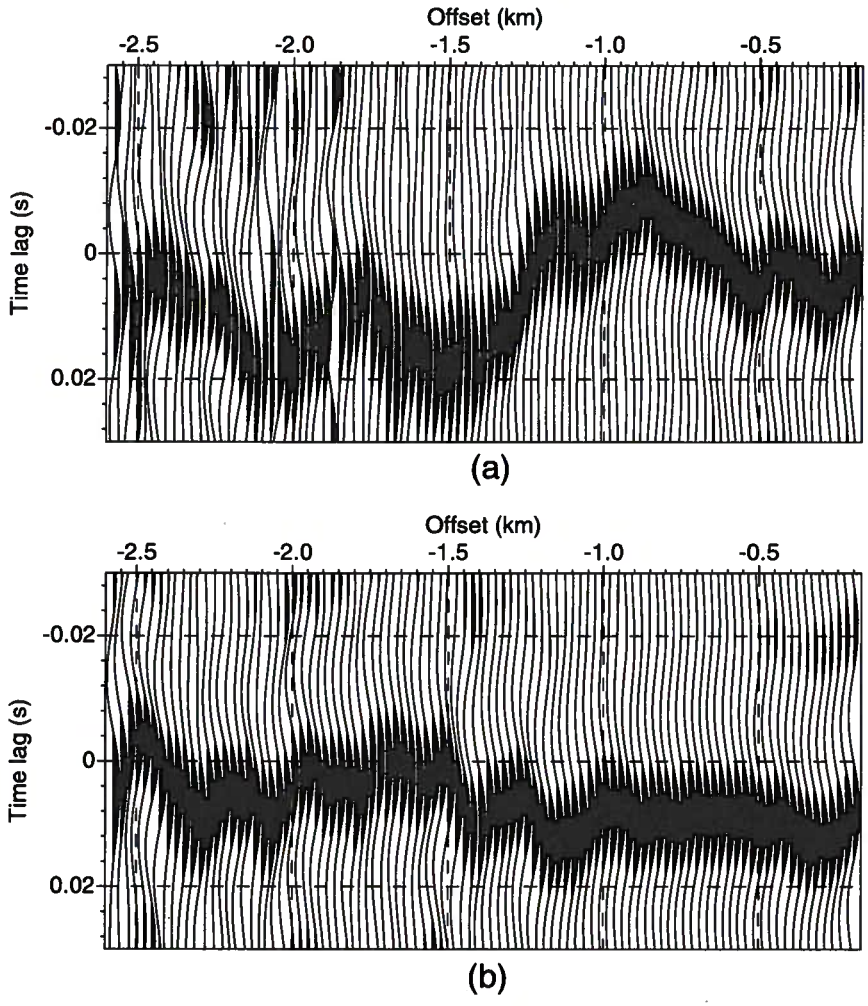

FIG. 4.14. Cross-correlation functions for (a) shot gather at location 7 km, and (b) shot gather at location 8.775 km. The cross-correlation is calculated between the original shots and those after the application of the methodology for modeling near-surface-induced time anomalies.

modeling scheme here because it cannot generate the first-arrivals associated with the new near-surface structure. Therefore, it is not possible to perform first-arrival refraction analysis on the modeled data after this process has been applied.

The distortions added to the Marmousi data by the wave-equation based methodology might seem too small to reduce our ability to obtain a good seismic image from this data set. To address this concern, I applied prestack depth migration to the original data, to be used as a reference, and to the data contaminated with residual time anomalies. The migrated section of the original data, seen in Figure 4.15a, exhibits good reflection continuity and sharp fault definition. By contrast, the migrated section obtained from the data contaminated with residual time anomalies, indeed exhibits poor reflection continuity almost everywhere, especially in the central part, where the model is highly complex. Away from the complex portion of the structural model, however, the image distortions are not so significant (see Figure 4.15b). These images thus confirm that these near-surface-induced time anomalies are large enough to distort the seismic data so much that it is impossible to get a good image if the anomalies have not previously been removed from the data. The estimation of a residual static solution for this particular problem requires special algorithms (Larner and Tjan, 1995) that take into account complications such as non-hyperbolic moveout, and event crossing in common-midpoint gathers. Those techniques, are beyond the scope of this research.

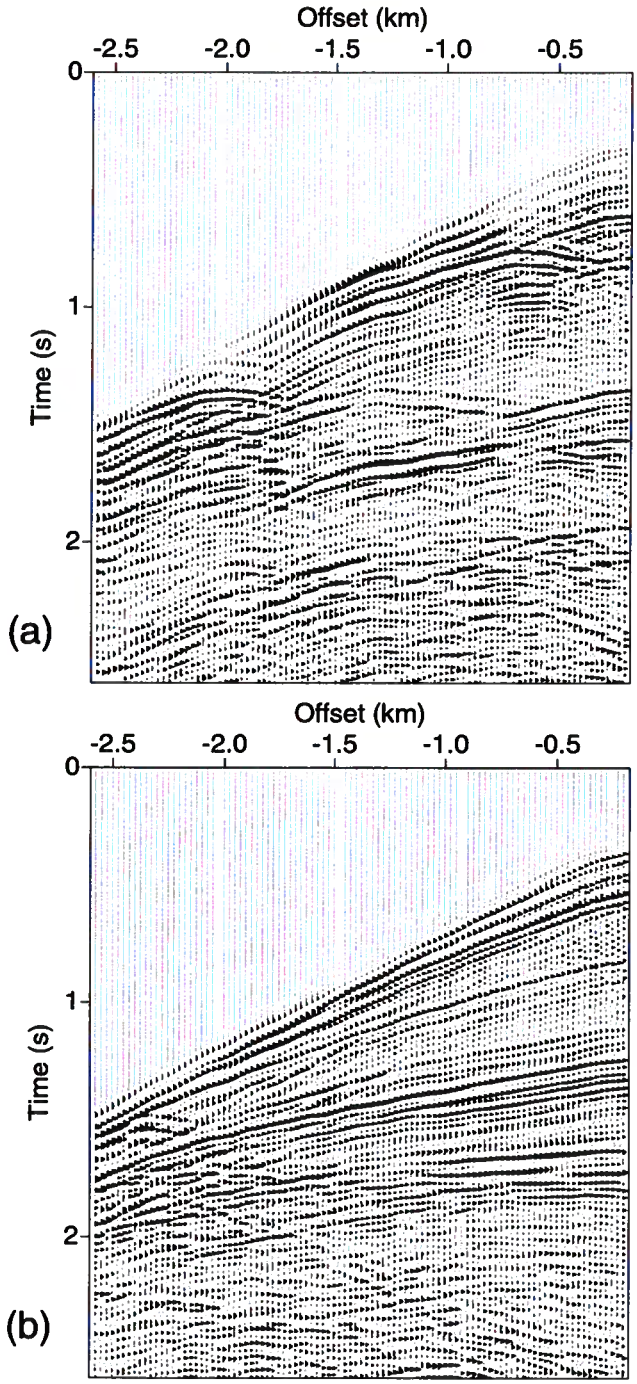

FIG. 4.13. Shot gathers at surface location (a) 7 km, and (b) 8.775 km after wave-equation datuming to go upward through the near-surface structure shown in Figure 4.9, followed by elevation-static corrections.

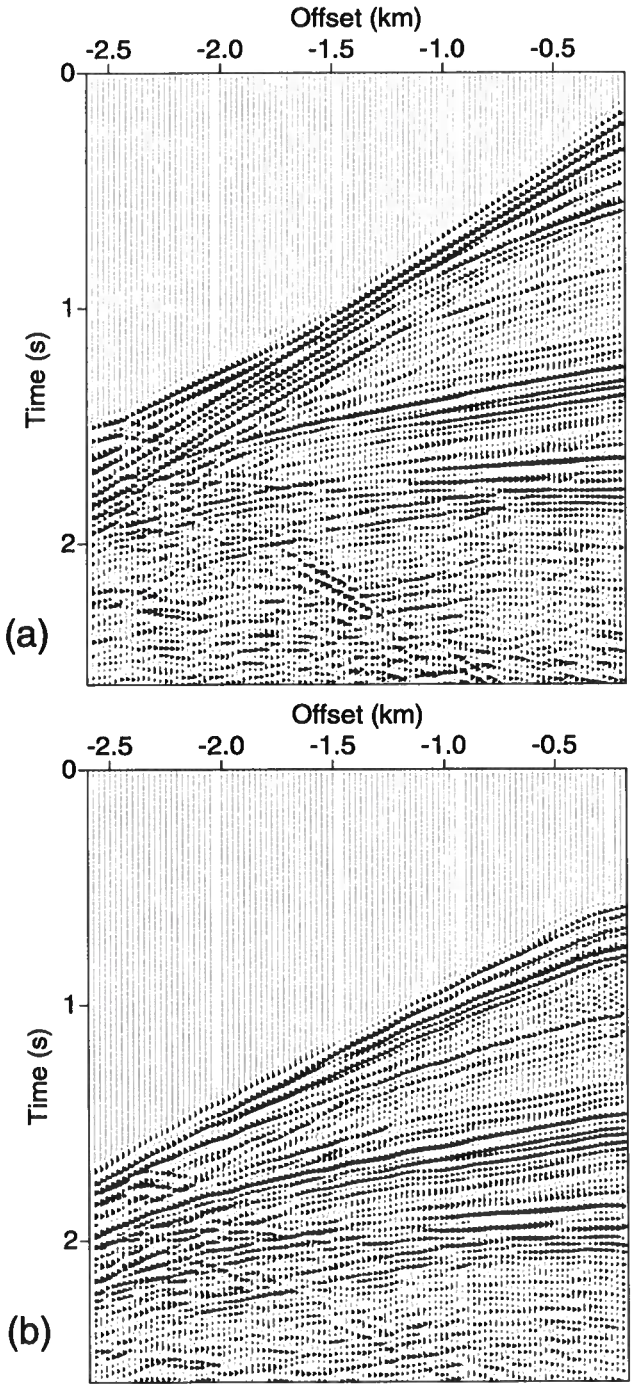

FIG. 4.12. Shot gather at location 8.775 km: (a) original data, and (b) data after wave-equation datuming to go upward through the near-surface structure shown in Figure 4.9.

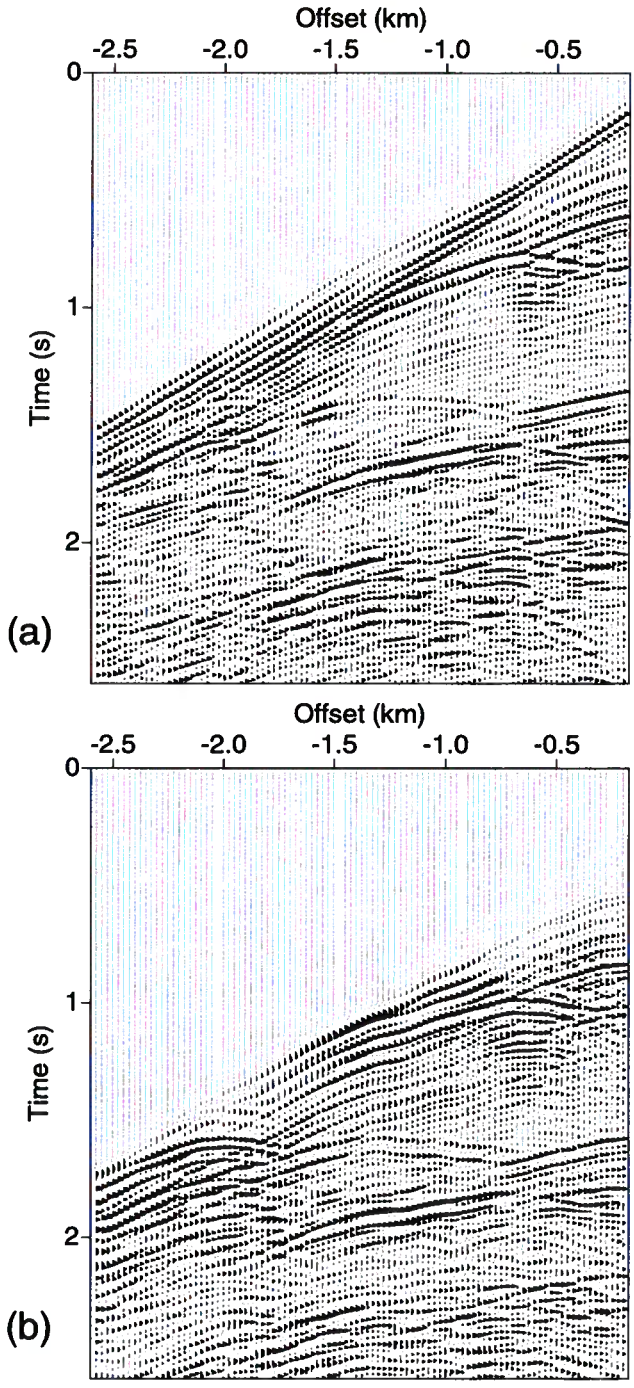

FIG. 4.11. Shot gather at location 7 km: (a) original data, and (b) data after wave-equation datuming to go upward through the near-surface structure shown in Figure 4.9.

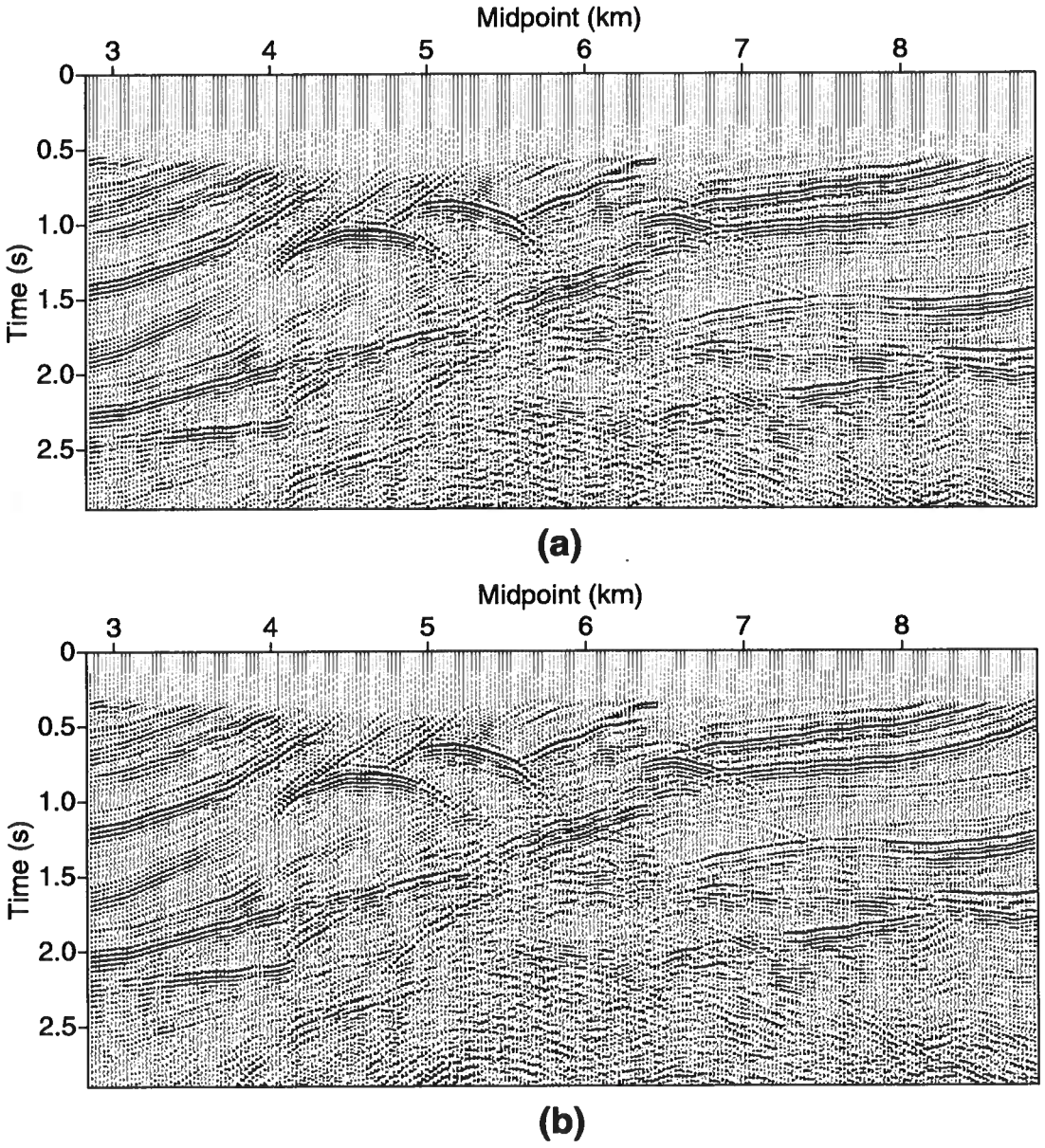

FIG. 4.10. Common-offset (300 m) time section from the Marmousi data set (a) after wave-equation datuming to go upward through the near-surface structure shown in Figure 4.9, and (b) after elevation-static corrections were applied to (a) to go down to the original datum.

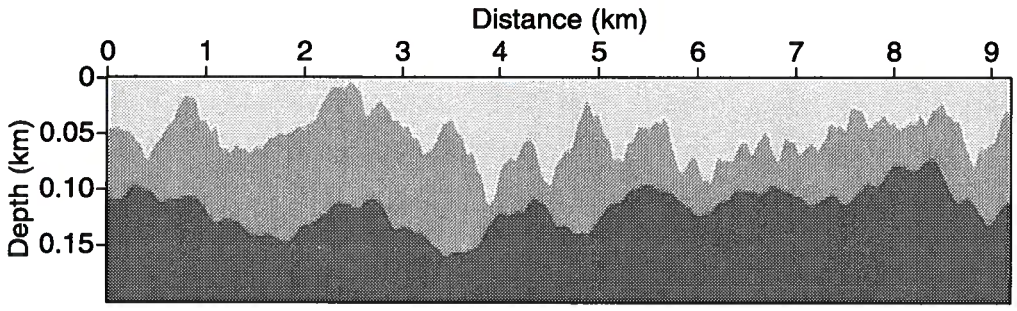

FIG. 4.9. Near-surface velocity structure to be superimposed on top the Marmousi structural model.

medium-frequency compare to those used by Larner and Tjan (1995) in their study; therefore, to obtain time distortions as large in amplitude and high in frequency as those, the near-surface model either has to be incredibly complex or we are overlooking something important in the wavefield-propagation process in the near-surface. The shallow velocity structure shown in Figure 4.9 generates total field-static corrections as large as 0.29 s.

Figures 4.11, and 4.12 show two shot records located at positions 7 and 8.775 km, respectively (see Figure 4.7), before and after the upward wave-equation datuming is performed. Figure 4.13 displays the two shot gathers after elevation-static corrections are applied to transfer the data to their original reference surface. Qualitatively, both shot gathers exhibit time distortions associated with the low-velocity layers. To verify quantitatively this observation, I compute cross-correlation functions between the original data and the resulting shot records of the modeling procedure (Figure 4.13). Figure 4.14 shows cross-correlations for the two shot gathers. These functions indicate that the near-surface-induced time distortions vary by as much as ± 20 ms, but they are not very short wavelength. The size of the distortions characterizes the complexity of the shallow velocity structure. Moreover, the time distortions exhibit long- and short-wavelength components similar to those commonly encountered in field data. Figure 4.14a shows a distortion pattern that includes not only high-amplitude, low-frequency components but also low-amplitude, high-frequency ones. On the other hand, Figure 4.14b shows only a high-frequency component, again with low-amplitudes in its distortions.

Additionally, we notice that since the energy associated with the first-arrivals is removed by the upward-continuation process, seismic events that were previously buried below their strong amplitudes are uncovered. Figure 4.11b shows a diffraction event at a time of 1.6 s and offset of -2.2 km that is hard to detect in Figure 4.11a. This particular action of the wavefield-extrapolation process has been discussed as a means for attenuating first-arrivals as well as ground-roll, by McMechan and Sun (1991). This characteristic of the wavefield-propagation process might represent a drawback of the

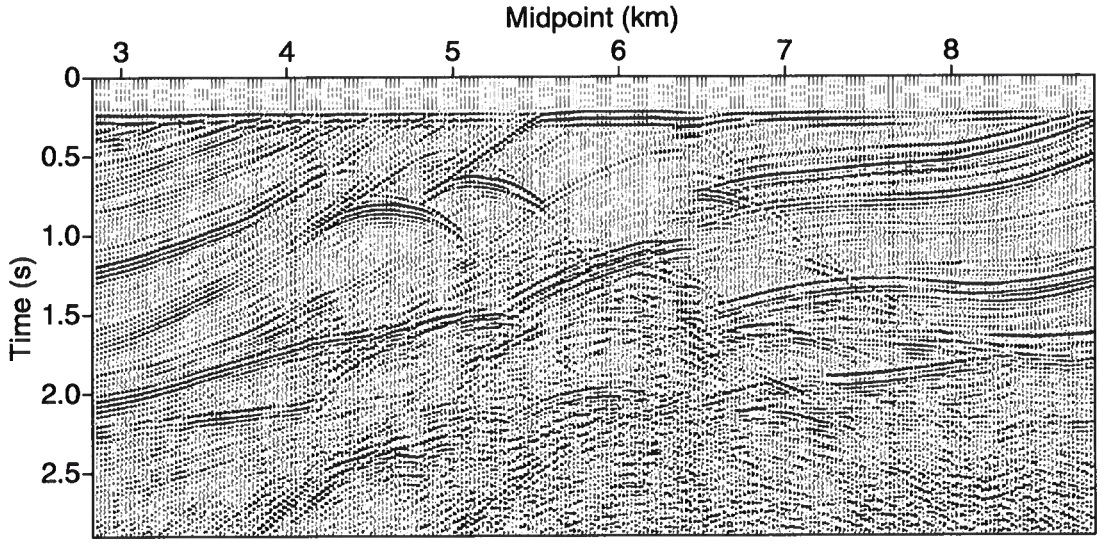

FIG. 4.8. Common-offset (300 m) time section from the Marmousi data set.

but also short-wavelength velocity anomalies associated with the near-surface (see Figures 4.10a, 4.11, and 4.12). The third and final step of this modeling approach is to redatum the seismic information to their original reference level by simulating application of elevation-static corrections. In practice, elevation-statics corrections are used to remove the long-wavelength components of the near-surface velocity anomalies to get the data to the stage where a residual statics analysis is required. Here, I estimate the time-invariant corrections assuming a constant velocity of 1560 m/s for the low-velocity structure. This velocity is computed by vertically and laterally averaging the velocity in the near-surface model (Figure 4.9). With this rough estimate of the near-surface velocity, I have tried to include the large uncertainties normally found in practice when first-arrival refraction-static analysis is used as a tool for velocity estimation.

To establish the distorting action of the near-surface velocity structure considered in this modeling study, I analyze the resulting data in the common-offset and shot domains. Figure 4.10b shows the common-offset section for a source-receiver distance of 300 m after the modeling methodology is applied. The section exhibits strong kinematic distortions in its central part, where the shallow structural model has maximum complexity (compare with Figure 4.8). Although not obvious from the display, at a time of 0.8 s and at about midpoint 7.5 km in the common-offset section, low-amplitude, medium-frequency time anomalies show the distorting action of the near-surface velocity model. Furthermore, most of the diffraction patterns are largely distorted. However, although the low-velocity layers used in the upward continuation process (Figure 4.9) offer high complexity, the time distortions associated with them are not as high-frequency as we expected. These time anomalies are low- to

section for a source-receiver distance of 300 m. This time section exhibits strong diffraction patterns that portray the distorting lateral velocity changes throughout the whole structural model.

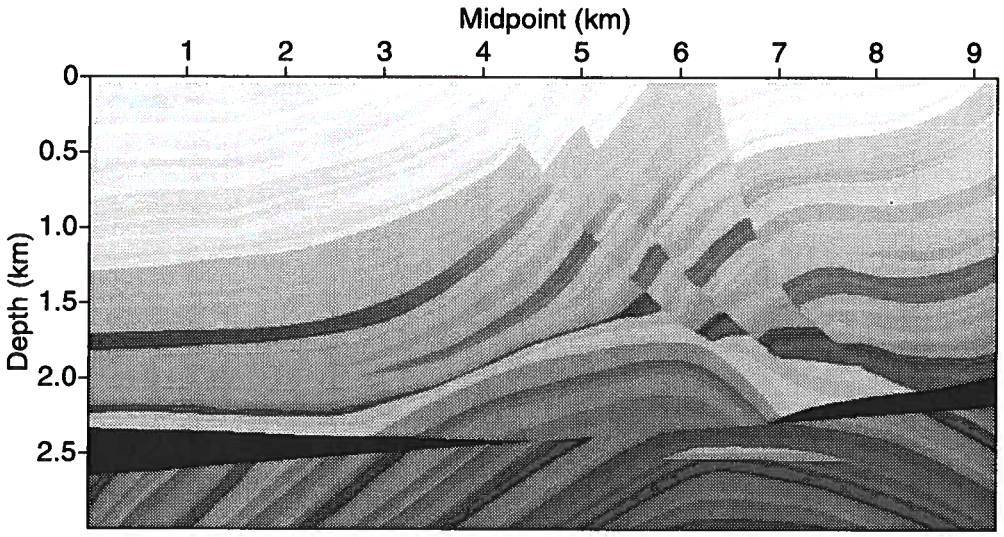

FIG. 4.7. The Marmousi structural model. The velocities range from 1500 m/s to 5500 m/s. The medium velocity is represented by the shading, the higher the velocity, the darker the shade.

Let us use the wave-equation-based methodology to contaminate the Marmousi data set with realistic time anomalies. The first step in this process is to build the near-surface velocity structure to be located on the top of the original velocity model. Modeling with realism is not a simple task considering the general lack of knowledge about the true complexity of the near-surface in practice. Furthermore, even if we were able to specify an acceptable near-surface velocity structure, there would be a doubt that results for any model studies could be sufficiently generalizable. On the other hand, I believe that much can be learned about this modeling methodology using complex near-surface structures such as that offered in Figure 4.9. This model consists of three near-surface layers with velocities of 1000, 1500, and 2000 m/s from top to bottom, respectively. The shallow velocity structure includes wavelengths as small as 100 m.

The second step of the modeling process is to upward continuation of the Marmousi prestack data through the shallow velocity structure using wave-equation datuming. To reduce artifacts as a results of the upward continuation process, the velocity field was smoothed with an operator length of 50 m. After this process, the data simulate the wavefield that would have been recorded if the original structural Marmousi model had included the shallow velocity structure illustrated in Figure 4.9. Now these data resemble land field data, in the sense that they contain not only long-wavelength

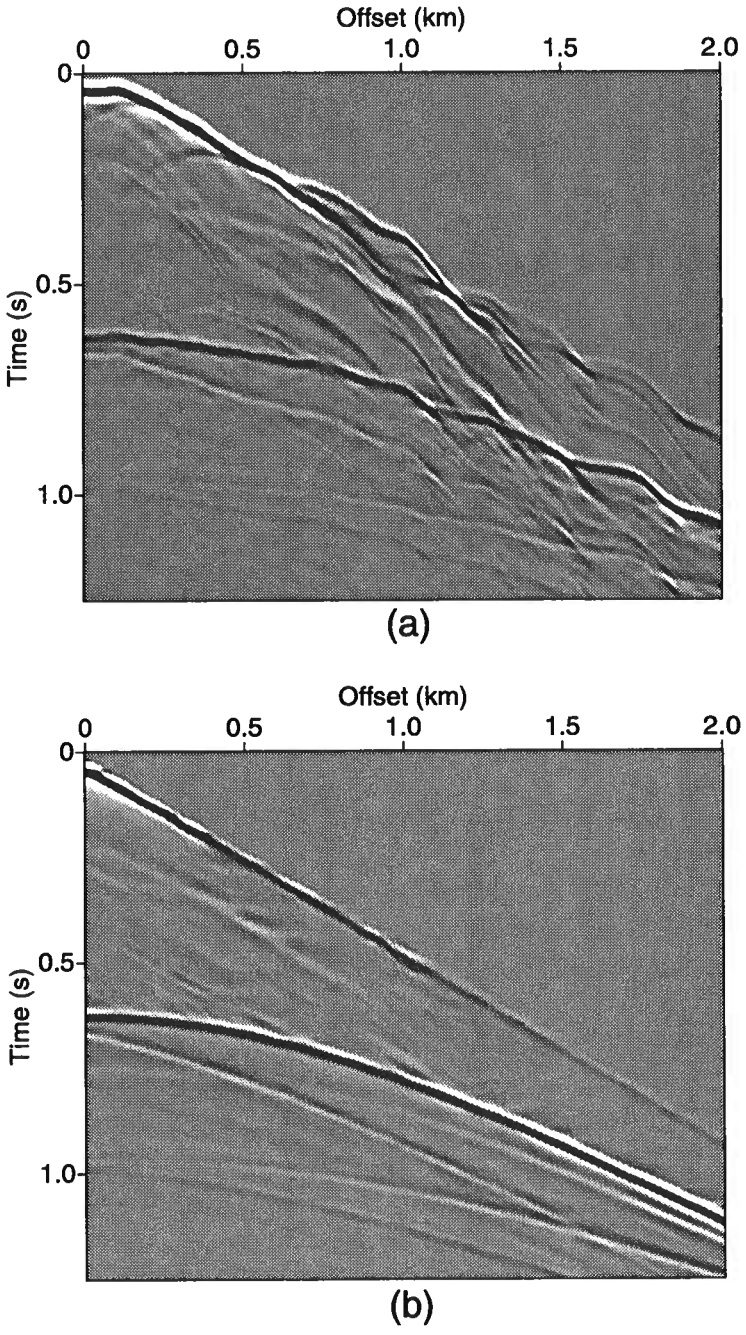

FIG. 4.6. Synthetic shot gather with geometry B after datuming the receivers down to a datum level at a depth of 350 m using (a) conventional static-time shifts, and (b) the Kirchhoff datuming.

estimation procedure by calculating and applying the required vertical-time shifts to the shot gather seen in Figure 4.5. The result of that process is shown in Figure 4.6a. The static time-shifts correct part of the kinematic distortions, especially those concentrated near the short-offsets, but cannot account for the focusing and defocusing action of the shallow-velocity structure.

Kirchhoff datuming, in contrast, gives an almost perfect result, as seen in Figure 4.6b. The diffraction patterns observed on Figure 4.5 are unraveled to a great degree, giving a result that simulates well a shot gather acquired with source and receivers located at a depth of 350 m.

The wavefield propagation throughout a complex near-surface velocity structure produces focusing and kinematic distortions on seismic data. From the results of these synthetic examples, I conclude that the static-corrections can solve, with some degree of accuracy, purely kinematic distortions, but cannot correct any distortions associated with focusing. On the other hand, Kirchhoff datuming can accurately unravel kinematic and focusing distortions from seismic data. For this reason, wave-equation datuming should prove to be a good tool for modeling near-surface-induced time distortions in the testing of alternative static-estimation algorithms.

4.3.2 Marmousi model contaminated with near-surface time anomalies

I now explore the applicability of the modeling methodology, described in the previous section, for superimposing a complex near-surface structure on top of the Marmousi data set and generating realistic residual-time anomalies. This data set has been used in several papers as a testbed for multiple purposes. In particular, Larner and Tjan (1995) tested their algorithm for residual static estimation, with promising results, on structurally complex areas using the Marmousi data set simplistically contaminated with surface-consistent-static time shifts that did not include wavelength longer than the cable length. Moreover, their static time shifts were random, zero-mean, and uniformly distributed between -20 and 20 ms.

Here, I use a wave-equation-based methodology to contaminate the synthetic data in an attempt to simulate realistic time anomalies that might resemble those commonly found in land data. The Marmousi data set consists of 240 shot gathers each of them with noise-free 96-channels (sampled at 4-ms interval). The first and last shot points are located at 3 and 9 km, respectively, from the west edge of the model (see Figure 4.7). Both the shotpoint spacing and receiver group interval are 25 m, yielding a maximum CMP fold of 48, and offsets range from 200 m to 2575 m. The synthetic data simulate an off-end marine geometry. The structural model exhibits large folding and faulting; therefore, the velocity across the model varies significantly. The outcropping formations around the midpoint located at 6 km in the model generate good examples of time distortions due to near-surface long-wavelength lateral velocity variations; however, short-wavelength lateral variations associated with a low-velocity structure are not present in the original data set. Figure 4.8 displays the common-offset time

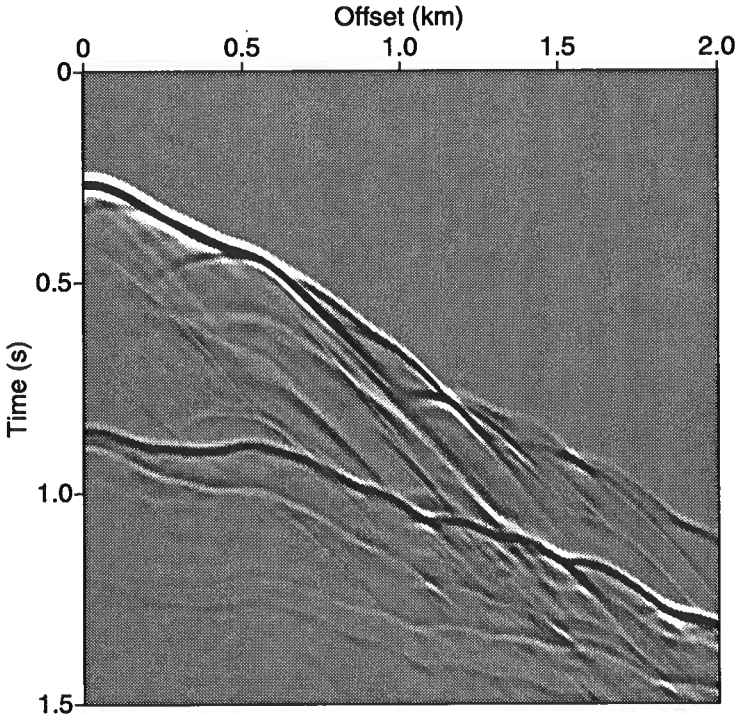

FIG. 4.5. Synthetic shot gather using geometry B generated with a full waveform FD modeling algorithm.

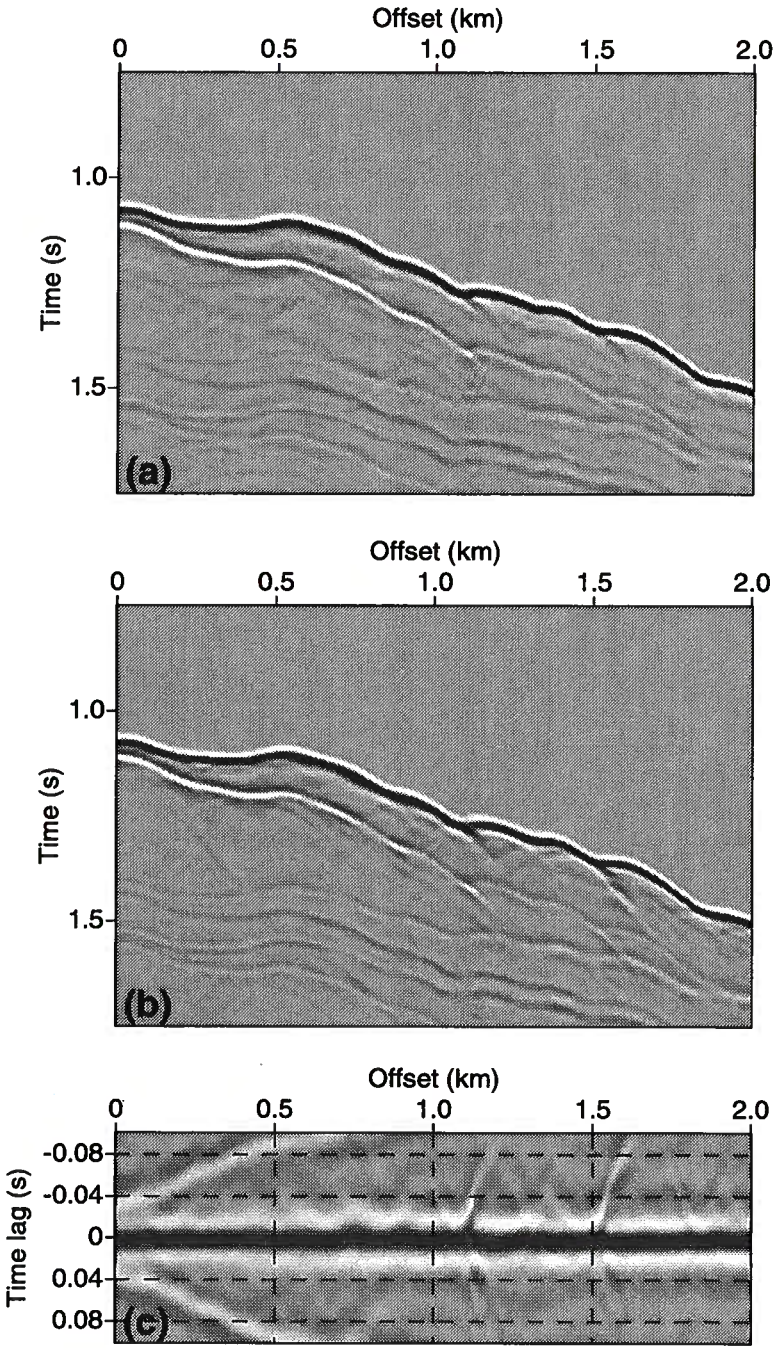

FIG. 4.4. Modeling of near-surface time anomalies: (a) synthetic shot gather with geometry A after using datuming to effectively reposition the receivers at the surface, (b) synthetic shot gather modeled with the source and receivers located on the surface, and (c) cross-correlation function between (a) and (b).

multiples, however, is supported by this remodeling scheme. To transfer the receivers from a depth of 350 m to the surface, I use a Kirchhoff datuming approach applied in the shot domain. The result of that process is shown in Figure 4.4a. Several features in the shot gather are worth noticing. Time and focusing distortions are evident in the reflection from the deeper interface as a result of propagating the wavefield throughout the shallow low-velocity structure (see Figure 4.2a).

Phantom diffraction patterns (Claerbout, 1985), are strong evidence of the focusing and defocusing action of the low-velocity distorting medium. Because such diffractions have nothing to do with the deep horizontal interface on which they are seen, they are termed phantom diffractions. It is hard to believe that a similar action could be simulated using just surface-consistent, static-time shifts. In practice, those diffraction patterns might produce instability in the traveltime picking process in residual-static estimation schemes (Perez, 1996).

To evaluate the accuracy of this modeling procedure, I cross-correlate the shot gather modeled with the source and receivers on surface seen in Figure 4.4b, with the synthetic gather generated with the upward extrapolation process shown in Figure 4.4a. The cross-correlation function of the shot gathers displayed in Figure 4.4c, illustrates a fairly good match between them (i.e., nearly zero shift of the dominant peak). The small differences between the two shot gathers could be attributed to inaccuracies in the ray-tracing procedure and definitely to the use of two different modeling approaches. At this point, I have to acknowledge that although the Kirchhoff formulation is a wave-equation-based approach, it, itself, is still just an approximation. The two-step modeling scheme could be much less expensive than full waveform FD modeling algorithm for the complete velocity structure.

Geometry B was used to compare the conventional static-estimation approach with the Kirchhoff datuming technique when applied to an heterogeneous near-surface velocity structure. Figure 4.5 shows the shot gather generated using the geometry B. Since the receivers are located on the surface and the shot is buried at a depth of 350 m, the distorting action of the low-velocity layers is observed only on the upgoing waves of the wavefield. Time and amplitude changes in both the direct-arrivals and reflection from the deeper interface are strong evidence of the distorting action of the weathering. Phantom diffraction patterns as a result of the focusing and defocusing processes due to the shallow velocity structure sometimes could mimic those associated with true faulting.

Figures 4.4a and 4.5 exhibit high similarity in the shape of the reflection event from the deeper interface. The large timing difference between the two shot records is due to differences in the location of the source for the two cases. For the shot gather displayed in Figure 4.4a, the source is located on the surface of the velocity model (Figure 4.2), while for the shot record in Figure 4.5, the source is buried at a depth of 350 m.

To transfer the receivers from the surface to a datum level at a depth of 350 m where the source is located, one could use a conventional static-estimation scheme or the Kirchhoff datuming approach. Let us now explore the conventional static-

features could violate the high-frequency approximation implied by the ray-tracing process in the Kirchhoff formulation (Bleistein, 1984).

I use geometry A to model time anomalies attributable to the top two low-velocity layers. Figure 4.3 shows the shot gather acquired with geometry A; it consists of 400 traces, with 1000 samples per trace at 2-ms sample interval and 5-m trace interval, and the source wavelet is a Ricker wavelet with a dominant frequency of 25 Hz. To simplify the interpretation of the time distortions on the deeper reflector, I subtract the energy associated with the first-arrivals (i.e., direct-arrivals, multiples, and diffractions) from the original synthetic shot record. To eliminate the first-arrivals from the original shot gather, I model a new shot gather using a velocity structure similar to the one used originally but that does not include the deepest interface. Then, I subtract the new shot record from the original one. Of course, the elimination of the conflicting events was perfect with this procedure.

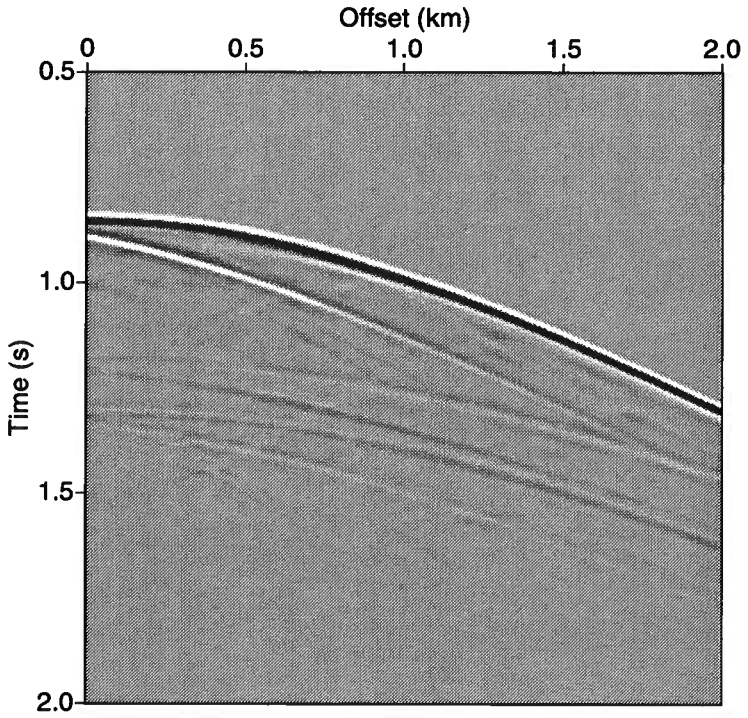

FIG. 4.3. Synthetic shot gather for geometry A generated with a full waveform FD modeling algorithm.

Here, the low-velocity structure acts only on the downgoing waves of the wavefield while the upgoing waves recorded by the receivers are not distorted, as illustrated by Figure 4.3. The distorting action of the near-surface velocity structure on the upgoing wavefield could be added to the shot gather of Figure 4.3 just by upward continuation of the data all the way to the surface where the source is located. No energy from

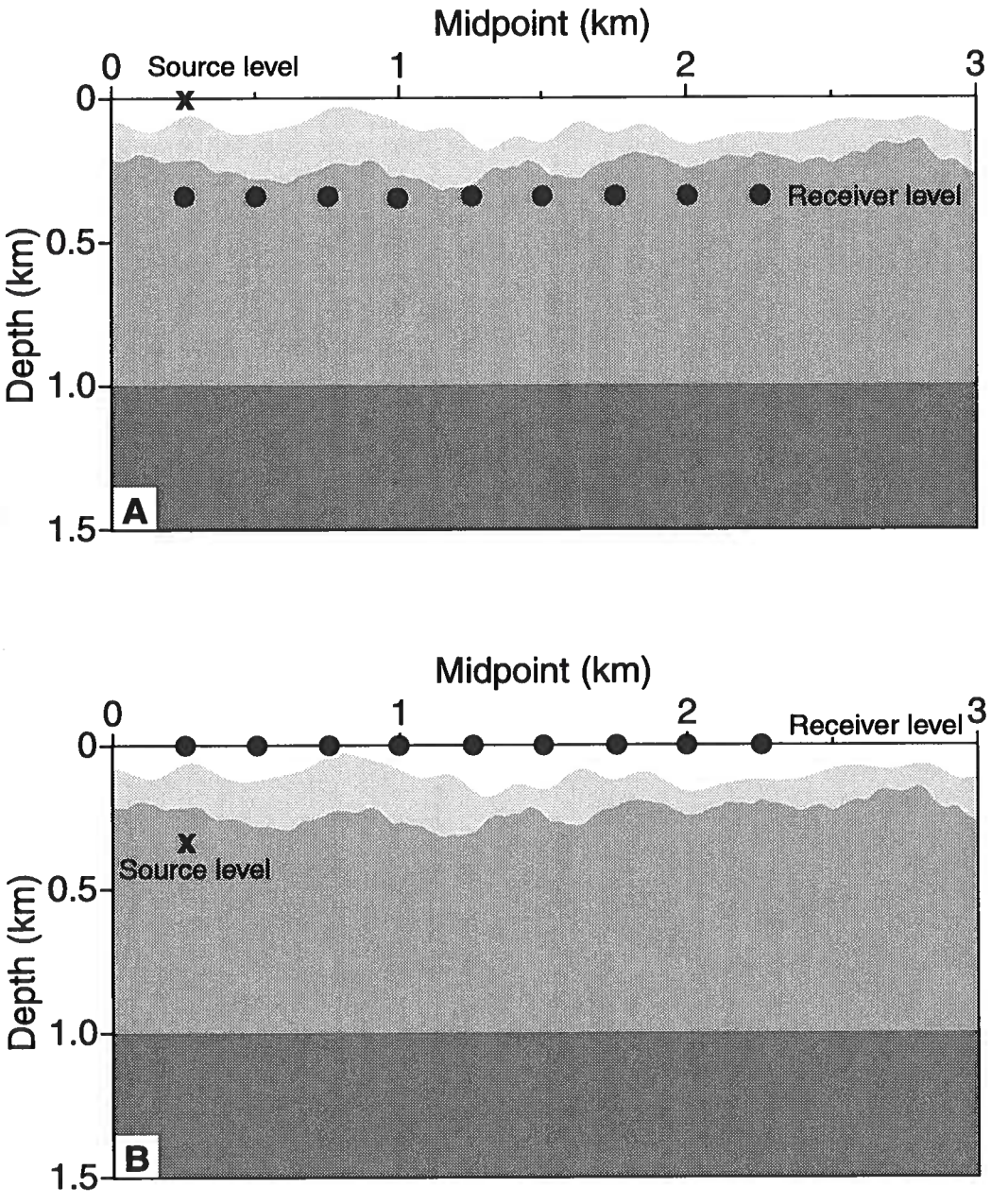

FIG. 4.2. Shot geometries A and B for a four-layer model. The velocity model consists of four layers of 1000, 1500, 2200, and 3000 m/s from top to bottom respectively.

using a fast algorithm such as ray-tracing, or a complex subsurface with a finite-difference modeling code. Then, using the procedure for remodeling the near-surface, any complex overburden can be superimposed atop the subsurface model. Here, we are interested in including topographic variation as well as laterally changing near-surface conditions above the subsurface velocity model. Wave-equation datuming is used to transfer the data from a flat original datum level to a curved surface that simulates topographic relief. Once the data are referenced to the topographic surface, elevation statics simulating the application of field-static corrections are applied to go back down to the original horizontal-recording surface, thus simulating field data that have had elevation statics applied. To compute the elevation-static corrections, we could use a smoothed version of the velocity structure used in the upward continuation step, or any other approximate velocity model selected for this purpose. The final result of this procedure is a data set contaminated not with residual statics but with residual time anomalies. This procedure simulates what is done in practice to get to the stage where residual-static analysis is required.

4.3.1 Modeling study for a single shot

In this section, I use the just-mentioned remodeling procedure to analyze its applicability and usefulness to modeling of near-surface time anomalies. Here, I test the procedure using a single shot. Later in this chapter, I offer a synthetic data example involving a complete seismic line. As mentioned in Chapter 2, prestack Kirchhoff datuming is applied first to the shot gathers, and then to the sorted receiver gathers (Figure 2.1). Therefore, to apply this process to a single shot, I use a particular set of geometries that do not require shot datuming. The algorithm is applied to the receivers exclusively. The geometries are:

- Geometry A.
  The shot position is located on the surface but the receivers are located 350 m below the surface (see Figure 4.2a). This geometry will be used to model near-surface-induced time anomalies.

- Geometry B.
  The shot position is located 350 m below the surface but the receivers are located on the surface (see Figure 4.2b). This geometry will allow to perform a comparative analysis between the conventional static approach and the Kirchhoff datuming technique to compensate for near-surface-induced wavefield distortions.

In order to compare the results of this procedure with its counterpart shot gather modeled with source and receivers on the surface, instead of using ray-tracing I use a full waveform 2D finite-difference modeling code (Fei, 1994). The velocity structure used in this modeling study is illustrated in Figure 4.2. The top two layers of the shallow-velocity structure include features with wavelength as small as 100 m. Smaller

Particularly important for this research is the presence of rugged terrain and complex near-surface characteristics that will allow us to compare different imaging strategies in an attempt to find an approach that is well suited to deal with such a large complexity.

In general, the synthetic data set offers good accuracy and data complexity. Spurious events, nevertheless, are also present in the data; for example, reflections from the sides of the model arise, indicating that the performance of the absorbing boundaries used in the modeling process was not perfect. Fortunately, I found that these noise patterns were not significantly troublesome for the imaging comparisons.

5.3 Comparison of datuming approaches

5.3.1 Static shift versus Kirchhoff datuming

Here, I explore the benefits of using wave-equation datuming as opposed to the conventional static approach when the velocity information of the near-surface is perfect. The overthrust model exhibits a complex near-surface characterized by high-velocity outcropping formations and important changes in topographic elevation throughout the seismic profile. For reference, a detail of the shallow velocity structure is given in Figure 5.4. The high-velocity wedge in the middle of the model gives rise to large raypath deviations from the vertical as the waves propagate through the near-surface; this situation compromises the performance of the simple static-correction approach in this overthrust acquisition environment. Moveout distortions attributable to the large static corrections greatly conspire against the accuracy of subsequently applied wave-equation-based processes; this problem is particularly significant in prestack depth migration because of its sensitivity to timing errors in the input data.

Most of the imaging algorithms used in the processing of the synthetic examples shown in this dissertation follow a nonrecursive Kirchhoff formulation, and all of them depend greatly upon ray-tracing to build their extrapolation operators. As in other high-frequency approximations, accuracy in the paraxial ray-tracing for prestack Kirchhoff datuming and prestack depth migration requires some degree of smoothing of the input velocity structure. For the smoothing, the velocity field was subjected to the damped least-square minimization procedure proposed by Liu (1993). The procedure attenuates the first spatial derivatives of the field, minimizing in the least-square sense, a weighted sum of the deviations between the true velocity structure and the smoothed one. After testing different operator lengths from 50 m to 300 m (165 ft to 985 ft), a length of 150 m (490 ft) in both vertical and horizontal directions was chosen, qualitatively, based on imaging quality.

Now let us compare the performances of the wave-equation-based and the static datuming approaches in the shot domain for the gathers at locations A and B; later, we will study the differences in terms of imaging quality after prestack depth migration. Figure 5.5 shows the shot gathers after transferring the sources and receivers from

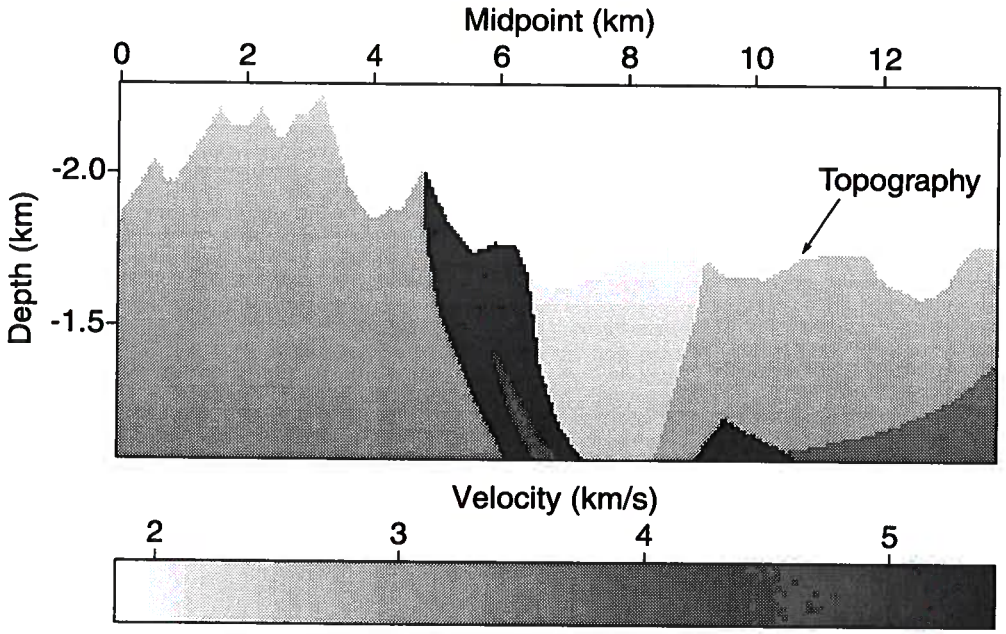

FIG. 5.4. True near-surface velocity model.

topography to a datum level of -1.22 km using Kirchhoff datuming. Comparing these shot records with those in Figure 5.2 and 5.3, we see that the most severe of the time distortions associated with the shallow-velocity structure are largely corrected. The residual nonhyperbolic moveout is related to the strong lateral velocity variations in the subsurface structural model beneath the datum level. Quite nicely, the diffracted energy (i.e., phantom diffraction patterns such as those observed in shot record A in Figure 5.2) associated with the edges of the high-velocity anomaly in the near-surface is focused after Kirchhoff datuming. Some artifacts are also observed in the resulting shot gathers presumably caused by aliasing in the input data (e.g., those high-dipping events observed in the deeper portion of the shot gathers in Figure 5.2). Overall, shot gathers A and B in Figures 5.5 and 5.3 exhibit satisfactory agreement. Differences, however, are evident such as these sequence of steeply sloping events in Figure 5.3a, which are largely attenuated by the dip-filtering action of the Kirchhoff datuming process. Other features at times larger than 3 s also show some differences; however, these events are mainly multiple reflections and reflections from the edges of the model that do not contribute to the final image.

For comparison, Figure 5.6 shows shot records A, and B after static corrections have been applied to redatum the data from the acquisition surface to a reference level of -1.22 km. Although they too have accomplished much correction of the data seen in Figure 5.2, unlike Kirchhoff datuming, static corrections are incapable of collapsing the diffraction patterns generated by the laterally-changing near-surface conditions.

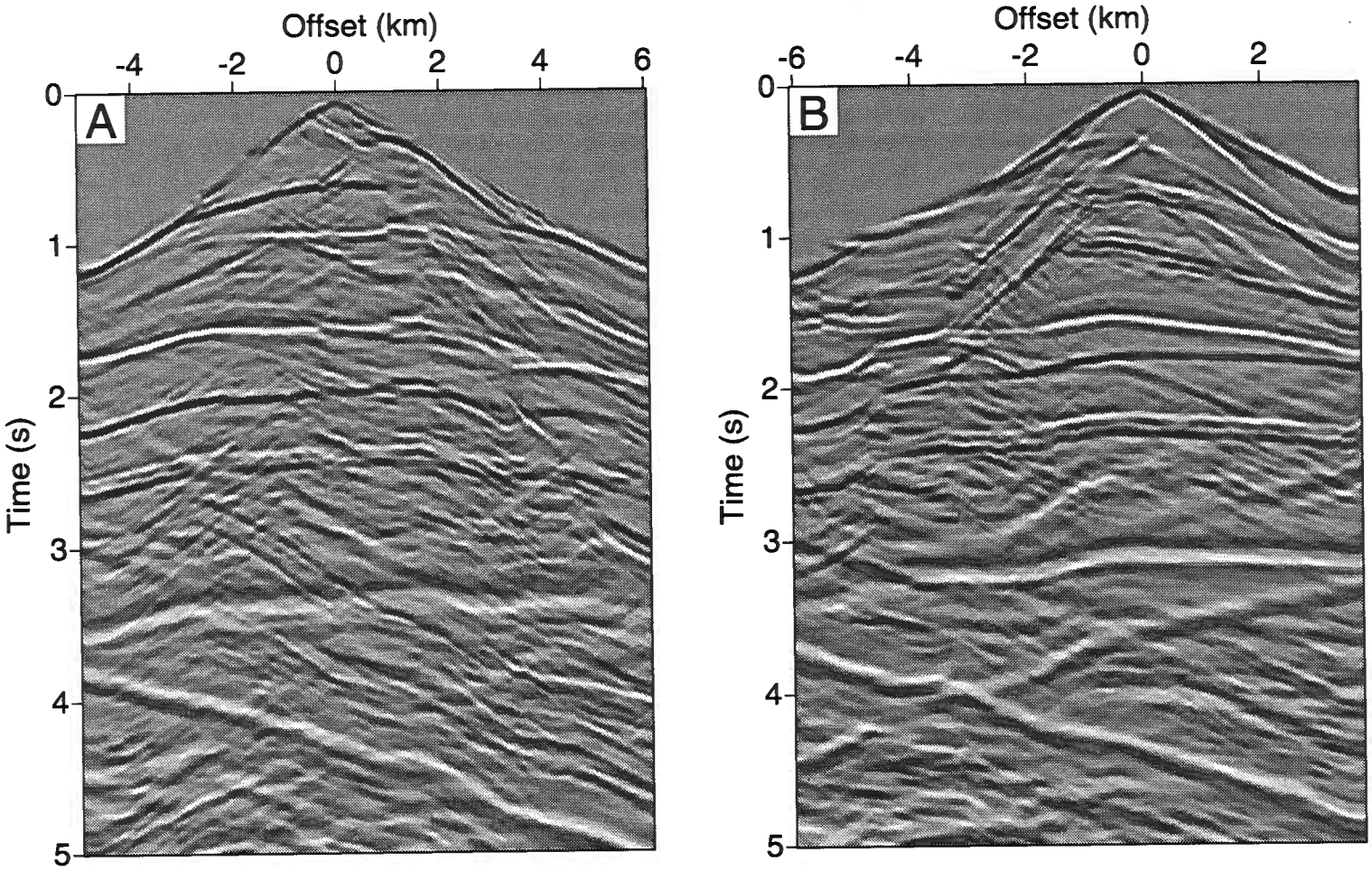

FIG. 5.5. Synthetic shot gathers after Kirchhoff datuming has been applied to transfer the data from topography to a datum level of -1.22 km.

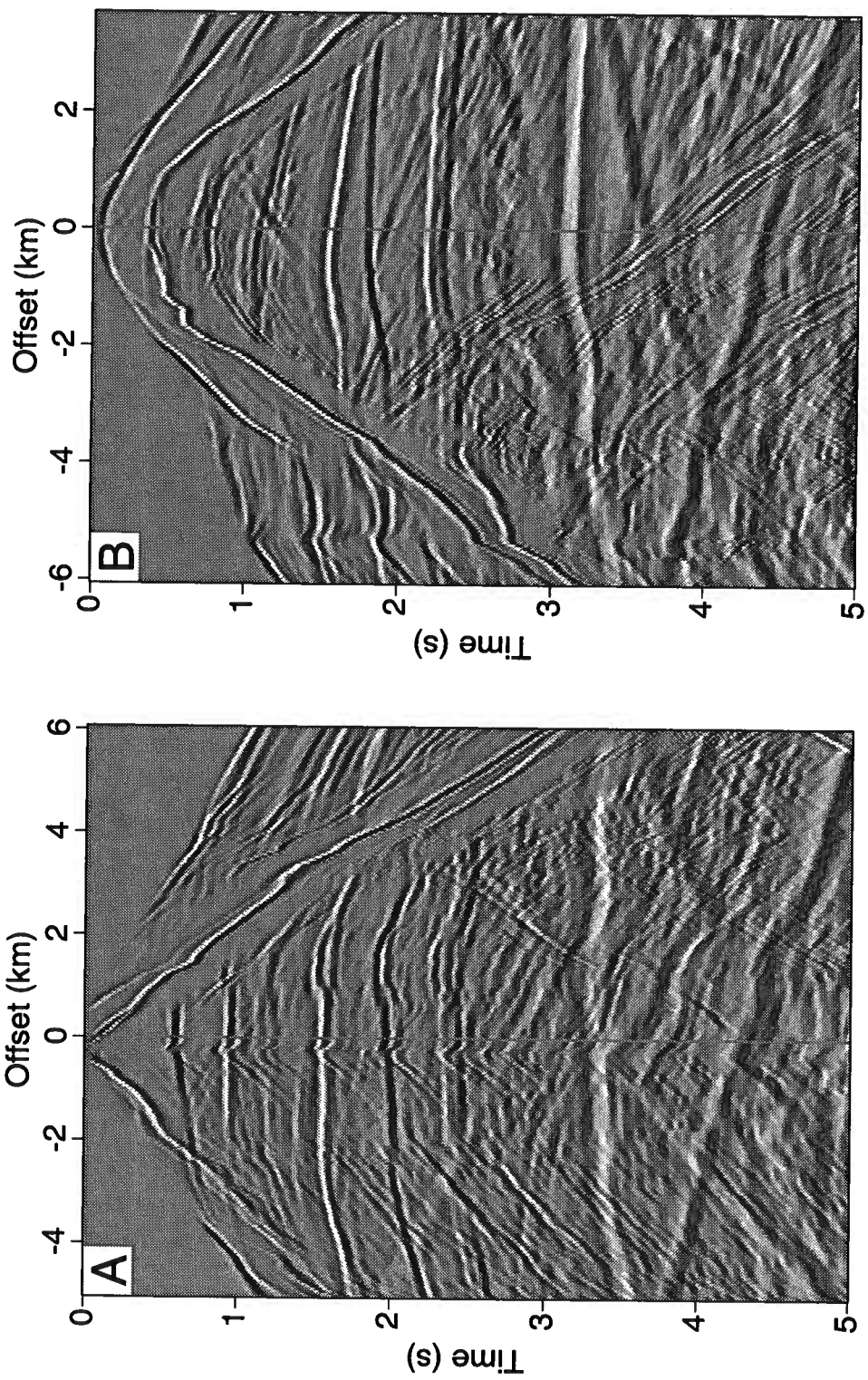

FIG. 5.6. Synthetic shot gathers after static corrections have been applied to transfer the data from topography to a datum level of -1.22 km.

Vertical-time shifts account for only kinematic distortions (and poorly so), modifying, the moveout of the seismic events in a manner inconsistent with the wave-theory.

Let us see the differences between the two approaches in terms of images quality after prestack depth migration. Figure 5.7a shows a migrated section obtained from the data processed with Kirchhoff datuming using the true near-surface velocity structure. The upper part of the data necessarily was muted during the downward continuation process; thus, the images are shown from the datum level at -1.22 km down. As desired, the image displays the general features exhibited by the structural model seen in Figure 5.1.

The deeper reflectors are well located relative to the structural model, and the upper fold at midpoint 8 km associated with the overthrust faults is well delineated, as are the fault planes. Also, the deeper folded structure below the elongated high-velocity feature at midpoint 5 km and depth of 1.5 km shows good reflector continuity in the horizontal direction, and quite nicely, even in the vertical direction at midpoint 7 km where the dipping interface has dip as large as 85 degrees. At a depth of 2 km, and a surface location of 8.5 km, the highest-velocity feature in the model is accurately resolved by the migrated section. To image this dipping reflector a total aperture of 10 km was required. Use of such a large migration aperture, however, generated strong artifacts on the resulting image; noise patterns, for example, are observed at the edges and at the bottom of the migrated section. Unfortunately, even with that large aperture, reflectors with dip of about 90 degrees are not imaged well enough, precisely because of aperture limitations. As is well known, in practice, to be able to image steep reflectors in any environment a sufficiently large aperture in time and space must be used; otherwise, steep features will be highly attenuated.

Figure 5.7b shows the migrated section obtained from the data processed with static-corrections. As mentioned earlier, the main problem for the conventional static datuming approach is concentrated in the area below the high-velocity anomaly of the near-surface. In that zone, the raypaths of the wavefield propagation deviate significantly from vertical, making the data obtained from the static solution not good enough for imaging of the deeper folded structure as well as when the Kirchhoff datuming is used. Likewise, the upper fold located at midpoints from 7 to 8 km is distorted giving an unsmooth structure that shows breaks not seen in the velocity model (Figure 5.1). On the other hand, the deeper sub-horizontal events at depths from 3 to 5 km in both Figures 5.7a and 5.7b show basically similar imaging quality; both are well defined relative to the structural model. As pointed out in Chapter 3, the shallower events can be more sensitive than the deeper ones to moveout distortions as a result of erroneous treatment of the near-surface time anomalies.

Outside the range of influence of the high-velocity wedge in the near-surface, both migrated sections exhibit similar imaging quality, indicating that for those areas the moveout distortions due to the conventional static corrections seem to be not too significant. This observation suggests that in areas where the near-surface is characterized by velocity that varies dominantly with depth, as in this portion of the model, the static approach could offer a satisfactory solution. This situation could

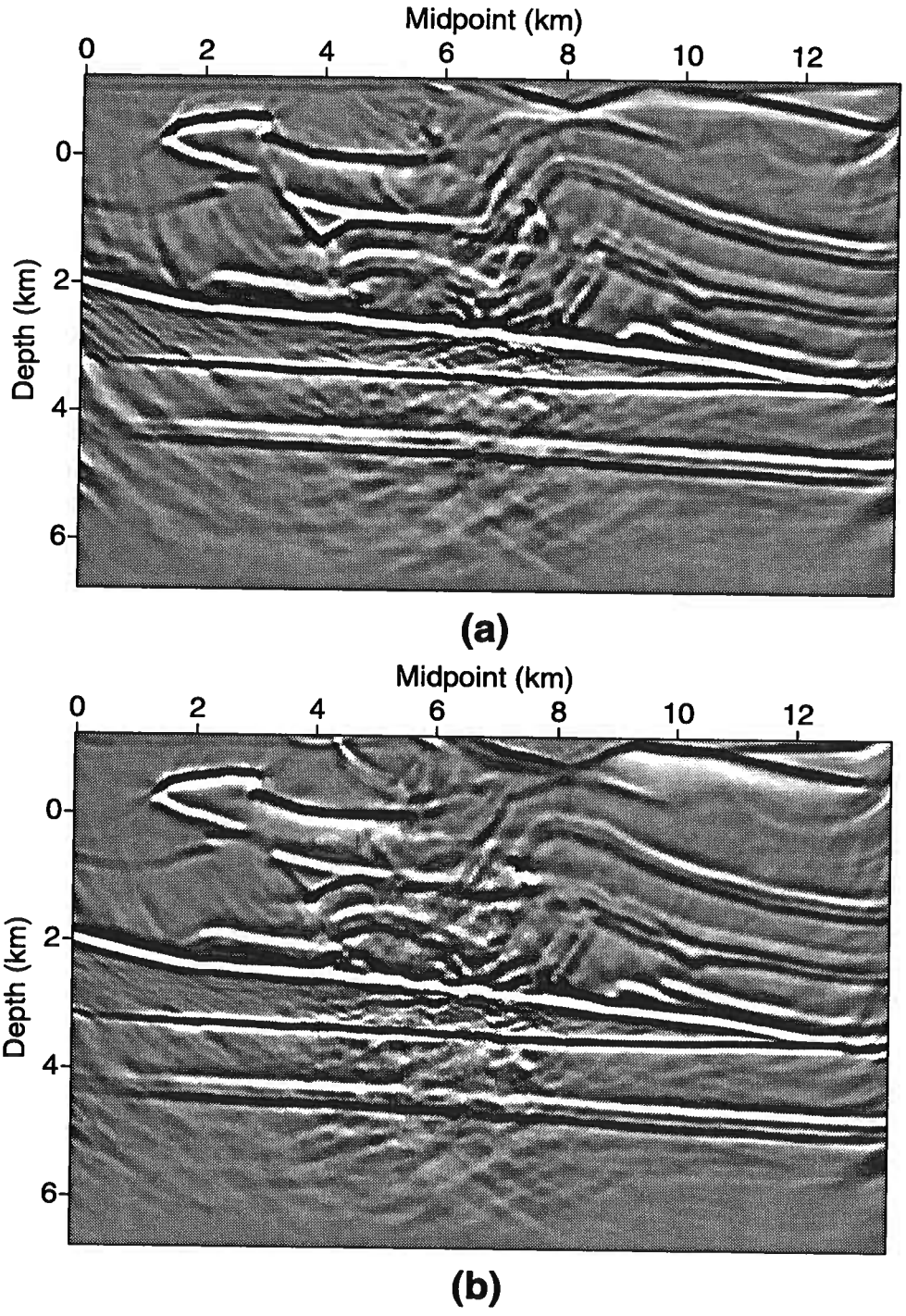

FIG. 5.7. Prestack Kirchhoff depth migration after (a) Kirchhoff datuming and (b) static-corrections, using the true-velocity model.

be explained by considering the general behavior of rays traced in $v(z)$ media. Close to the source the raypath is almost vertical, resembling the general characteristics of surface-consistent statics. Since the aperture of the wave-equation datuming is relatively small, the differences between the two datuming procedures (i.e., vertical-ray static and wave-equation-based) should not be extremely large. On the other hand, if the near-surface consists of high-velocity rocks that outcrop at the surface (e.g., the high-velocity wedge in this model), the statics solution is far from being acceptable because raypaths in the near-surface depart significantly from the vertical. Under those circumstances, the wave-equation-based methods seem to be required (at least in those cases in which the near-surface velocity structure is well known).

From this example, we can infer that since wave-equation datuming applies dynamic datuming corrections rather than static ones, reflection and diffraction events tend to be better reconstructed and, therefore, better images can be obtained after prestack depth migration, as long as the velocity model for the near-surface is accurate.

5.3.2 Finite-difference wave-equation datuming

As mentioned in Chapter 2, wave-equation datuming could be implemented using either a Kirchhoff integral formulation or finite-difference following the zero-velocity layer concept. One source of difference we can expect in results obtained with these two approaches is that the Kirchhoff approach, as implemented here, works with first-arrival, ray-traced times rather than those associated with the arrivals having the strongest energy. Here, for comparison I provide the finite-difference solution obtained with the commercial software ProMAX. This approach yields a full-waveform solution intended as a benchmark to assess the quality of my Kirchhoff datuming implementation. Shot gathers and Kirchhoff migrated sections from data processed with the zero-velocity, layer-datuming approach are shown in Figures 5.8 and 5.9.

Although the shot record A processed with finite-difference datuming (Figure 5.8) contains stronger artifacts (dispersion-related perhaps) than does the Kirchhoff result in Figure 5.5, it also better reconstructs some features in the data. In Figure 5.8, shot gather A has a reflection event at a time 1.2 s and offset 2.5 km that is better-defined than that in Figure 5.5.

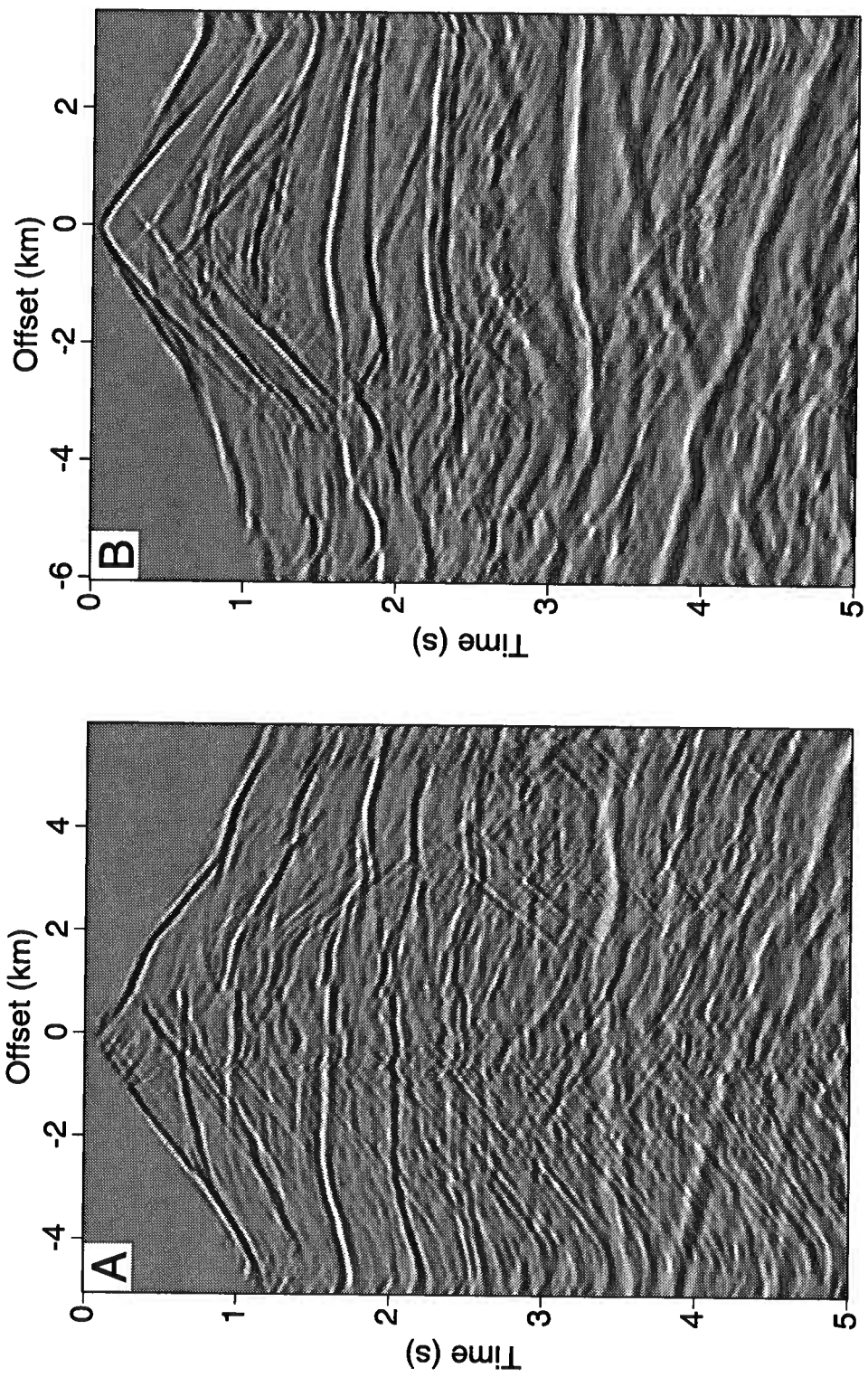

FIG. 5.8. Synthetic shot gathers after finite-difference wave-equation datuming has been applied to transfer the data from topography to a datum level of -1.22 km.

At an offset of 3 km and a time of 1.8 s is another example in which finite-difference results are better to some degree than the Kirchhoff ones. On the other hand, in shot gather B, the Kirchhoff approach gives a result close to that of the finite-difference method.

Not surprisingly, the discrepancies in reconstruction quality observed in these shot records are concentrated beneath the high-velocity anomaly in the near-surface. The main inaccuracy observed in the Kirchhoff datuming approach comes from the ray-tracing step. Even though the paraxial ray-tracing method has proven to work acceptably in many complex velocity models, it has limitations as do all ray-tracing algorithms. The near-surface high-velocity wedge represents an extreme case, with velocity changing abruptly from 2135 m/s to 5120 m/s (7000 ft/s to 16800 ft/s). Under these conditions, a full waveform finite-difference algorithm is more likely to produce better wavefield-extrapolation results.

For comparison between the migrated sections from the two datuming approaches (i.e., finite-difference and Kirchhoff), Figure 5.9a is a repeat of Figure 5.7a, while Figure 5.9b shows the migrated section obtained from the data processed with the finite-difference datuming approach. The two images are quite similar although the finite-difference result is somewhat sharper, with slightly more reflection continuity, as it was for the shot gathers. The slight loss of frequency content in the Kirchhoff implementation can be attributable to the action of the operator anti-aliasing filter, an important feature that is less severe in the finite-difference approach.

On the other hand, the Kirchhoff results in general exhibit better definition of the largest dips in the model than do those of the finite-difference scheme. For example, the dipping feature located at surface midpoint 8.5 km and depth 2 km, is better resolved on the image after Kirchhoff datuming than on that after the finite-difference approach. Similarly, the image processed with the Kirchhoff datuming exhibits better reflection continuity for the central fold located at surface midpoint 7 km and depth 1.5 km (i.e., dip of 85 degrees) than does the image processed with its finite-difference counterpart.

From this comparative analysis, I conclude that the finite-difference datuming implementation yields a slightly better solution than does the Kirchhoff approach under extreme laterally-changing near-surface conditions. Under these circumstances, the ray-tracing procedures, on which the Kirchhoff datuming approach is based, face difficult issues such as multi-valued traveltimes and head-waves that are implicitly taken into account in the full waveform finite-difference solution.

On the other hand, unlike my Kirchhoff implementation, this finite-difference datuming scheme has dip limitations that attenuate the steepest features in the data; in this sense, the Kirchhoff scheme is superior to this finite-difference implementation despite shortcomings associated with multi-valued traveltimes and the required smoothing of the velocity field.

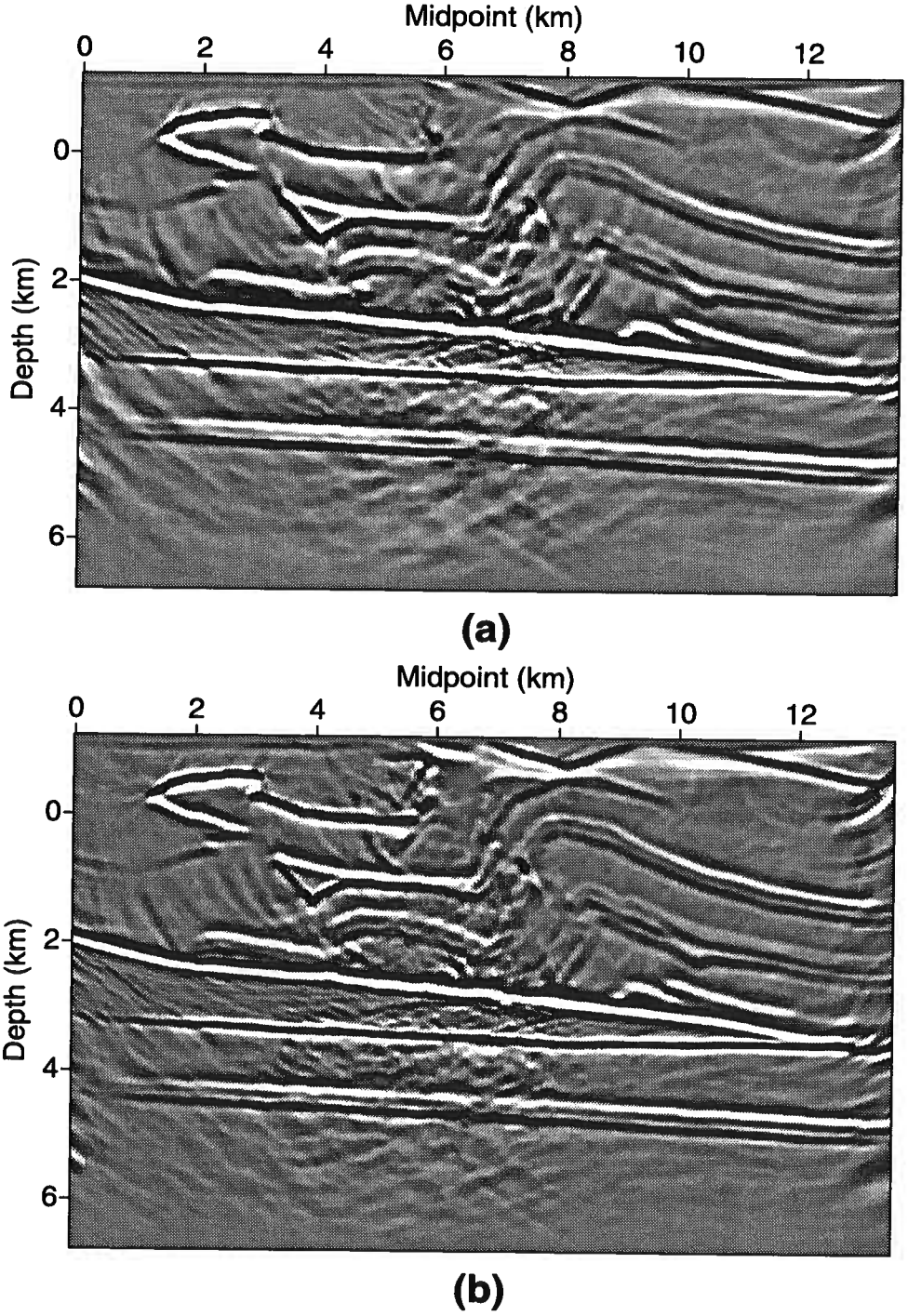

FIG. 5.9. Prestack depth migration after wave-equation datuming using a (a) Kirchhoff formulation and (b) finite-difference approach. Both processings were performed with the same velocity field.

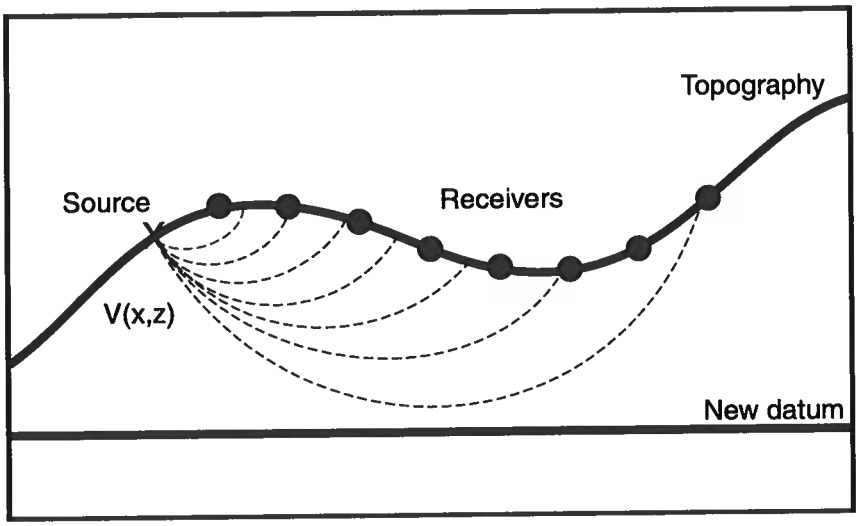

FIG. 5.10. Turning-ray tomography concept.

5.3.3 Turning-ray tomography analysis

An essential element to perform the datuming process is to have a reliable estimate of the near-surface velocity structure. Historically, first-arrival refraction-static analysis have been used as a tool to obtain information on the near-surface velocity structure. Unfortunately, refraction-static analysis can give poor results in overthrust areas, where frequently the near-surface geology includes high-velocity rocks outcropping at the surface, yielding geometries that are far from the simple layered model. Conventional refraction-static analysis depends upon the existence of head waves or diving waves generated by identifiable high-velocity refractors; thus, the first-arrivals are modeled as refracted energy traveling along the interfaces between layers.

An alternative technique for estimating the near-surface velocity structure is turning-ray tomography. Applications of tomographic velocities to account for near-surface time anomalies have come into practice recently (Zhu et al., 1992, and Stefani, 1995). Unlike refraction methods, turning ray-tomography incorporates vertical and horizontal velocity gradients in the representation of the near-surface structure. In the turning-ray concept, the first-arrivals represent continuously refracted direct raypaths propagating in a continuous, general $v(x, z)$ medium. The velocity gradients in the velocity field make downgoing rays turn gradually, bending the rays upward and back to the surface where they are recorded (see Figure 5.10). Perhaps the primary drawback of this technique is that it still depends upon the quality of picked first-breaks, as does refraction-static analysis. It does not, however, require one to associate arrival times with specific refracting interfaces.

In practice, the target medium is discretized into a grid of rectangular cells, each of which contains a single velocity. The basic procedure for estimating near-surface velocities using turning-ray tomography involves an iterative minimization of

the differences between the picked first-arrivals and predicted traveltimes obtained by tracing turning-rays through this discretized medium. Using all the raypaths and those traveltime differences, the initial velocity field is adjusted to reduce the traveltime residuals.

To estimate the near-surface velocity field of the overthrust structural model, I used results of turning-ray tomography. Dr. Xianhuai Zhu of Union Pacific Resources performed this tomography analysis, and kindly provided me his tomographic solution for the shallow-velocity model. The near-surface structure included in the tomography analysis went from the topographic surface to a datum level of -1 km. The size of the rectangular cells was 50 m (165 ft) in the horizontal direction, and 12.5 m (41.25 ft) in the vertical direction, and the initial guess consisted of a constant vertical gradient in velocity starting from the irregular topographic surface.

Figure 5.11 shows the near-surface velocity structure obtained from the tomographic analysis. The tomographic model is a smooth approximation of the true velocity field (Figure 5.4), with the high-velocity anomaly in the central part of the model satisfactorily resolved considering the complexity of the inversion problem. Below, I will use this tomographic model for part of an analysis of sensitivity of the datuming techniques to error in the near-surface velocity structure. I also use it in the analysis of the influence of such errors on the quality of the stacking velocity functions.

5.3.4 Tomo-statics versus tomo-datuming

Once the near-surface velocity model is estimated from a tomography analysis, two alternative approaches could be pursued to correct for near-surface-induced time distortions: (1) statics correction (tomo-statics), and (2) wave-equation datuming (tomo-datuming) (Zhu et al., 1992, 1995). Figure 5.12 shows shot gathers A and B after the tomo-statics solution was applied. These shot records should be compared with those in Figure 5.6. Since the tomographic velocity model agrees reasonably well with the long-wavelength component of the true velocity structure, it is hard to find much difference between the static-corrected shot gathers in Figure 5.12 and those in Figure 5.6. The medium- to short-wavelength components in the true near-surface model not resolved, in the smoother result of the inversion technique, are responsible for the differences seen in Figures 5.6 and 5.12, such as those at offset 1.5 km and from time 1.5 s to 2.5 s in shot gather A. Later, we will see that these small differences distort significantly the quality of the images after migration.

Figure 5.13, on the other hand, shows shot records A and B after tomo-datuming. If the tomography-based estimates of the near-surface velocity structure are sufficiently accurate, wave-equation datuming would yield better results than those obtained with statics corrections (Figure 5.12) because, even though both processes use the same velocity model, tomo-datuming honors the wave-theory. Shot record A after tomo-datuming (Figure 5.13), nevertheless, seems to show more time distortion than does shot record A after tomo-statics. This should not be surprising, since in Chapter 3 simple synthetic examples exhibited the same relative behavior when the near-surface

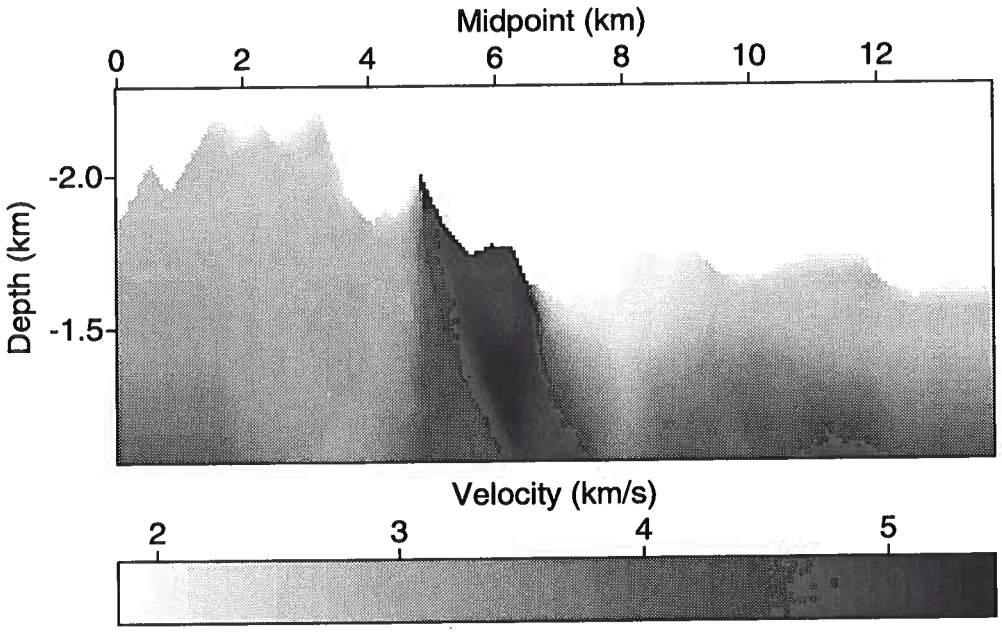

FIG. 5.11. Near-surface velocity model obtained from a turning-ray tomographic analysis.

velocity model was not perfect. Furthermore, the shot gathers in Figure 5.13 show a small bulk downward time shift with respect to those corrected with the true-velocity model (Figure 5.5). This situation suggests that the tomographic velocity model has average-velocities that are slightly higher than the true ones, at least in the central part of the near-surface velocity structure.

This observation is supported by looking at the shading, which indicates the velocity of the layers in the models shown in Figures 5.11, and 5.4. Also, the size of the high-velocity feature in the middle of the near-surface velocity structure is larger than the true one; although, its velocity is not as large. This overestimation of the high-velocity portion of the model is a common situation in tomography analysis (Wielandt, 1987). It seems that the rays are deflected around low-velocity anomalies resulting in a preferential sampling of the high-velocity regions. The size of low-velocity anomalies, as a result, may be considerably underestimated. Both actions bias the results of the inversion process toward higher-average velocities.

Now, let us compare the results of the datuming processes using the tomographic model in term of imaging quality after prestack depth migration from a horizontal reference surface. For the migration, we use the correct velocity model beneath the datum level.

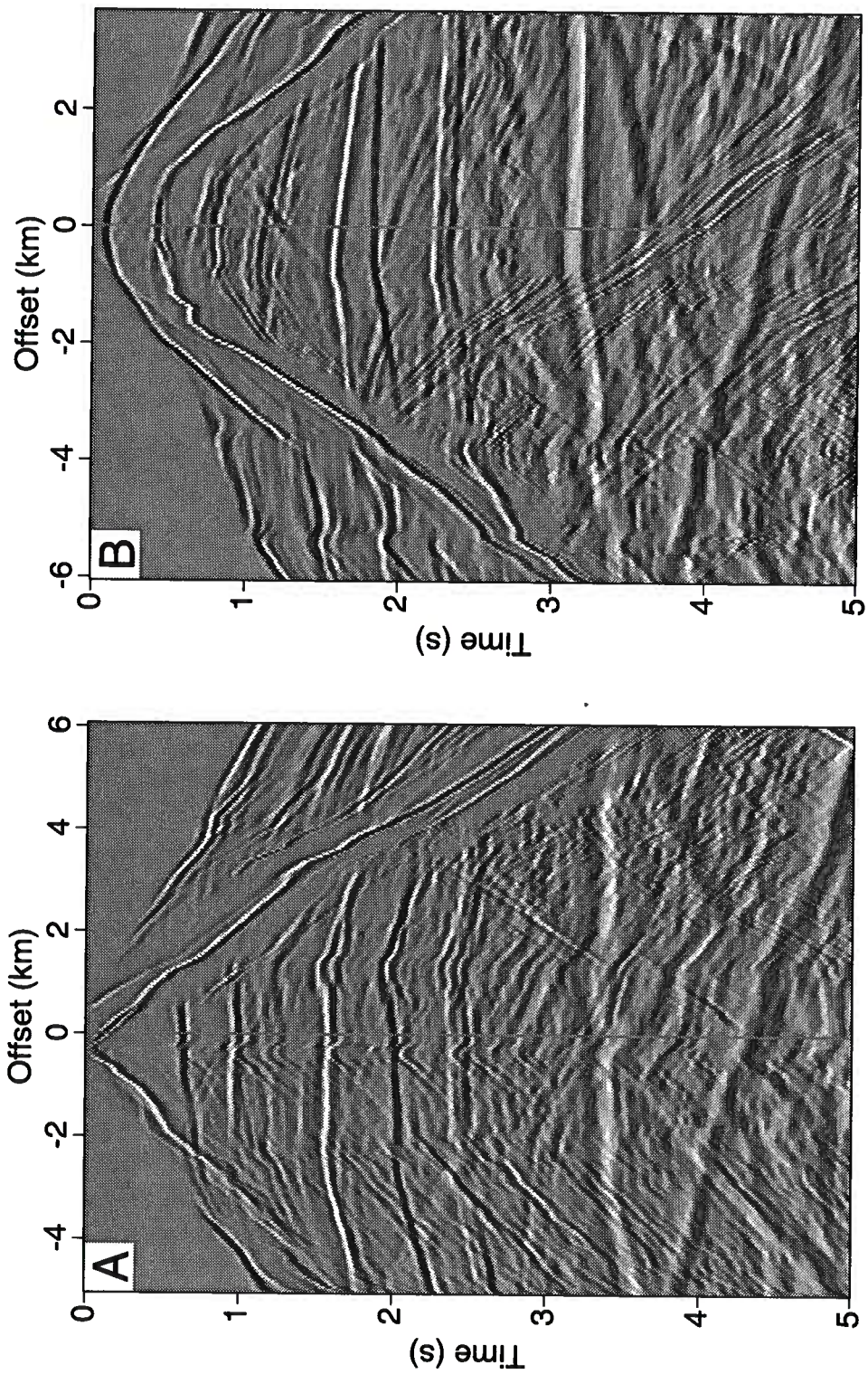

FIG. 5.12. Synthetic shot gathers after tomo-static corrections have been applied to transfer the data from topography to a datum level of -1.22 km.

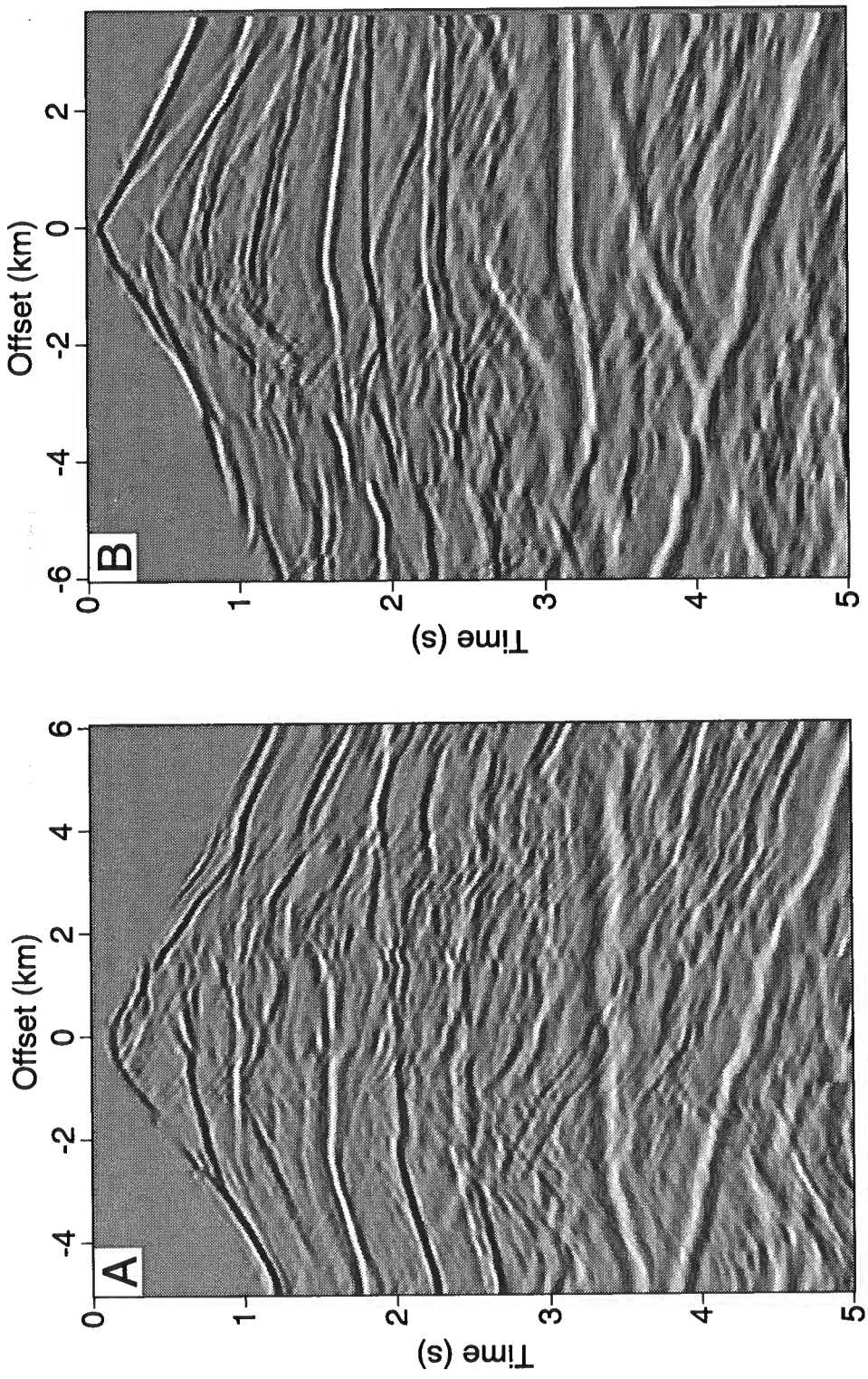

FIG. 5.13. Synthetic shot gathers after Kirchhoff-based tomo-datuming has been applied to transfer the data from topography to a datum level of -1.22 km.

Figure 5.14 shows the migrated sections generated after the data are processed with tomo-datuming and tomo-statics. Overall, unfortunately, neither of these migrated sections obtained from data processed with the tomographic near-surface velocity model offers as good a solution to this challenging imaging problem as we would wish. Note, for example, the disrupted image of the deeper, sub-horizontal reflectors on both results. Moreover, the deeper reflectors are more continuous in the image from tomo-statics (Figure 5.14b) than in that from tomo-datuming (Figure 5.14a). Similarly, the dipping feature located at surface midpoint 8.5 km and depth 2 km is better defined on the migrated section from the static solution than on that from the tomo-datuming solution.

Even though turning-ray tomography inversion does not yield a perfect near-surface velocity model, it likely is as good or better than conventional refraction statics approaches for estimating a near-surface velocity model for statics correction, and no other practical alternatives are available (Zhu et al., 1992, 1995). As we have seen with this synthetic example, although the tomographic velocity model exhibits, quite well, the main features of the true near-surface velocity model, it does not reproduce them with the accuracy required to appreciate the benefit of the more sophisticated wave-equation-based datuming over the conventional static-datuming approach. Thus, we can expect that wave-equation datuming will not be worth the effort unless the near-surface velocity structure is accurately estimated; otherwise, the better option is the static solution. Even though the conventional static scheme does not yield a better image than that obtained with Kirchhoff datuming, at least it is not worse and definitely is much less expensive.

5.4 Prestack depth migration from the recording surface

Another wave-theoretic approach for treating near-surface-induced time distortions is prestack depth migration from the acquisition surface. This approach incorporates the laterally-changing near-surface conditions and the topographic information directly into a fully prestack algorithm. Since the characteristics of the near-surface must be included in the velocity structure used in the migration process, this approach will suffer from the same problem as does wave-equation datuming when working with erroneous shallow-velocity models. The shortcoming is even more troublesome for this migration approach than it is for wave-equation datuming since, after the datuming step, subsequent processes such as residual-statics analysis are available to compensate for errors in the rough estimate of the near-surface velocity structure. After depth migration little can be done to correct for those short-wavelength time anomalies that remain in the data as a consequence of imperfect knowledge of the near-surface velocity model.

A practical way to get around this problem might be to estimate the short-wavelength components of the near-surface-induced time distortions by conventional residual-static procedures and apply them before the migration from topography is performed. This approach, however, has its problems, considering that the residual-static

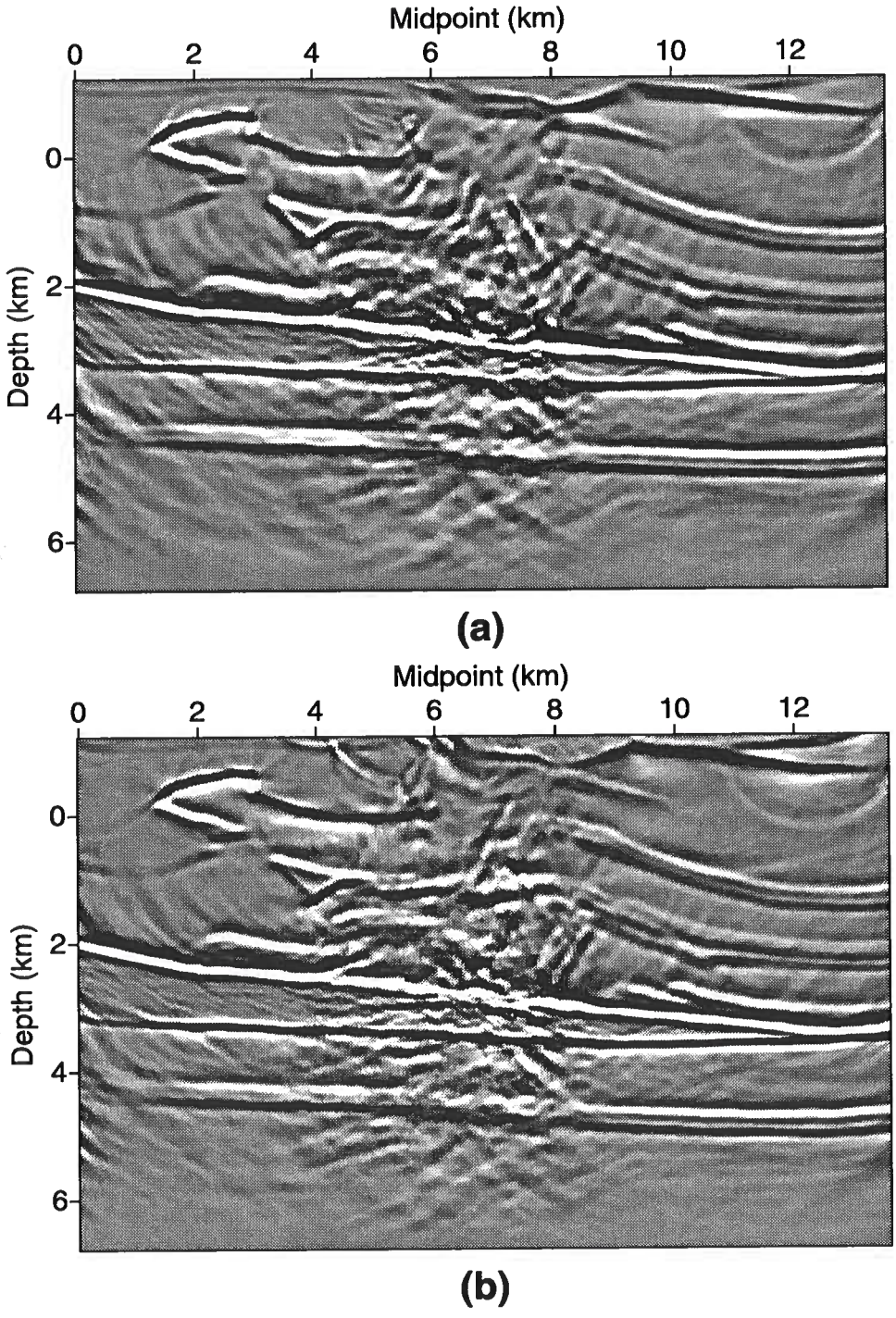

FIG. 5.14. Prestack depth migration after (a) tomo-datuming, and (b)tomo-statics. The processing was performed with the same tomographic-velocity field.

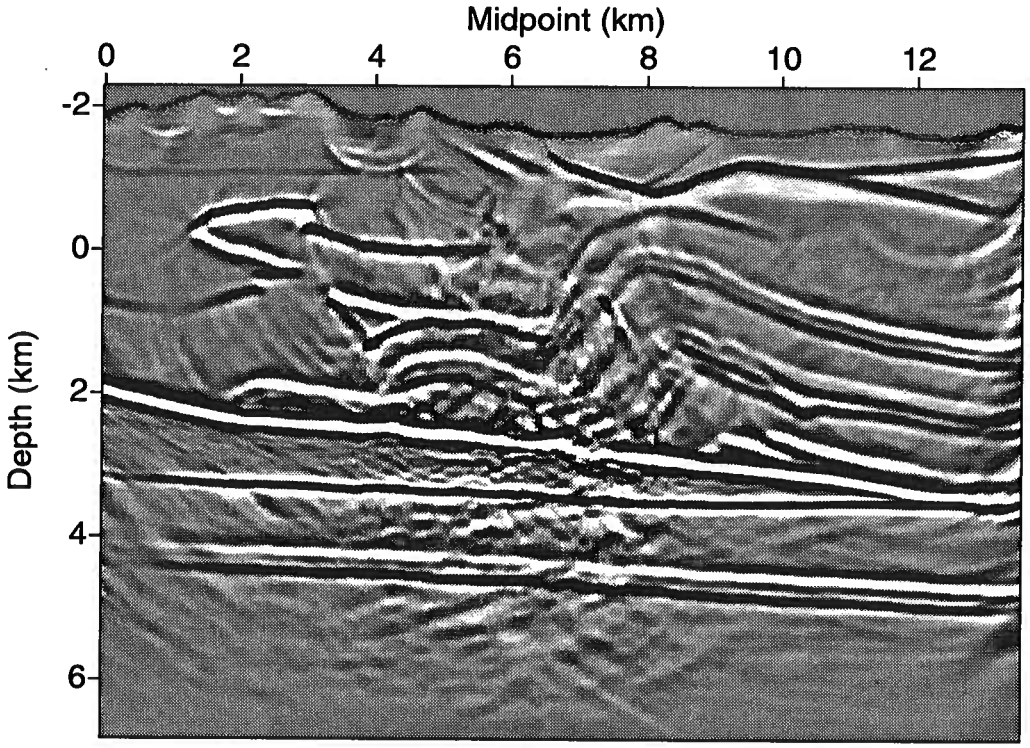

FIG. 5.15. Prestack Kirchhoff depth migration from topography. The true-velocity model is used in the migration process.

solution depends upon previously applied corrections for the long-wavelength components of the time anomalies. Therefore, since we likely change the long-wavelength component of the solution when migrating from topography, the short-wavelength static corrections applied to the data before migration would no longer be optimum. This complication could be seen as a chicken-and-egg kind of problem.

Now, let's analyze our ability to migrate from topography as opposed to wave-equation datuming followed by depth migration from a horizontal reference surface. Figure 5.15 shows the migrated section when the algorithm works from the acquisition surface. This image should be compared with that seen in Figure 5.7a. Overall, the two processes yield similar imaging quality, with a slight edge to the result of migrating of the data after datuming. The image of the dipping reflector at surface midpoint 7 km and depth 1.5 km shown in Figure 5.7a exhibits better reflection continuity than does the image obtained by migration from topography. Also, the seismic reflector located at surface midpoint 3.9 km and depth 1 km is slightly better defined in Figure 5.7a than it is in Figure 5.15. On the other hand, the image of the deeper folded structure located between surface midpoints 4 and 6.5 km at depth 1.5 km shows better reflection continuity in the image obtained by migration from topography than does the image obtained after Kirchhoff datuming and depth migration. Those differences, however,

are relatively small and some of them might be due to ray-tracing inaccuracies when the migration process works from topography as explained below.

When the imaging process is divided into prestack Kirchhoff datuming followed by prestack depth migration as opposed to migrating from topography, the overall traveltime calculation is split into two steps: (1) from topography to the datum level, and (2) from the datum level to the points in the subsurface, as illustrated in Figure 5.16. Since in the two-step processing the first-arrival traveltime calculation in each step is not allowed to evolve as long as it does in the migration from topography, the first-arrival traveltimes are more likely associated with the most energetic part of the seismic wavefield, and thus the adverse action of multi-valued arrivals might not develop, or it is less severe. This observation was shown by Bevc (1995) using his layer-stripping Kirchhoff migration.

The major advantage of migration from the acquisition surface over Kirchhoff datuming followed by prestack depth migration is that the former approach allows one to image the near-surface geologic structure; this information is important for tying a seismic data interpretation to any available surface geology data (e.g., outcrops).

5.5 Imaging distortions induced by imperfect near-surface velocity models: Versteeg's approach

In a study of the sensitivity of prestack depth migration to the subsurface velocity model, Versteeg (1993) searched for the smoothest velocity model that still would generate an accurate depth image of the Marmousi model. After comparing depth images obtained with velocity models of different degree of smoothing, he concluded that, given the frequency content in that data set, the minimal spatial wavelength required in the velocity model to generate an accurate image from the Marmousi data set is about 200 m (655 ft).

Using a similar approach, I have analyzed the imaging-induced distortions due to inaccurate shallow-velocity structures. Knowing that the kinematic characteristics of the seismic data are determined by the long-wavelength components of the velocity model, it is reasonable to expect that some smooth versions of the velocity field (in this study the near-surface structure) can still yield good images. To study the importance of accuracy in the definition of the shallow velocity structure to the performance of the datuming algorithms, I applied different degrees of smoothing to the near-surface velocity model. The subsurface structural model was smoothed with a minimum-operator length of 150 m (490 ft), as in previous sections, to ensure a stable and accurate solution in the ray-tracing procedure.

The operator lengths, L, considered in this analysis are: 300, 450, 600, and 900 m (985, 1475, 1970, and 2950 ft). The sensitivity of the wave-equation-based, and the conventional static datuming approaches to the degree of smoothing of the near-surface velocity model is analyzed in terms of imaging quality after the corrected data are migrated. I judge the quality by comparing the migrated sections with the structural velocity model (Figure 5.1). The three smoothed near-surface models

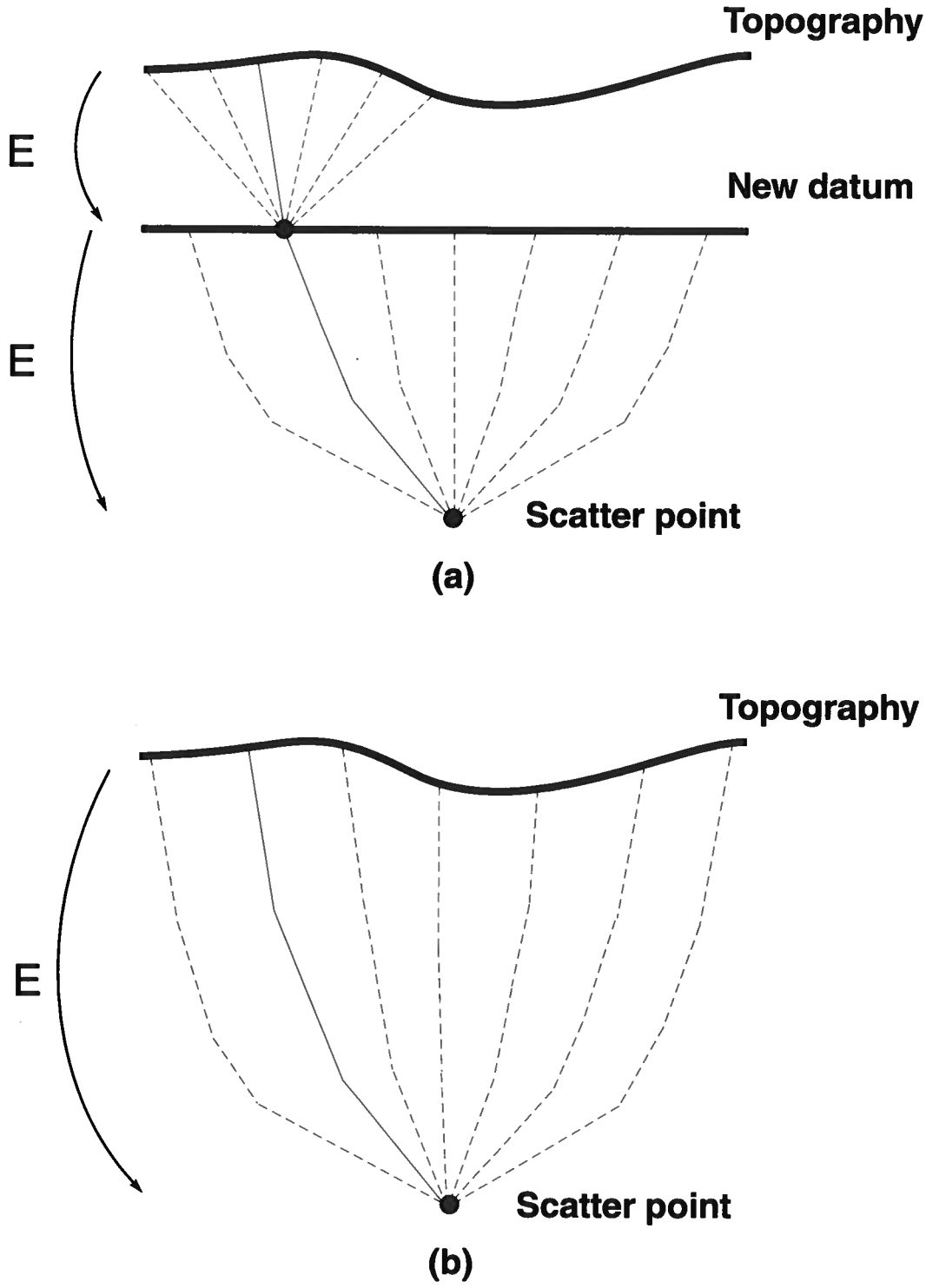

FIG. 5.16. Migration (a) after wave-equation datuming, and (b) from variable-topography acquisition surface.

shown in Figure 5.17 should be compared with those in Figures 5.4, and 5.11. The details in the shallow-velocity model associated with the small spatial wavelengths are increasingly attenuated by an augmentation in the length of the smoothing operator. The depth images obtained for $L = 300$ m after each of the two datuming approaches are applied, shown in Figure 5.18, resemble quite well those in Figure 5.7. The images associated for $L = 450$ m and 600 m (Figures 5.19, and 5.20) start to degrade in the central part of the model, where the high-velocity wedge offers the maximum complexity in the near-surface.

Note that the deterioration of the images is more rapid for the data processed with the Kirchhoff datuming than is that for those processed with the conventional static solution. For a small amount of smoothing, the better solution is given by the Kirchhoff datuming approach (Figures 5.7, and 5.18), but as the length of the smoothing operator gets larger, the difference in imaging quality of the two datuming schemes reduces to a point where is hard to distinguish the quality of the depth images (Figure 5.21).

This analysis gives qualitative support to the conclusion that when working with imperfect near-surface velocity information (the situation typically encountered in practice), the conventional static approach could be more robust than wave-equation datuming in treating time anomalies associated with the near-surface. On the other hand, if the shallow velocity structure is sufficiently accurate, wave-equation-based datuming offers the best image.

5.6 Ambiguities in stacking velocity analysis due to datuming procedures

In the previous sections, I studied the action of the datuming techniques in terms of the quality of the resulting prestack-depth-migrated images where the velocity structure below the datum level is perfectly known. Now, let's focus on the action of the datuming techniques on stacking velocity analysis both where knowledge of the near-surface velocity field is perfect and where it is not. As covered in Chapter 3, the moveout distortions observed in each of the datuming approaches deteriorate, quite strongly, the overall quality of the depth images. Where a conventional CMP processing sequence is subsequently undertaken, we can expect the moveout distortions to also lead to ambiguities in stacking velocity analysis.

For subsurface velocity structures as complex as that studied in the previous section, a conventional CMP processing sequence is not convenient. Furthermore, considering that our main interest in this section is in the distorting action of the near-surface for stacking velocity analysis, I use a different synthetic data set for this study. The new velocity field consists of the shallow-velocity structure shown in Figure 5.22, and a simple subsurface velocity structure. The new subsurface velocity model includes five constant-velocity layers with the geometry shown in Figure 5.23. The velocity in the model ranges from 2500 m/s (8200 ft/s) in the first layer to 5000 m/s (16400 ft/s) in the deepest one. Since the overall lateral velocity variation is mild, conventional CMP processing is appropriate.

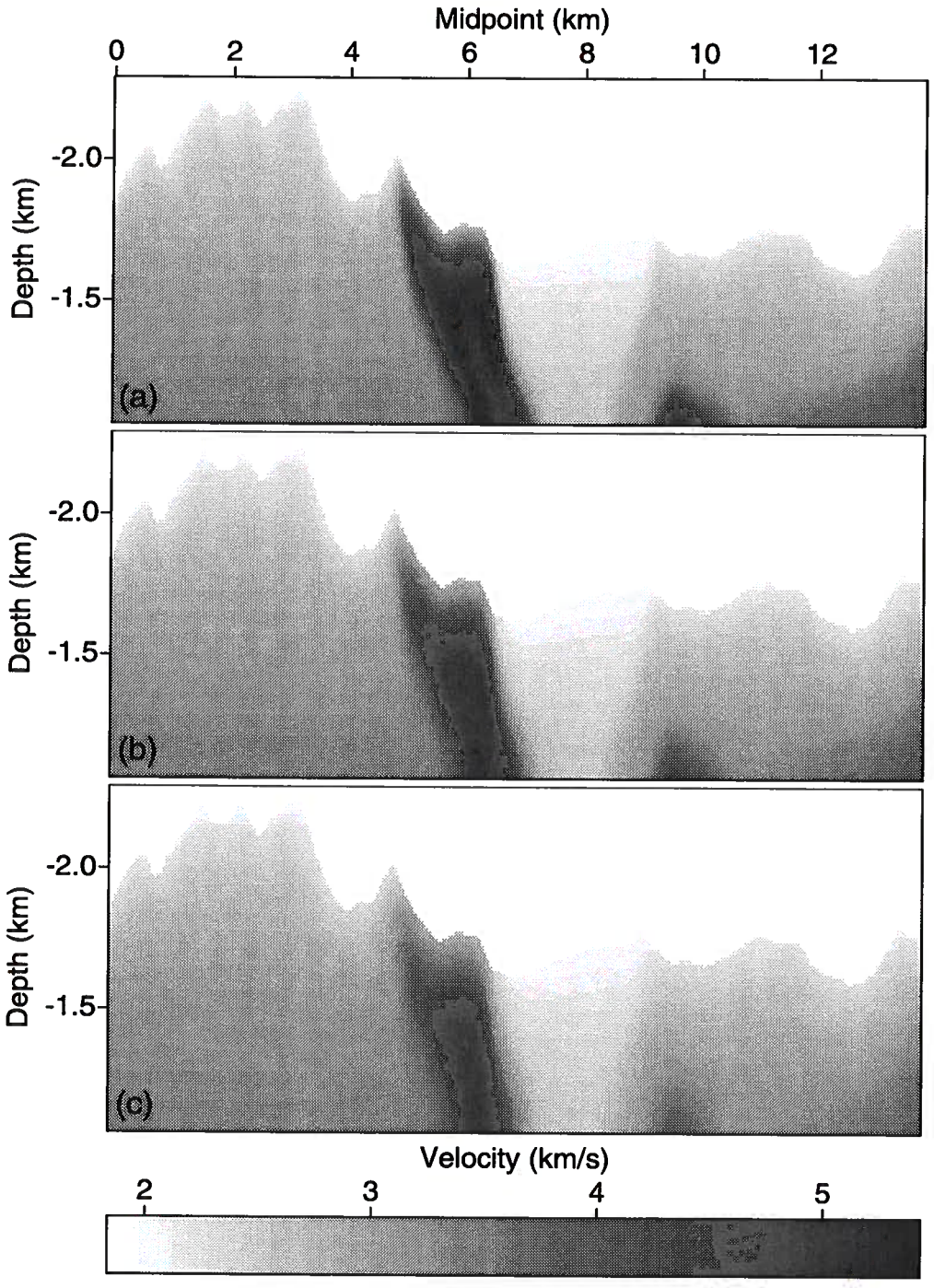

FIG. 5.17. Near-surface velocity model after smoothing with an operator length of (a) 300 m, (b) 450 m, and (c) 600 m.

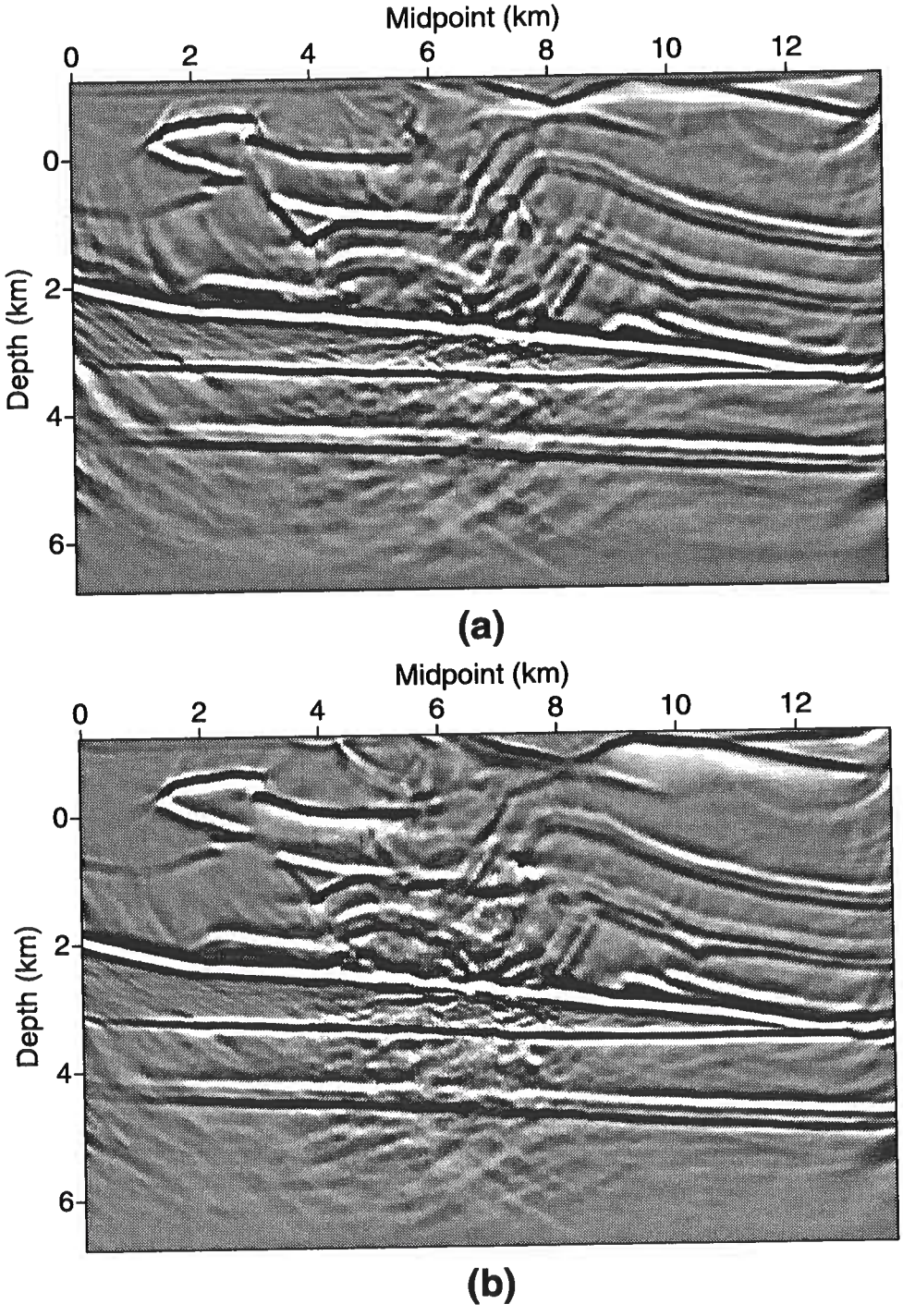

FIG. 5.18. Depth migration after (a) Kirchhoff datuming, and (b) static-corrections, using a smoothed velocity model obtained with an operator length of 300 m.

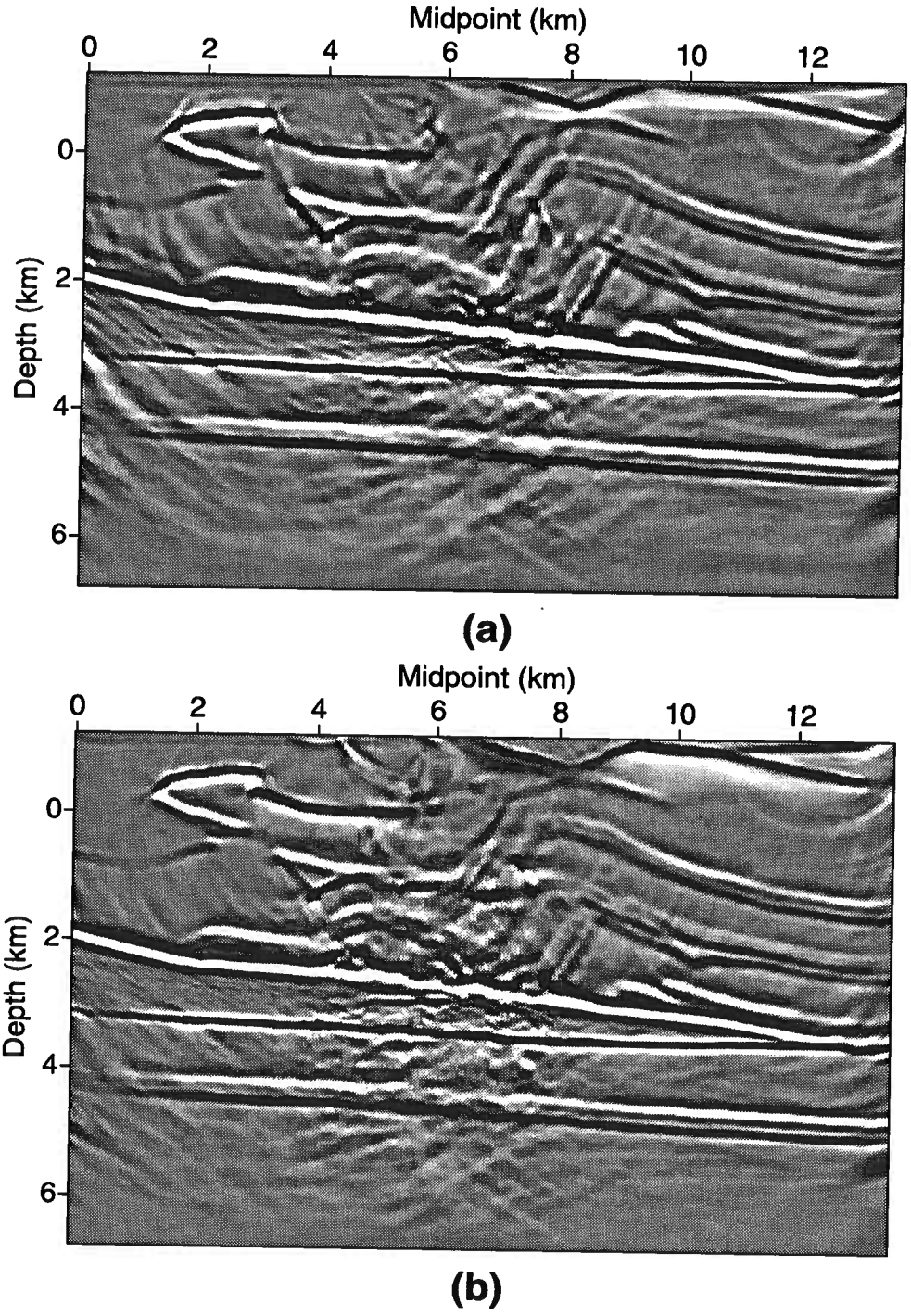

FIG. 5.19. Depth migration after (a) Kirchhoff datuming, and (b) static-corrections, using a smoothed velocity model obtained with an operator length of 450 m.

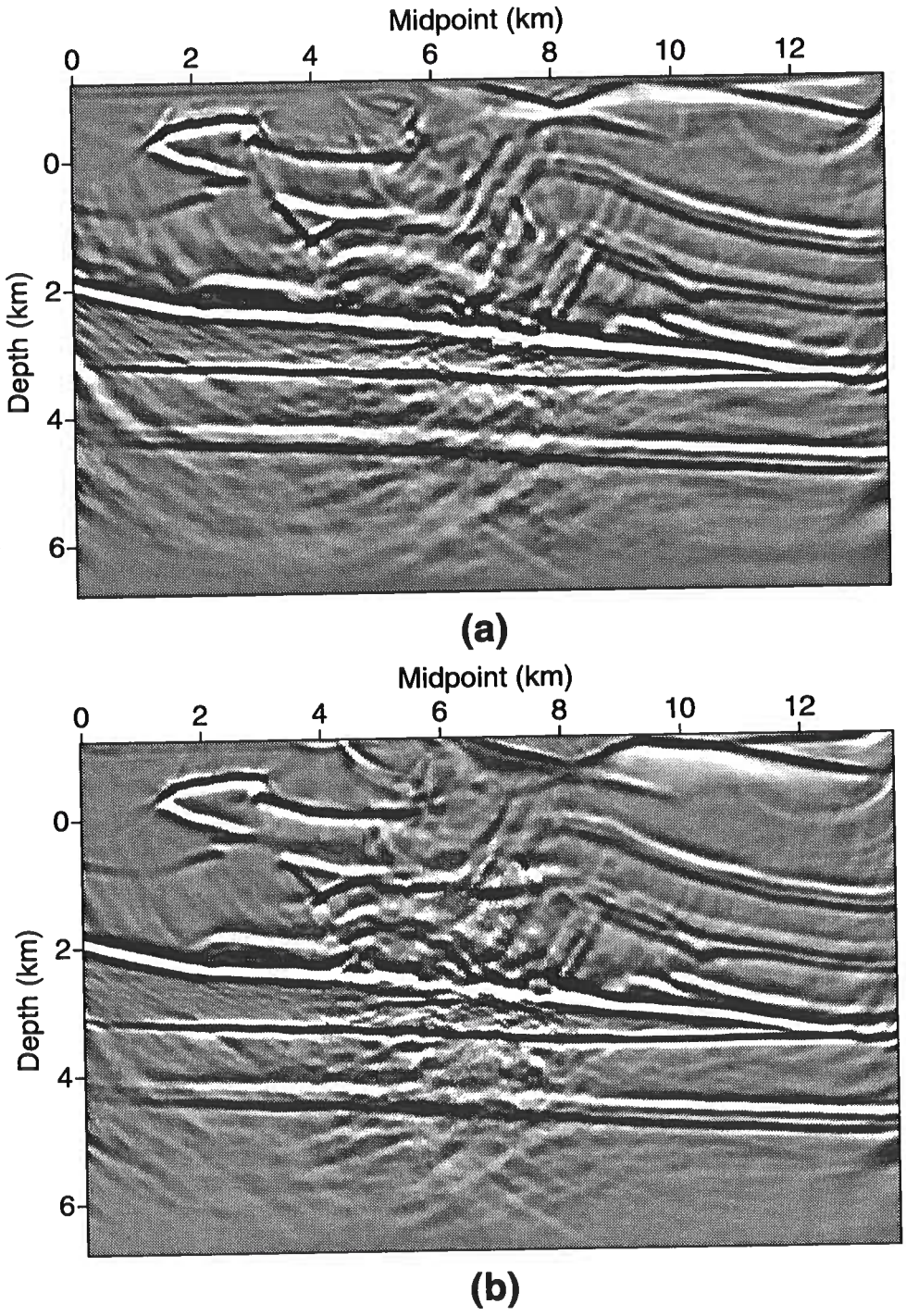

FIG. 5.20. Depth migration after (a) Kirchhoff datuming, and (b) static-corrections, using a smoothed velocity model obtained with an operator length of 600 m.

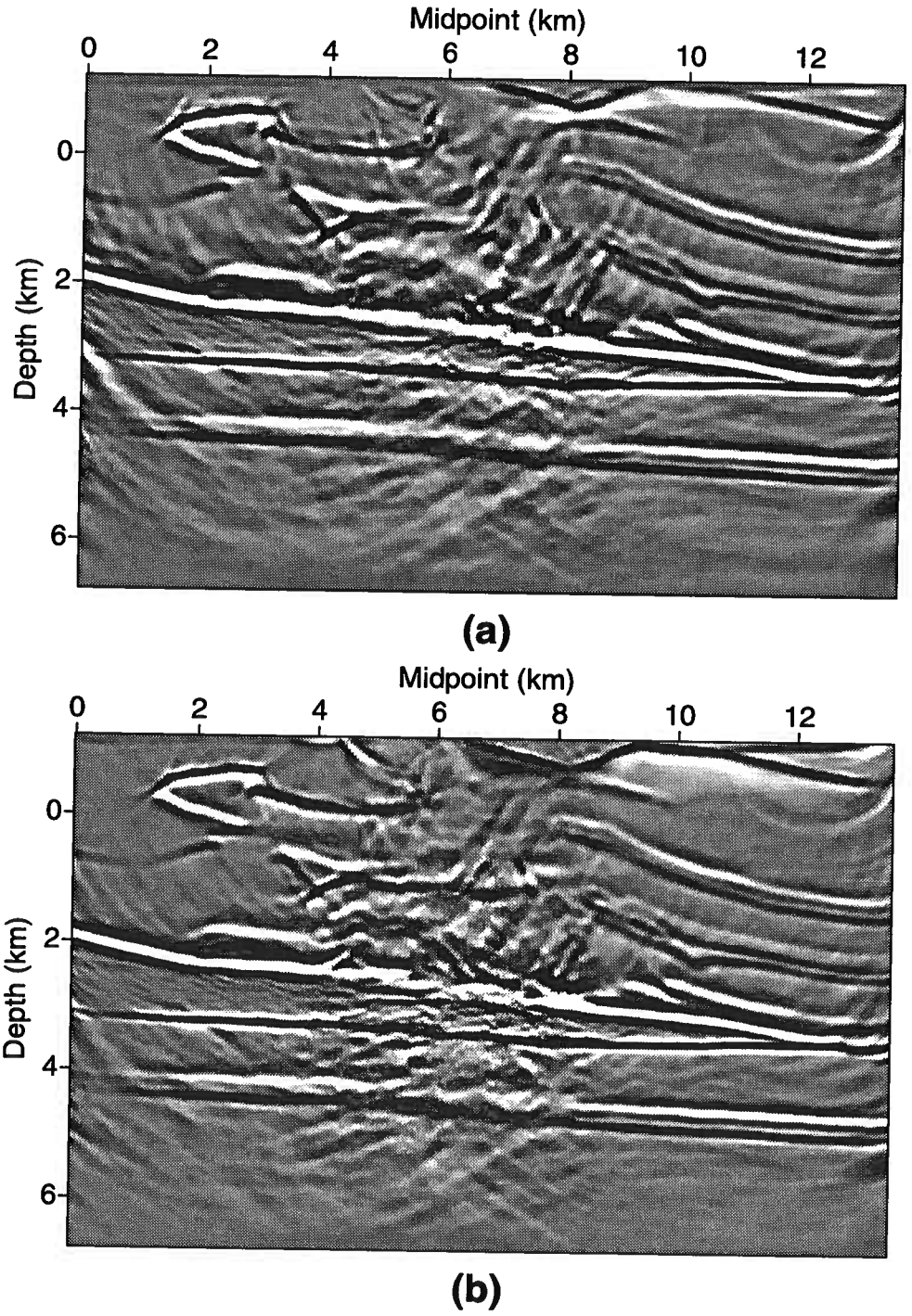

FIG. 5.21. Depth migration after (a) Kirchhoff datuming, and (b) static-corrections, using a smoothed velocity model obtained with an operator length of 900 m.

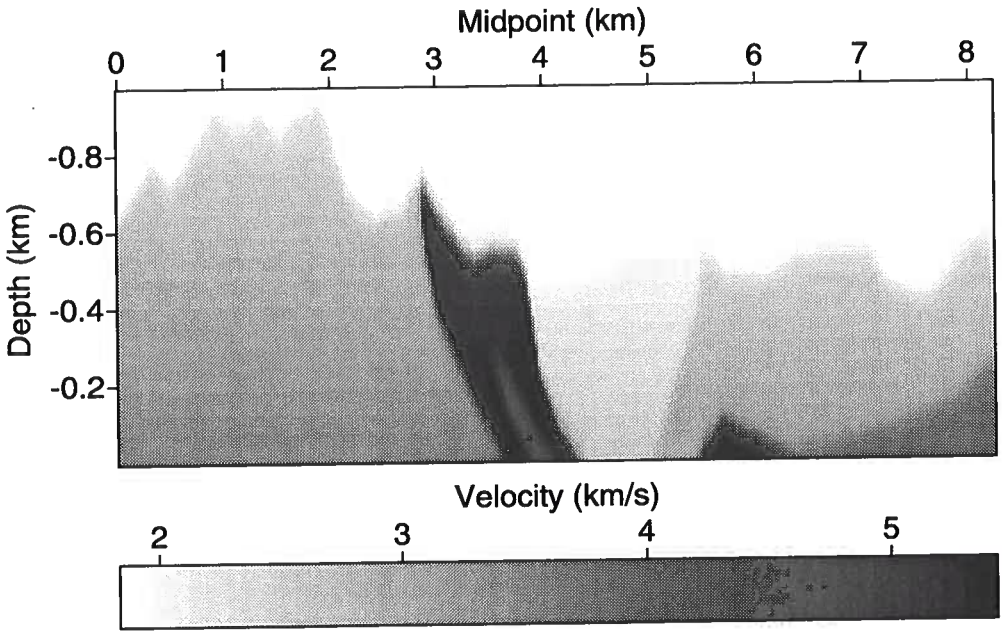

FIG. 5.22. Slightly smoothed overthrust near-surface velocity structure.

Since the subsurface velocity structure is simple enough, instead of using an expensive full-waveform finite-difference code to generate the synthetic data, I use the more efficient two-step modeling procedure presented on Chapter 4. There, I suggested modeling data from the deeper subsurface once, and then using wave-equation datuming to superimpose whatever complex shallow-velocity structure is desired. This two-step modeling procedure allows us to test the influence of different near-surface velocity fields without having to remodel the subsurface structure. Two shot records from the first step of the modeling scheme (i.e., ray-tracing modeling) are shown in Figure 5.24. Direct arrivals and refraction energy are not modeled in this synthetic data set. The earliest reflection exhibits the familiar dip-related shifted hyperbolic moveout, and the two latest ones have moveout that is approximately a shifted hyperbola; these characteristics of the two deeper reflections evidence the lateral velocity variation in the subsurface model. The reflection from the anticlinal structure in the central part of the model shows nonhyperbolic moveout.

Once the synthetic data set from the horizontal surface is available, I perform upward continuation through the shallow-velocity structure displayed in Figure 5.22, by means of Kirchhoff datuming. The result of this near-surface modeling scheme is displayed in Figure 5.25. The new shot records simulate the wavefield that would have been recorded if the sources and receivers had been located on the topographic surface of the near-surface velocity model shown in Figure 5.22. As expected, the complex near-surface structure strongly distorts the moveout of the reflection events, giving rise to sharp discontinuities, some of which are associated with topographic changes, and others are related to abrupt lateral velocity variations. The shot gathers displayed

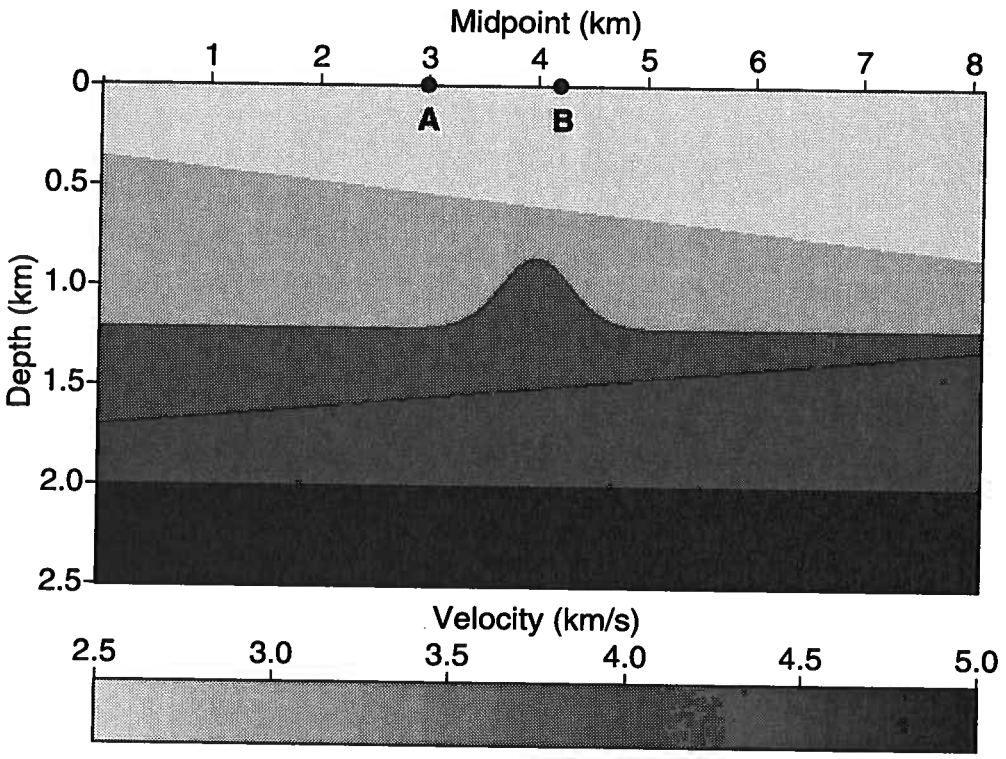

FIG. 5.23. Simple subsurface velocity structure beneath a datum depth of zero. This model is used to analyze the distorting action of datuming procedures. The darker the shading, the higher the layer velocity. The dots A and B indicate the positions of the shot gathers shown in coming figures.

in Figure 5.25 are located at the zone of influence of the near-surface high-velocity anomaly. The sharp edges of the high-velocity wedge generate not only strong time distortions, but also phantom diffractions that evidence the defocusing action of the near-surface.

Once the data referenced to the topographic surface are available, I remove the near-surface-induced time distortions by performing layer replacement with each of two approaches: (1) the conventional static scheme, and (2) Kirchhoff datuming. In the layer-replacement procedure, I transfer the data from topography to the original reference surface (i.e., depth = 0 m). Then, again, I transfer the data upward to their final reference surface using a constant velocity of 2500 m/s, that is the velocity of the first layer of the subsurface model (Figure 5.23).

I use this layer-replacement step rather than simply doing the datuming, as above, in order to provide a fair comparison of these datuming approaches. In this example, because the topography and the datum level are 1 km apart in some parts of the model, static corrections would be extremely large. As we know, large static corrections applied to nonzero-offset data change significantly the moveout of the reflection events making the static approach inappropriate. By using the layer-replacement scheme I

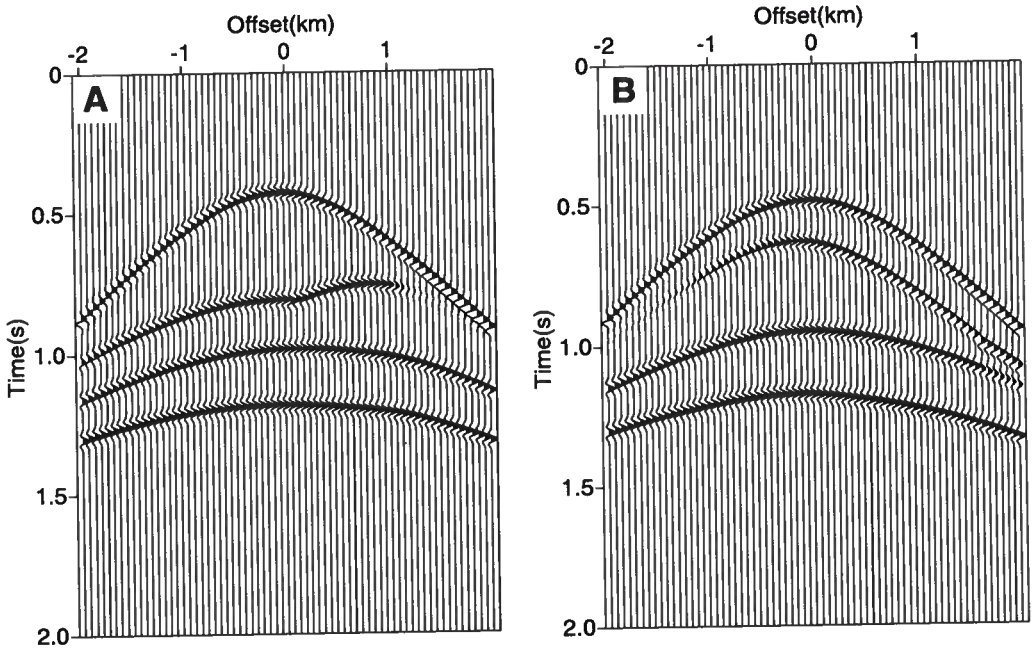

FIG. 5.24. Synthetic shot gathers recorded on a horizontal surface at depth equal to zero. Shots records A and B are located at lateral positions 3 km and 4.2 km, respectively.

reduce the size of the static corrections to a level where they would not be at an unacceptable disadvantage as compared with time corrections by wave-equation datuming. To minimize the size of the static-corrections, I locate the final datum level at -560 m, the average elevation of the topographic profile.

For reference, I estimate the stacking velocity functions from a synthetic data set modeled with sources and receivers at the final datum level; these velocity functions will be referenced as "true stacking velocity functions" in this section. Figure 5.26 shows semblance functions for the true stacking velocities at midpoints 4 and 5 km, estimated from the data modeled at a final datum level.

Moreover, I consider two situations based on the level of accuracy of the shallow velocity information used in the datuming processes. First, I consider a scenario in which knowledge of the near-surface velocity field is perfect. In this case, even though the true velocity model is used, the data processed with the static-correction approach yield stacking velocity profiles that are too high or too low, as well as less resolved, compared to the true velocity functions (Figure 5.27).

In general, the stacking velocity field should vary smoothly throughout a seismic profile. Abrupt changes in the behavior of the stacking velocities may indicate that some near-surface time anomalies are still in the data. Since the static-corrections do not consider the slant-path component the wave-propagation process in the near-

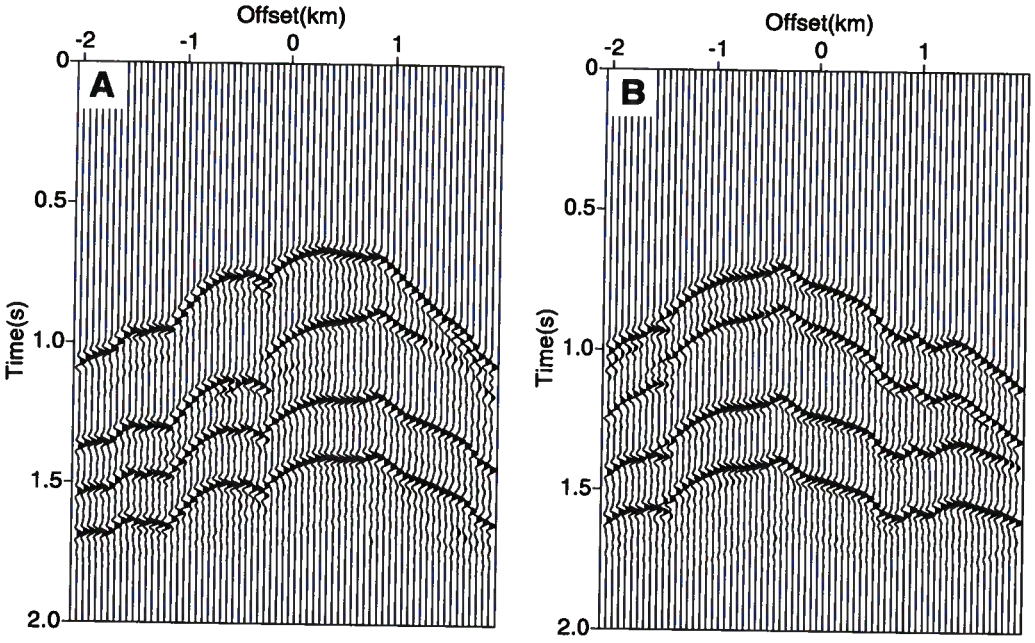

FIG. 5.25. Synthetic shot gathers after wave-equation datuming is performed to upward continuation of the data through the overthrust near-surface velocity model shown in Figure 5.21.

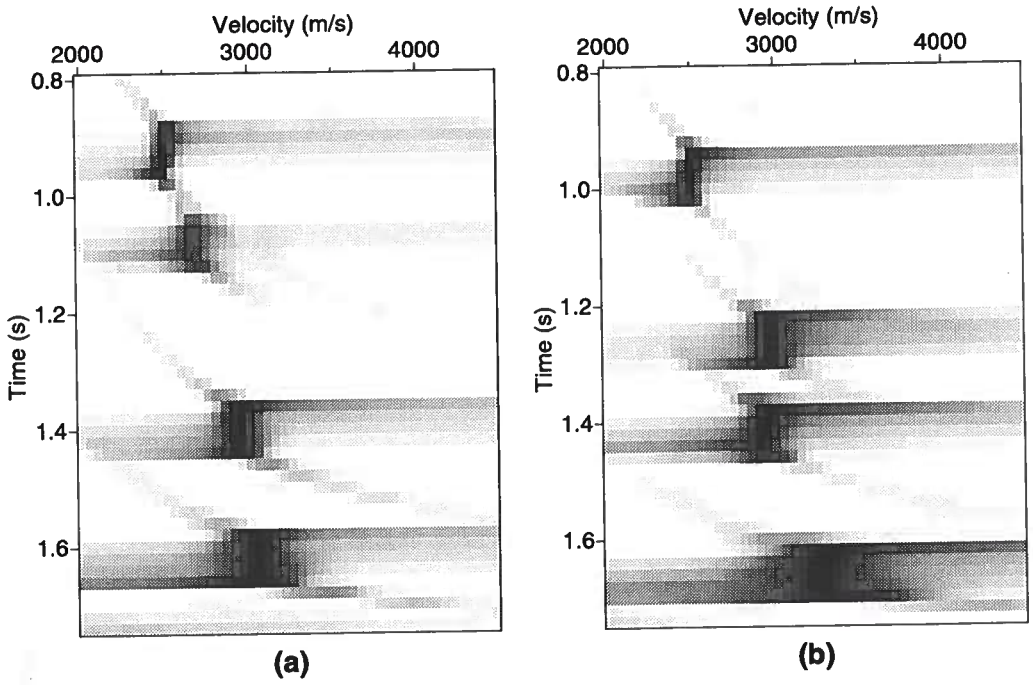

FIG. 5.26. Semblance velocity analysis at lateral positions (a) 4 km, and (b) 5 km calculated from data modeled at a depth of -560 m, the final datum level.

surface, distortions on the reflection moveouts arise; those distortions generate ambiguities in the velocity analysis and compromise the success of any subsequently applied wave-equation based processes. Figure 5.27 shows that not only do the semblance functions after static corrections lead to stacking velocities that differ from the true ones but also their interpretation is difficult and ambiguous; these semblance functions exhibit a smeared and blurred character, especially the one located close to the problematic near-surface high-velocity wedge (Figure 5.27a).

Kirchhoff datuming, on the other hand, accurately accounts for the time anomalies associated with the near-surface, properly reconstructing the hyperbolic moveout on the reflection events in a way consistent with the wave-theory. Therefore, the data treated with the Kirchhoff datuming yield stacking velocities (Figure 5.28) almost identical to the true stacking velocity functions. Furthermore, these semblance functions are sharp and easy to interpret.

Now, let us consider a second scenario in which the layer-replacement processes are performed using a velocity field derived from a tomography analysis. Although this near-surface velocity model is a good approximation to the true velocity field (Figure 5.22), it is imperfect, giving us the opportunity to study the influence of errors in the near-surface velocity structure through the datuming process to estimates of the stacking velocity functions.

For comparison of the stacking velocity functions derived from the two scen-

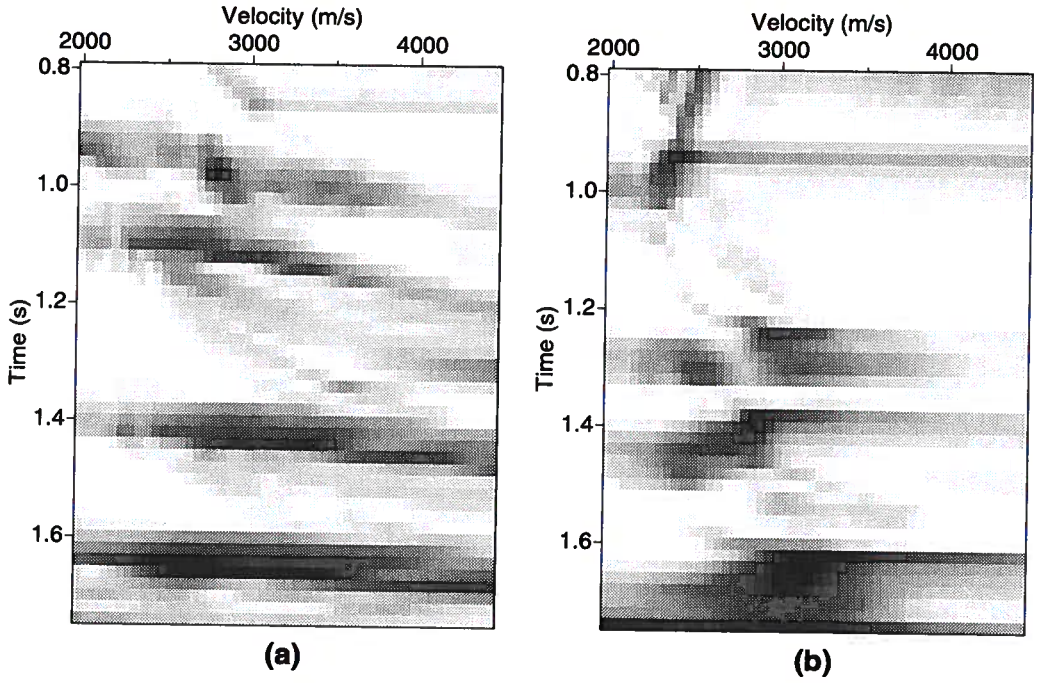

FIG. 5.27. Semblance velocity analysis after the application of static-corrections at lateral positions (a) 4 km, and (b) 5 km.

arios and the two datuming schemes, these functions are displayed together in Figures 5.29, 5.30, and 5.31 for three midpoint locations. Stacking velocity profile from data processed with Kirchhoff datuming and the true near-surface velocity model change smoothly along the synthetic seismic line, offering consistent solutions. The well-behaved velocities after Kirchhoff datuming indicate that successful stacking can be performed. These velocities match, quite nicely, with those obtained from the data modeled at the final datum level.

On the other hand, stacking velocity functions from data treated with statics estimated from the perfectly known velocity model depart from the "true" stacking velocities especially at the shallow reflectors, indicating that time anomalies still remain in the data (see Figures 5.29, 5.30, and 5.31). Since the static datuming approach does not correct properly the near-surface time anomalies, the stacking velocities attempt to compensate for the remaining distortions in the data offering a compromise solution that tries to correct one error by another. In practice, when data are contaminated with long-wavelength components of near-surface-induced time distortions, the interpreted stacking velocities fluctuate around the true stacking velocity profiles from one CMP location to another.

The stacking velocity profiles obtained from data processed with tomo-datuming and tomo-statics exhibit large variability, also fluctuating around the true stacking velocities functions, but the data treated with tomo-datuming give stacking velocity

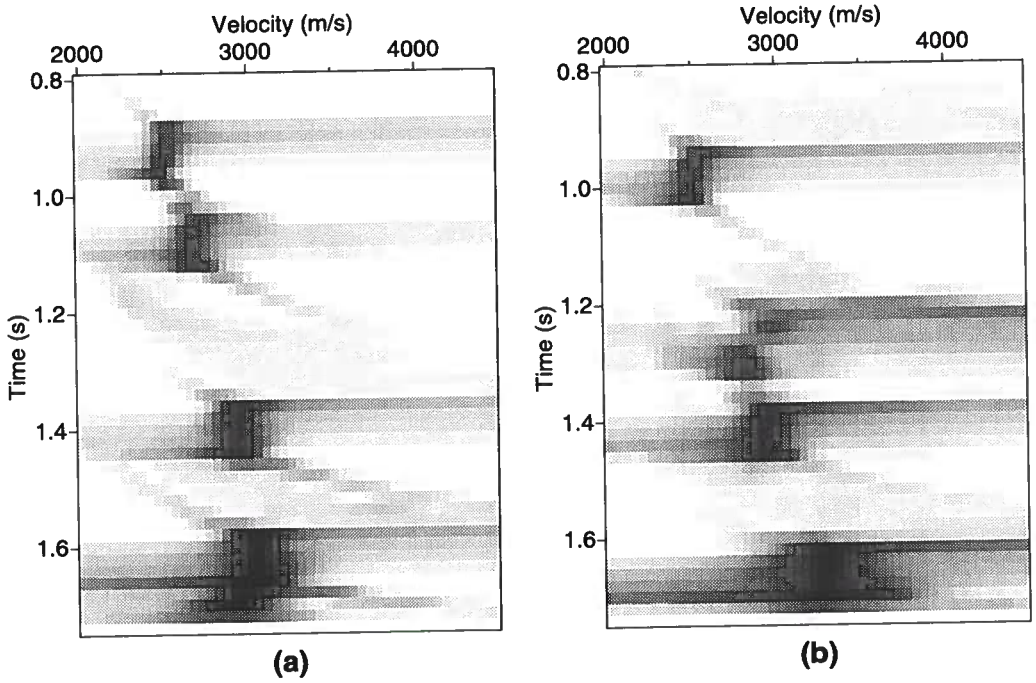

FIG. 5.28. Semblance velocity analysis after Kirchhoff datuming at lateral positions (a) 4 km, and (b) 5 km.

profiles that are closer to the true ones than those obtained from data processed with tomo-statics. According to these results, tomo-datuming reduces the ambiguity in the velocity analysis avoiding unnecessary moveout distortions in the reflection events.

Now, let us see the action of the datuming approaches on the stacking process itself, and how the stacking quality varies for the different schemes. Where the perfectly known, shallow velocity structure is used, the stack from data treated with Kirchhoff datuming exhibits satisfactory reflection continuity (see Figure 5.32a). Beneath midpoint position 3.2 km, however, there are small breaks that evidence the presence of the high-velocity rock mass in the near-surface velocity model, and thus, imperfections in the ray-tracing procedure (Figure 5.22). Also, some artifacts in the stack section are due to aperture limitations and edge effects in the wavefield extrapolation process. At this point, we have to remember that the original data have gone through the datuming process three times, once in the modeling task and twice in the velocity-replacement scheme.

Figure 5.32b shows the stack section from data processed with static corrections evaluated from the true shallow velocity structure. This stack section shows significant reflection discontinuities that are stronger for the shallow reflectors. These are evidence of the limitations of the static approach for treating time anomalies under absolute knowledge of the near-surface velocity field.

Figure 5.33 shows the stack section from data treated with tomo-datuming and

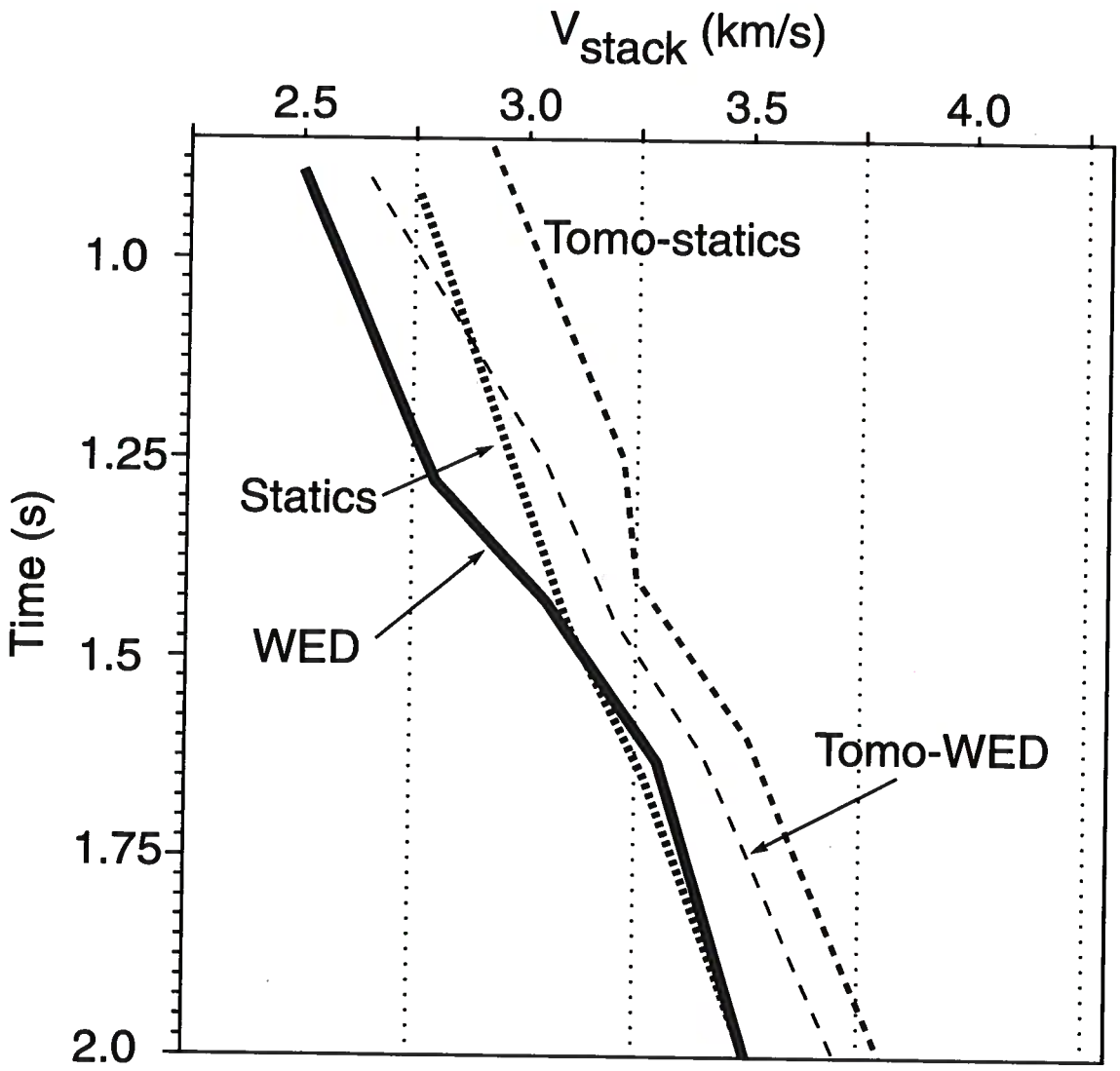

FIG. 5.29. Interpreted stacking velocity functions at the CMP at lateral position 3 km. The velocity functions are derived from data processed with the following methods: (1) wave-equation datuming (WED) and (2) conventional static correction with a perfectly known near-surface velocity model (Statics), and (3) tomo-datuming (Tomo-WED) and (4) tomo-static correction with the near-surface velocity model obtained from a tomographic analysis.

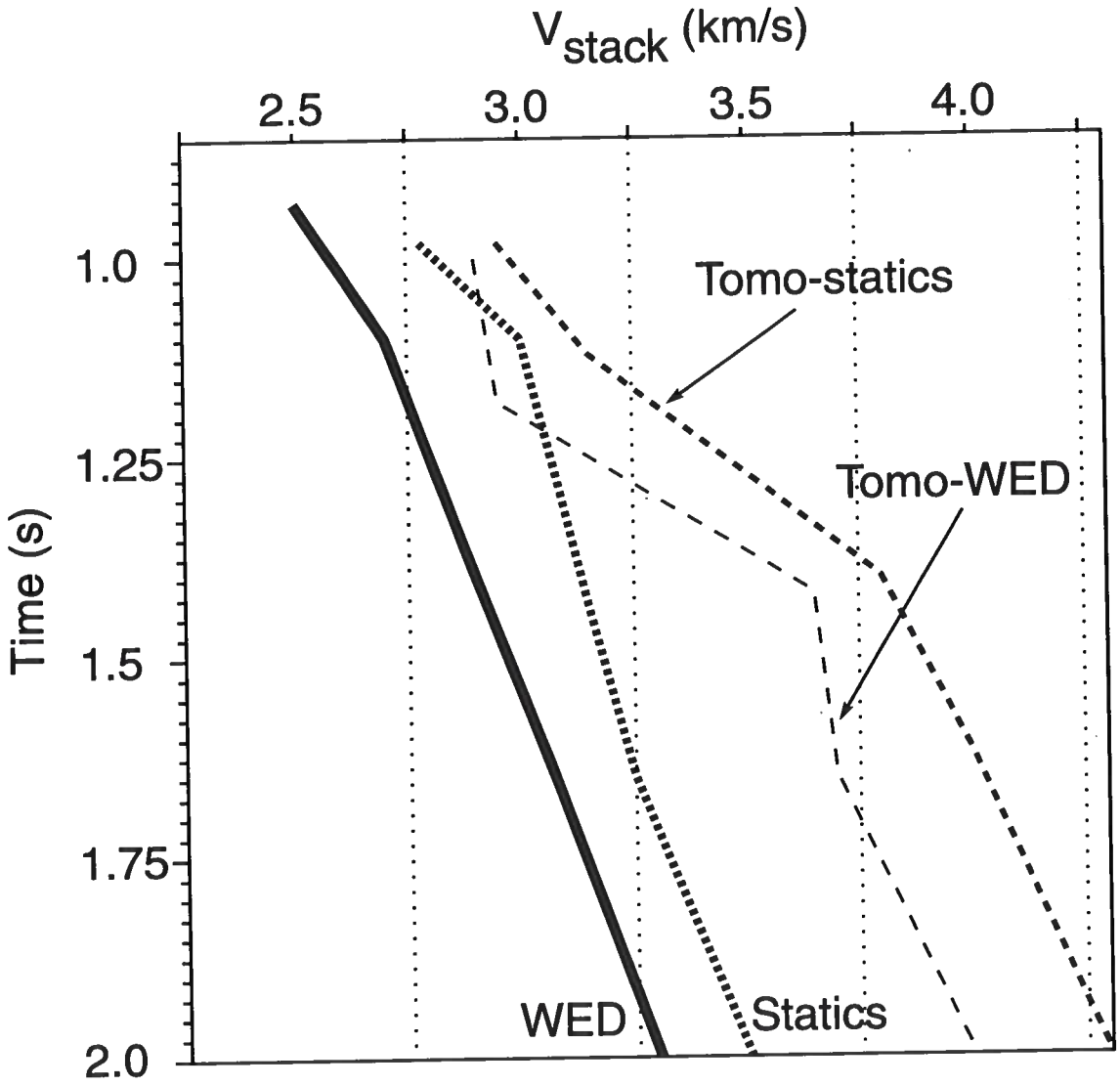

FIG. 5.30. Same interpreted stacking velocity functions as in Figure 5.29, but at lateral position 4 km.

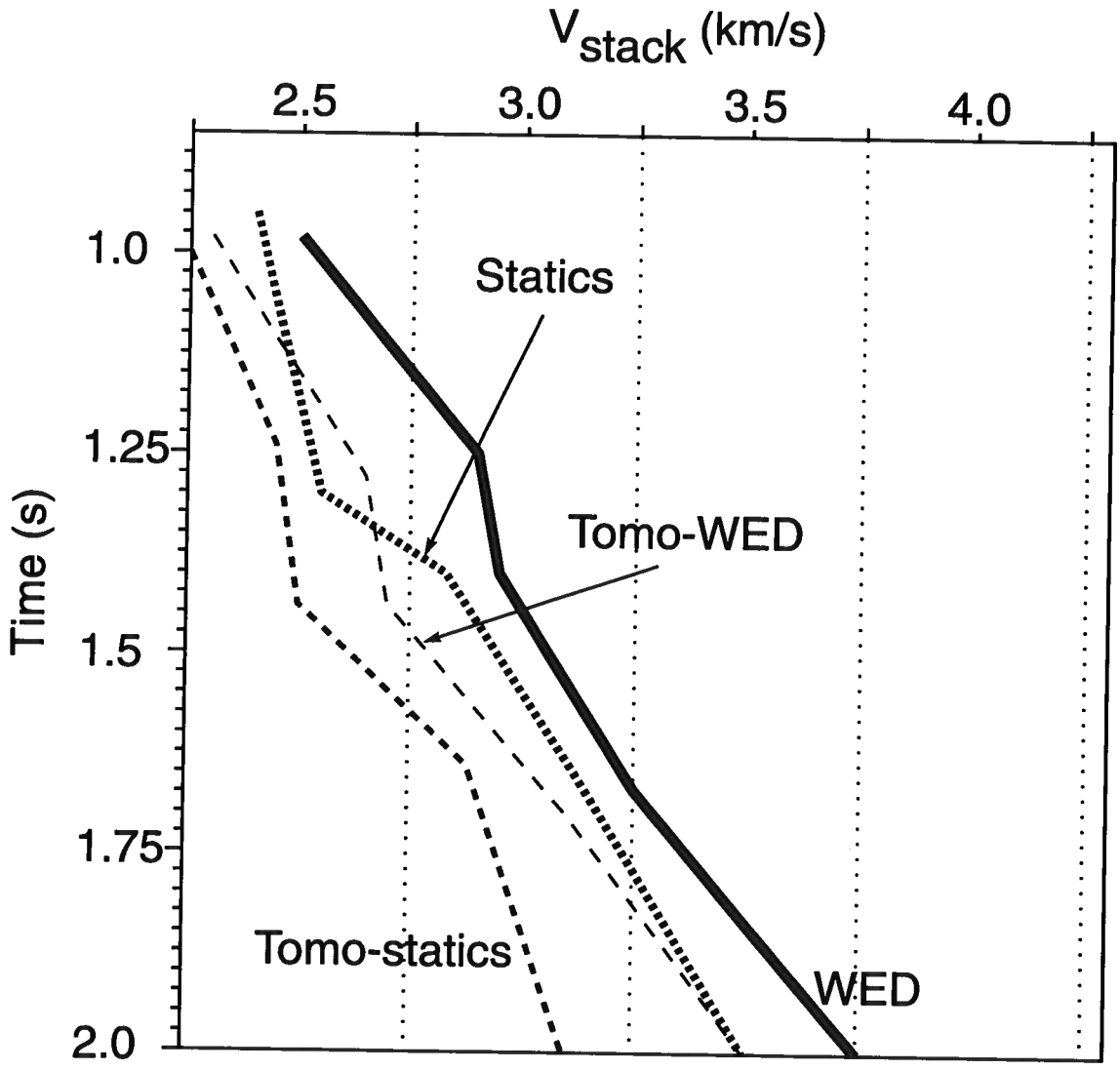

FIG. 5.31. Same interpreted stacking velocity functions as in Figure 5.29, but at lateral position 5 km.

tomo-statics. The deterioration of the stacking quality is apparent in both seismic sections. Furthermore, since the data are contaminated with both long- and short-wavelength time anomalies due to the imperfection in the tomographic model, the Kirchhoff datuming smears the short-wavelength component of the time anomalies, resulting in data with a slightly lower-frequency content than that from data treated with the tomo-static approach where no smearing occurs. It is difficult to decide which stack section is better in term of stacking quality and reflector continuity. This indicates that the degree of accuracy of the near-surface velocity model is extremely important in deciding which approach should be used in the treatment of the near-surface-induced time distortions.

From these examples, I conclude that the Kirchhoff datuming approach yields better stacking velocities and stacking quality than does the conventional static approach when the datuming processes are performed with a perfectly known near-surface velocity model. When the datuming processes use an imperfect tomographic near-surface velocity model, the stack sections obtained from the two datuming approaches yield similar stacking quality, although the stack section processed with Kirchhoff datuming exhibits slightly better reflection continuity in some portions of the seismic profile. It is explained by noticing that the stacking velocity functions are closer to the true ones when the data are processed with tomo-datuming as opposed to tomo-statics. Since the stacking velocity functions interpreted from data processed with static corrections are much more variable from one CMP location to another, the stacking quality varies significantly along the seismic profile as opposed to when the true velocity model below datum is used for NMO correction. For the static-corrections scheme, this particular behavior of the interpreted stacking velocities would demand more frequent control of the stacking velocities along the seismic line in order to achieve stacking quality similar to that obtained from data treated with Kirchhoff datuming.

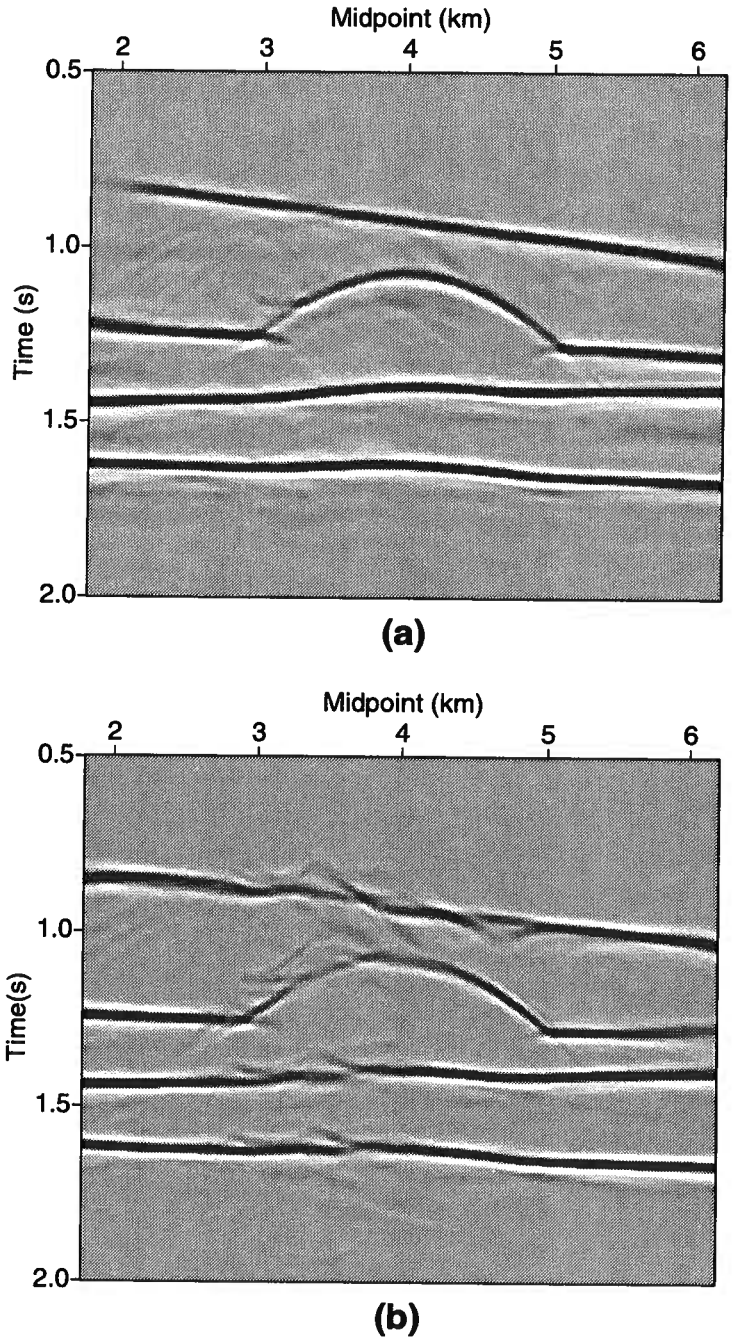

FIG. 5.32. Stack sections from data processed with (a) wave-equation datuming, and (b) conventional static corrections. The datuming processes are performed with true near-surface velocity model in Figure 5.21.

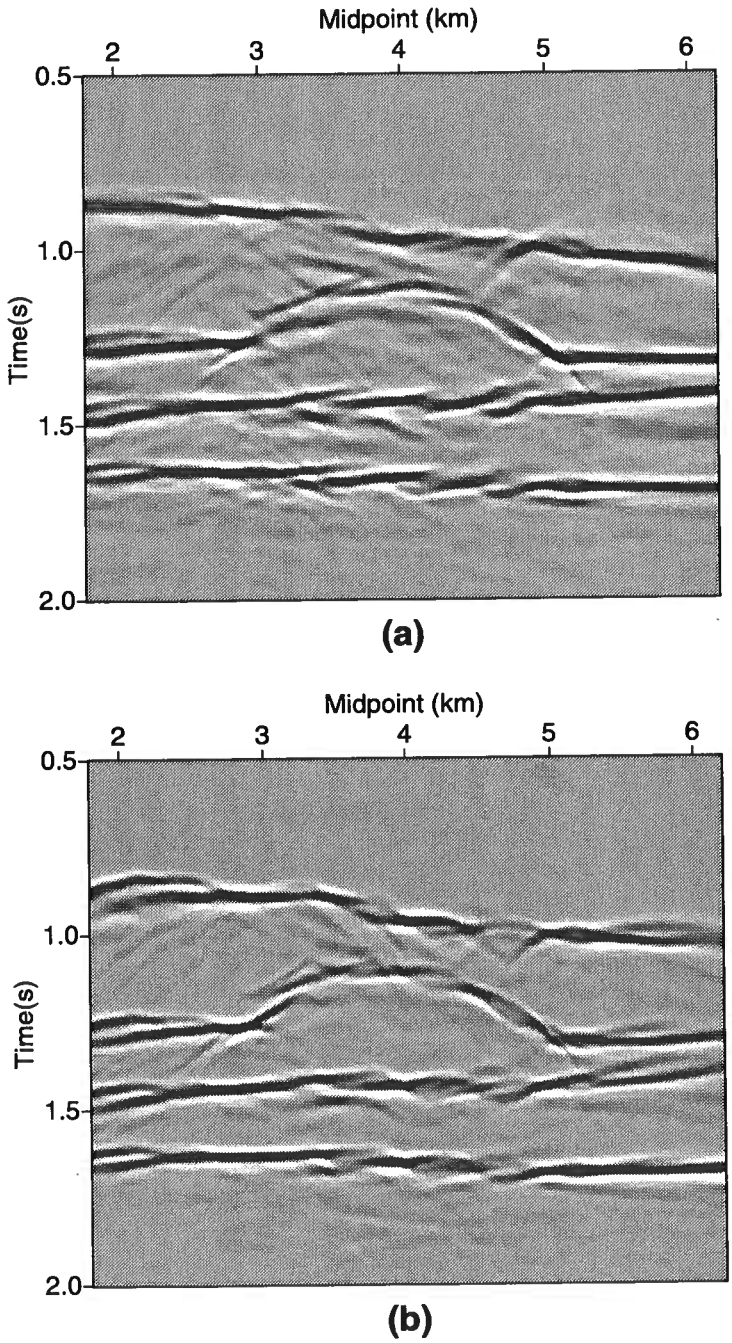

FIG. 5.33. Stack sections from data processed with (a) tomo-datuming, and (b) tomo-statics. The datuming processes are performed with a tomographic near-surface velocity model.

Chapter 6

CONCLUSIONS

Near-surface-induced time distortions play an important role in the imaging process, one that is especially apparent in overthrust and rough terrain areas. In this dissertation, I have reviewed three possible approaches to treating time distortions associated with variable-topography recording surface and laterally-changing near-surface conditions: (1) The conventional static-correction approach, (2) wave-equation datuming (Berryhill, 1984), and (3) migration from the recording surface. The wave-equation-based and the simple static datuming approaches were compared in terms of imaging quality after prestack depth migration, assuming that the subsurface velocity model beneath the datum level is known. This comparative analysis considered two scenarios: (1) an absolute knowledge of the shallow velocity structure, and (2) a realistic degree of accuracy in the near-surface velocity information. For the latter scenario, I used a near-surface velocity model derived from a turning-ray tomography analysis. Following are the main conclusions.

6.1 Imaging in areas of rough terrain

6.1.1 Accurate near-surface velocity model

As is known, the wavefield propagation throughout a complex near-surface velocity structure produces focusing and kinematic distortions on seismic data. The static-corrections approach can solve, to some degree of accuracy, purely kinematic distortions but definitely cannot correct distortions associated with focusing. Wave-equation datuming, in contrast, offers an accurate theoretical solution to dealing with near-surface-induced distortions in the process of imaging. When the information of the near-surface velocity is perfect, the wave-equation datuming unravels time distortions associated with laterally-changing near-surface conditions accurately, accounting for kinematic and focusing distortions in seismic data and preparing them for a conventional CMP processing sequence. Since no moveout distortions are left in the data after wave-equation datuming, reliable velocity analysis can be carried out. Unlike wave-equation datuming, the static-corrections approach cannot remove properly the nonhyperbolic moveout distortions associated with the near-surface, compromising the performance of subsequently applied processes such as velocity analysis, DMO, and migration. Moveout distortions in the data caused by improper treatment of the near-surface time anomalies seem to influence more significantly the shallow reflections than the deeper ones.

If the general processing problems are the rugged topography and the laterally-

changing near-surface conditions but the subsurface model is expected to be structurally simple, Kirchhoff datuming followed by time migration provide a less expensive solution than does prestack depth migration. Kirchhoff datuming transfers the data from an irregularly-sampled rough surface to an ideal, regularly-sampled, horizontal new reference surface beneath the near-surface velocity anomalies.

Full-waveform finite-difference datuming works somewhat better that does the Kirchhoff datuming approach under extreme lateral velocity variation on the near-surface such as those frequently found in overthrust areas. Furthermore, finite-difference datuming solutions exhibit higher-frequency content than those from a Kirchhoff datuming implementation. The main reason for this is the attenuating action of the operator anti-aliasing filter. However, the differences in the results of these two implementations of the wave-equation datuming process are relatively small when the true near-surface structure is used and they are negligible when the information of the shallow velocity model is imperfect. Therefore, in practice, Kirchhoff datuming would be preferred over finite-difference datuming, considering its computational efficiency and its robustness to handle irregular sampling in the data, characteristics typically found in land-acquisition geometries.

An alternative wave-theoretical approach for treating near-surface-induced time distortions is prestack depth migration from topography. Unlike wave-equation datuming, migration from topography does not lose any data from the near-surface in the downward continuation process, giving structural information that is important for tying a seismic interpretation to any available surface geology data (e.g., outcrops). When an accurate ray-tracing algorithm is used in the estimation of the extrapolation operators, the quality of the images generated from migration after datuming and those obtained with migration from topography is quite similar.

6.1.2 Imperfect near-surface velocity information

For modest degree of velocity smoothing, the wave-equation datuming gives better results than does the static-correction approach when a smooth version of the true shallow velocity structure is used in the imaging process. In some situations, however, the static-datuming approach can be more robust than the wave-equation datuming scheme. I have demonstrated with synthetic data examples that the static-datuming technique might work better when the velocity used in the datuming processes is higher than the true velocity field. When the velocity used in the datuming process is lower than the true velocity field, both algorithms comparably distort the data, giving poor imaging quality after prestack depth migration. In general, prestack depth migration is highly influenced by timing errors in the input data. Therefore, good control of the near-surface-induced time distortions is required in order to get a satisfactory image quality.

In the presence of errors in the overburden velocity model, it is difficult to see differences in imaging quality on migrated sections obtained from data processed with tomo-static and tomo-datuming. To exploit the accuracy of the tomo-datuming

algorithm, the near-surface velocity obtained by turning-ray tomography must portray quite accurately the features in the true velocity field. Otherwise, both corrective procedures would yield similarly poor images. Therefore, the conventional static-correction approach would be preferred over the more sophisticated Kirchhoff datuming considering its simplicity and low cost.

On the other hand, on conventional CMP processing, Kirchhoff datuming gives better stacking-velocity functions than does the static-corrections approach by avoiding unnecessary moveout distortions on reflection events. Since the stacking velocity functions interpreted from data treated with static-corrections can change considerably from one CMP location to another, the stacking quality can vary along the seismic line unless fine control of the velocities is used along the profile. This observation suggests that under similar sampling conditions of the stacking velocities, the stacking quality given by data treated with Kirchhoff datuming is superior to that offered by data processed with the static-corrections approach.

The conclusions from the last two paragraphs seem to be contradictory. In the work done by following a depth processing sequence (e.g., with prestack depth migration), the static approach proved to be more robust than the Kirchhoff datuming when using imperfect near-surface velocity information. Under the same circumstances, for the time processing, the Kirchhoff datuming gave better stacking velocity functions than those obtained from static-corrected data. Perhaps, the explanation for this contradictory situation is the relative sensitivity to error of the two domains in which the processing is done (i.e, depth and time). As is known, depth processing is extremely sensitive to time anomalies and velocity uncertainty. Time processing, on the other hand, is more tolerant of velocity errors and time distortions. In any case, more study will be required to better understand the nature of this dichotomy.

6.2 Modeling of near-surface time anomalies

Wave-equation datuming proved to be a good tool for efficiently adding near-surface time anomalies to model data. Traditionally, static-estimation schemes have been tested using synthetic data contaminated with pseudo-random surface-consistent statics. In contrast to the conventional methods for adding in statics, the wave-equation-based methodology works with a near-surface velocity model. This approach honors the multi-directional nature of the propagation paths, giving more realistic time anomalies. This methodology thus offers an inexpensive way to study near-surface problems, allowing us to remodel just the near-surface structure of the velocity model without having to repeatedly model the subsurface velocity structure. Particularly if the subsurface velocity structure is complex, an expensive modeling algorithm (e.g., finite-difference) may need to be used for the deep subsurface, after which wave-equation datuming performs the modeling of just the near-surface. The two-step methodology is thus less expensive than using the full-waveform finite-difference approach for every new near-surface situation that needs to be studied. When the near-surface velocity structure exhibits more complexity and detail than that which Kirchhoff da-

tuming can handle with accuracy, a full-waveform finite-difference datuming could be used instead, and the general methodology would be still valid.

6.3 Software developed

Computational tools were required to process the synthetic data presented in this thesis. Some of the codes are extensions of existent programs and others are new developments that use available subroutines. Aiming at preserving full portability to different computer systems, I developed the codes in standard ANSI C. All these codes run as part of the Seismic Unix (SU) environment (Cohen and Stockwell Jr., 1996). The following codes will be available in the Seismic Unix (SU) package:

- Prestack Kirchhoff datuming from and to a variable-topography surface: **sudatumk2dcr.c** and **sudatumk2dcs.c**. This datuming algorithm is implemented in the time domain; those codes are designed to operate first on receiver gathers (cr) and then on shot gathers (cs) (See Figure 2.1). These codes are based on a far-field approximation of equations (2.14) and (2.15). As input, they require traveltime tables, which can be estimated with the code **rayt2d.c**.

- Migration from the recording surface: **sumigtopo2d.c**. This code is an extension of the program **sukdmig2d.c** implemented by Dr. Zhenyue Liu. The new version offers the important option to migrate data directly from the variable-topography acquisition surface. As with the previous codes, it requires traveltime tables as input.

- Ray-tracing from topography. This code is an extension of the program **rayt2d.c** implemented by Dr. Zhenyue Liu. This program is an implementation of the paraxial ray-tracing method (Beydoun and Keho, 1987). The new version allows estimation of traveltime tables from a variable recording surface.

6.4 Future work

Although the theory required to do wave-equation datuming in the shot and receiver domain is well known, it would be valuable to develop a different Kirchhoff approach that works in the common-offset domain. In practice, the prestack Kirchhoff datuming approach is performed in the shot domain and then in the receiver domain. This multi-step approach is computationally inefficient, and it has aperture problems and edge effects. These inconveniences are even worse in 3-D, where the shot spacing is often large compared to the receiver spacing. A wave-equation datuming approach in the common-offset domain would be an ideal solution not only in terms of imaging quality but also in terms of computational efficiency. One-step Kirchhoff datuming would reduce costs, decreasing the input and output data requirements. Furthermore, that new approach would reduce artifacts due to aperture limitations and edge effects.

Recent work has indicated that anisotropy has significant importance in seismic data imaging. Appropriate changes to this Kirchhoff implementation would enable it to handle downward continuation of the data through an anisotropic medium. The real problem for this approach would be in estimating the required parameters to define well enough the anisotropic behavior of the media in order to compensate for near-surface-induced time distortions.

Ray-tracing is the heart of any Kirchhoff-type implementation, thus an improved ray-tracing code that considers not only the first-arrival but multi-valued arrivals would increase the quality of these extrapolation and migration schemes.

The methodology presented here for modeling near-surface time distortions was used to generate realistic time anomalies on the Marmousi data set. Such contaminated data sets could be a good testbed for analyzing the applicability of new residual static-estimation approaches, such as that by Larner and Tjan (1995). Unlike the surface-consistent static shifts imposed in their tests, these time anomalies are non-surface-consistent.

BIBLIOGRAPHY

Beasley, C. and W. Lynn (1992). The zero-velocity layer: Migration from irregular surfaces. *Geophysics*, **57**, no. 11, 1435–1443.

Berkhout, A. (1985). *Seismic migration - Imaging of acoustic energy by wavefield extrapolation : A. Theoretical aspects.* Elsevier, Amsterdam and New York.

Berryhill, J. A. (1986). Submarine canyons - velocity replacement by wave equation datuming before stack. *Geophysics*, **51**, no. 8, 1572–1579.

Berryhill, J. R. (1979). Wave equation datuming. *Geophysics*, **44**, no. 8, 1329–1344.

Berryhill, J. R. (1984). Wave equation datuming before stack (short note). *Geophysics*, **49**, no. 11, 2064–2067.

Bevc, D. (1993). Data parallel wave equation datuming with irregular acquisition topography. In *63rd Annual Internat. Mtg., Soc. Expl. Geophys., Expanded Abstracts*, Volume 93, pp. 197–200.

Bevc, D. (1994). Near-surface velocity estimation. In *64th Annual Internat. Mtg., Soc. Expl. Geophys., Expanded Abstracts*, Volume 94, pp. 996–999.

Bevc, D. (1995). Imaging complex structures with first-arrival traveltimes. In *65th Annual Internat. Mtg., Soc. Expl. Geophys., Expanded Abstracts*, Volume 95, pp. 1189–1192.

Beydoun, W. B. and T. H. Keho (1987). The paraxial ray method. *Geophysics*, **52**, no. 12, 1639–1653.

Bleistein, N. (1984). *Mathematical methods for wave phenomena.* Academic press, New York.

Bleistein, N. (1987). On the imaging of reflectors in the earth. *Geophysics*, **52**, no. 7, 931–942.

Bleistein, N., J. K. Cohen, and F. G. Hagin (1987). Two and one-half dimensional born inversion with an arbitrary reference. *Geophysics*, **52**, no. 1, 26–36.

Burke, N. L. and S. Knapp (1994). Advances in imaging in the colombian foothills. In *64th Annual Internat. Mtg., Soc. Expl. Geophys., Expanded Abstracts*, Volume 94, pp. 1651–1655.

Claerbout, J. (1985). *Imaging the earth's interior.* Blackwell Scientific Publications, Inc.

Cohen, J. and J. W. Stockwell Jr. (1996). Cwp/su release 28, a free seismic software environment for unix platforms. Technical report, Center for Wave Phenomena.

Docherty, P. (1991a). A brief comparison of some kirchhoff integral formulas for migration and inversion. *Geophysics*, **56**, no. 8, 1164–1169.

Docherty, P. (1991b). Documentation for the 2.5-d common shot program cshot. Technical Report U08R, Center for Wave Phenomena.

Ellis, N. and P. Kitchenside (1989). Recursive implementation of redatuming, imaging, and layer replacement for irregular topography. In *59th Annual Internat. Mtg., Soc. Expl. Geophys., Expanded Abstracts*, Volume 89, pp. 482.

Fei, T. (1994). *Elimination of numerical dispersion in finite-difference modeling and migration by flux-corrected transport.* Ph. D. thesis, Colorado School of Mines.

Geoltrain, S. and J. Brac (1993). Can we image complex structures with first-arrival traveltime? *Geophysics*, **58**, no. 4, 564–575.

Larner, K., G. Perez, E. Jenner, and T. Salinas (1996). The quality of the surface-consistent assumption in residual-statics estimation. In *66th Annual Internat. Mtg., Soc. Expl. Geophys., Expanded Abstracts*, Volume 96.

Larner, K. and T. Tjan (1995). Simultaneous statics and velocity estimation for data from structurally-complex areas. In *65th Annual Internat. Mtg., Soc. Expl. Geophys., Expanded Abstracts*, Volume 95, pp. 1401–1404.

Liu, Z. (1993). A kirchhoff approach to seismic modeling and prestack depth migration. Technical Report CWP-137, Center for Wave Phenomena.

Lumley, D. E., J. F. Claerbout, and D. Bevc (1994). Anti-aliased kirchhoff 3-d migration. In *64th Annual Internat. Mtg., Soc. Expl. Geophys., Expanded Abstracts*, Volume 94, pp. 1282–1285.

Lynn, W., S. MacKay, and C. J. Beasley (1990). Efficient migration through irregular water-bottom topography. In *60th Annual Internat. Mtg., Soc. Expl. Geophys., Expanded Abstracts*, Volume 90, pp. 1297–1300.

MacKay, S. M. (1994). Efficient wavefield extrapolation to irregular surfaces using finite differences: Zero-velocity datuming. In *64th Annual Internat. Mtg., Soc. Expl. Geophys., Expanded Abstracts*, Volume 94, pp. 1564–1567.

McMechan, G. and R. Sun (1991). Depth filtering of first breaks and ground-roll. *Geophysics*, **56**, 390–396.

McMechan, G. A. and H. W. Chen (1990). Implicit static corrections in prestack migration of common-source data. *Geophysics*, **55**, no. 6, 757–760.

Nichols, D. (1994). Maximum energy traveltimes calculated in the seismic frequency band. In *64th Annual Internat. Mtg., Soc. Expl. Geophys., Expanded Abstracts*, Volume 94, pp. 1382–1385.

Perez, G. (1996). The quality of the surface-consistent assumption in residual-statics estimation. Master's thesis, Colorado School of Mines.

Rajasekaran, S. and G. A. McMechan (1995). Prestack processing of land data with complex topography. *Geophysics*, **60**, no. 6, 1875–1886.

Reshef, M. (1991). Depth migration from irregular surfaces with depth extrapolation methods (short note). *Geophysics*, **56**, no. 1, 119–122.

Rodriguez, S., J. P. Diet, and D. Paturet (1991). Dip move out in the case of irregular surfaces. In *61st Annual Internat. Mtg., Soc. Expl. Geophys., Expanded Abstracts*, Volume 91, pp. 1301–1304.

Scales, J. (1994). *Theory of seismic imaging*. Samizdat press, Golden.

Schneider, William A., J., L. D. Phillip, and E. F. Paal (1995). Wave-equation velocity replacement of the low-velocity layer for overthrust-belt data. *Geophysics*, **60**, no. 2, 573–579.

Shtivelman, V. and A. Canning (1988). Datum correction by wave equation extrapolation. *Geophysics*, **53**, no. 10, 1311–1322.

Stefani, J. P. (1995). Turning-ray tomography. *Geophysics*, **60**, no. 6, 1917–1929.

Versteeg, R. and G. Grau (1991). The marmousi experience. In *Proceedings of the workshop on Practical aspects of seismic data inversion, 1990, 52nd EAEG Meeting*. Eur. Assoc. Expl. Geophys.

Versteeg, R. J. (1993). Sensitivity of prestack depth migration to the velocity model. *Geophysics*, **58**, no. 6, 873–882.

Wielandt, E. (1987). On the validity of the ray approximation for for interpreting delay times. In G. Nolet (Ed.), *Seismic tomography with applications in global seismology and exploration geophysics*. The Netherlands: D. Reidel publishing company.

Wiggins, J. W. (1984). Kirchhoff integral extrapolation and migration of nonplanar data. *Geophysics*, **49**, no. 8, 1239–1248.

Wiggins, R. A., K. L. Larner, and R. D. Wisecup (1976). Residual statics analysis as a general linear inverse problem. *Geophysics*, **41**, 922–938.

Yilmaz, O. and D. Lucas (1986). Prestack layer replacement. *Geophysics*, **51**, no. 7, 1355–1369.

Zhu, X., B. G. Angstman, and D. P. Sixta (1995). Overthrust imaging with tomodatuming. In *65th Annual Internat. Mtg., Soc. Expl. Geophys., Expanded Abstracts*, Volume 95, pp. 1397–1400.

Zhu, X., D. P. Sixta, and B. G. Angstman (1992). Tomostatics: Turning-ray tomography + static corrections. *The Leading Edge*, **11**, no. 12, 15–23.